

**Mechanisms of Cell-autonomous Resistance
to *Toxoplasma gondii* in Mouse and Man**

Inaugural-Dissertation
zur
Erlangung des Doktorgrades
der Mathematisch-Naturwissenschaftlichen Fakultät
der Universität zu Köln

vorgelegt von
Aliaksandr Khaminets
aus Slonim, Weißrussland
Köln 2010

Berichterstatter:

Prof. Dr. Jonathan C. Howard

Prof. Dr. Thomas Langer

Tag der mündlichen Prüfung: 31.05.2010

Table of contents

1 Introduction	1
1.1 Infection and immunity	1
1.2 Interferons and their role in cell-autonomous immunity	2
1.3 Cellular responses to interferons	4
1.4 Immunity-related GTPases	7
1.4.1 Nomenclature and expression	7
1.4.2 Biochemical properties of IRG proteins	8
1.4.3 Cellular localisation of IRG proteins	9
1.4.4 Roles of IRG proteins in immunity	10
1.5 <i>Toxoplasma gondii</i> as a model pathogen to study human and mouse cell-autonomous response	12
1.6 Aims of the study	16
2 Material and Methods	18
2.1 Reagents and cells.	18
2.1.1 Chemicals, reagents and accessories	18
2.1.2 Equipment	18
2.1.3 Materials	18
2.1.4 Enzymes and proteins	19
2.1.5 Kits	19
2.1.6 Vectors and constructs used in the present study	19
2.1.7 Cell lines, bacterial and protozoan strains	19
2.1.8 Serological reagents	21
2.2 Molecular Biology	23
2.2.1 Agarose gel electrophoresis	23
2.2.2 Generation of the expression constructs	23
2.2.3 Cloning of PCR amplification products	25
2.2.4 Purification of DNA fragments from agarose gels	25
2.2.5 Ligation	25
2.2.6 Preparation of competent cells	26
2.2.7 Transformation of competent bacteria	26

2.2.8 Plasmid isolation	26
2.2.9 Determination of the concentration of DNA	27
2.2.10 Site-directed mutagenesis	27
2.2.11 DNA sequencing	27
2.3 Cell biology	28
2.3.1 Transfection	28
2.3.2 Immunocytochemistry	28
2.3.3 In vitro passage of <i>T. gondii</i>	28
2.3.4 Infection of cells with <i>T. gondii</i> for immunocytochemistry	29
2.3.5 <i>T. gondii</i> lysis	29
2.3.6 Live cell imaging	29
2.3.7 Inhibition of signalling pathways and microtubule polymerisation	30
2.3.8 Synchronisation of <i>T. gondii</i> infection	30
2.3.9 <i>T. gondii</i> proliferation assay	31
2.3.10 Quantification of IRG protein signal intensity at <i>T. gondii</i> PV	31
2.3.11 Western blotting	32
2.3.12 Colorimetric cell viability assay	32
2.3.13 Propidium iodide staining	33
2.3.14 Pulse-chase analysis	33
2.3.15 Immunoprecipitation	34
3 Results I	35
3.1 Time-course of endogenous IRG protein loading onto avirulent ME49 <i>T. gondii</i> vacuoles in mouse fibroblasts	35
3.2 Time-course of ectopically expressed IRG protein loading onto avirulent ME49 <i>T. gondii</i> vacuoles in mouse fibroblasts	37
3.3 Sequential loading of multiple IRG proteins on to the PV of avirulent ME49 <i>T. gondii</i>	38
3.4 Vacuolar loading with IRG proteins is independent of major signalling systems and microtubules	41

3.5 Vacuolar loading with IRG proteins is dependent on autophagic regulator Atg5	42
3.6 Reduced loading of IRG proteins onto the PVM of virulent <i>T. gondii</i> strains	46
3.7 Coinfection of mouse fibroblasts with <i>T. gondii</i> of different virulence and virulence-associated <i>T. gondii</i> proteins ROP18, ROP16 and ROP5 do not affect loading of PVM with IRG proteins	48
3.8 IRG complex formation is required for efficient loading onto <i>T. gondii</i> PV	51
3.9 Vacuolar loading with IRG proteins is required for <i>T. gondii</i> elimination	53
4 Results II	59
4.1 IDO-dependent and IDO-independent mechanisms of resistance against <i>T. gondii</i> in human cells	59
4.2 Disruption of <i>T. gondii</i> vacuoles is not apparent in IFN γ -induced primary human fibroblasts	61
4.3 IFN γ stimulates death of distinct types of <i>T. gondii</i> -infected human cells	63
4.4 Human cells, stimulated with IFN γ and infected with <i>T. gondii</i> , undergo necrosis but not apoptosis	66
4.5 Addition of tryptophan inhibits necrosis of human fibroblasts during IDO-dependent but not during IDO-independent course of IFN γ -mediated control of <i>T. gondii</i>	70
4.6 Pharmacological inhibition of IDO rescues <i>T. gondii</i> growth in IFN γ -stimulated HeLa cells but not in primary human fibroblasts	72
5 Discussion	75
5.1 Heterogeneity of IRG protein loading onto vacuoles with avirulent <i>T. gondii</i>	75
5.2 Regulation of IRG proteins by Atg5 in IFN γ -stimulated mouse fibroblasts	77

5.3 IRG complex formation is required for association with avirulent <i>T. gondii</i> PV	79
5.4 Passive vs. active model of IRG protein association with avirulent <i>T. gondii</i> PV	80
5.5 Reduced accumulation of IRG proteins on virulent <i>T. gondii</i> PVs is independent of ROP5, ROP16 and ROP18 virulence determinants of the parasite	82
5.6 Loading of IRG proteins onto <i>T. gondii</i> vacuoles is crucial for parasite elimination in IFN γ -induced mouse fibroblasts	85
5.7 Amount of cultured cells determines the mechanism of <i>T. gondii</i> growth inhibition in IFN γ -stimulated primary human fibroblasts	86
5.8 <i>T. gondii</i> infection stimulates necrosis of IFN γ -induced primary human cells	87
5.9 IDO-dependent and IDO-independent mechanisms of IFN γ -induced <i>T. gondii</i> growth restriction in human cells	89
6 Appendix	92
6.1 Figure 32. Association of wt, catalytic interface and secondary patch mutants of Irga6-cTag1 with ME49 <i>T. gondii</i> PV	92
6.2 Permeabilisation of avirulent <i>T. gondii</i> to cytoplasmic Cherry in IFN γ -stimulated infected MEFs	94
6.3 IFN γ induces death of <i>T. gondii</i> -infected human cells	95
6.4 Analysis of Hs27 cell viability by PI staining	96
7 References	97
8 Summary	124
9 Zusammenfassung	125
10 Acknowledgements	127
11 Erklärung	128
12 Teilpublikationen	129

13 Lebenslauf	130
----------------------------	------------

1 Introduction

1.1 Infection and immunity

Organisms evolve by interacting with each other and their environment. Numerous intricate interplays between organisms proved to be the source and the result of adaptations shaping life on the planet. Forms of relations between different species, also called symbiosis (Greek *syn* stands for “with” and *biosis* stands for “living”), were classified into mutualism (both sides benefit from relationship), commensalism (one side benefits while the other is not positively or negatively affected) and parasitism (one side exploits and harms the other). Various pathogens use their hosts in order to survive and reproduce whereas hosts attempt to eliminate the unwelcome guests. This underlies the everlasting battle between the host and the parasite leading to the co-evolution of species (Roy and Mocarski, 2007).

Hosts possess an arsenal of mechanisms, called the immunity system, to defend themselves from pathogens. Host barriers, such as plasma membranes or outer cell layers, represent the most ancient and primitive means of protection against parasites. Additionally, various molecules (e.g. complement, lysozyme, lactoferrin etc.) and processes (e.g. phagocytosis), capable of exerting antiparasitic action, account for a large portion of innate immune system. These immune mechanisms constitute a first line of defense against invasion which is deployed in a fast but unspecific manner (Janeway et al., 2008). In contrast to innate immunity, adaptive immunity (or acquired), found only in vertebrates (Medzhitov and Janeway, 1997), has a lag phase after initiation till the system is fully functional. Adaptive immunity is characterized by generation of high-specificity receptors to the antigens via somatic mechanisms of amplification and diversification, and by the phenomenon of immunological memory. The latter allows recognizing and mounting the immune response more rapidly and efficiently after repeated exposure to the same infectious agent (Janeway et al., 2008).

Central to triggering of the immune programs is recognition of the parasite. This step is achieved by the pattern recognition receptors (PRRs), present on cellular membranes (e.g. Toll-like receptors, scavenger receptors) or in the cytoplasmic space (e.g. CARD helicases, NOD-like proteins) which recognise the pathogen-associated molecular patterns (PAMPs) (e.g. LPS, DNA, double-stranded RNA) (Medzhitov, 2001; Akira, Uematsu, and Takeuchi, 2006; Fritz et al., 2006; Lee and Kim, 2007). Recognition of the parasite signals to the immune system to escalate the inflammatory

response, resulting in the recruitment of immune cells at the locus of invasion, secretion of cell-derived immune mediators and increased permeability of blood vessels. All these processes ensure containment and subsequent clearance of infection (Roy and Mocarski, 2007; Janeway et al., 2008).

Regulation of cell-to-cell communication, connection between innate and adaptive systems and the magnitude of the immune response are tightly regulated by cytokines.

1.2 Interferons and their role in cell-autonomous immunity

Cytokines (Greek *cyto* means “cell”, *kinos* means “movement”) are a group of peptides and proteins, secreted by both hematopoietic and non-hematopoietic cells, implicated in modulation of all steps of the immune response. Cytokines could be subdivided into chemokines, hematopoietins, tumor necrosis factor (TNF) family and interferons (Janeway et al., 2008). A prominent role in regulation of the immune system is orchestrated by interferons. Since the discovery of interferon as an antiviral drug (Isaacs and Lindenmann, 1957; Isaacs, Lindenmann, and Valentine, 1957), the cytokine was assigned a plethora of functions discussed hereafter. The family of the interferons include type I: IFN α (14-20, depending on species) (van Pesch et al., 2004), IFN β (Mogensen et al., 1999), IFN ω (Hauptmann and Swetly, 1985), IFN τ (Bazer, Spencer, and Ott, 1997), IFN ϵ (Pestka, Krause, and Walter, 2004), IFN δ (Lefevre et al., 1998); type II: IFN γ (Bancroft, 1993) and type III: IFN λ (Kotenko et al., 2003). Type I interferons are secreted by virtually all types of cells, however the major producers of IFN α and IFN ω are hematopoietic cells whereas fibroblasts are the main source of IFN β (Bach, Aguet, and Schreiber, 1997). In addition to T-cells and NK cells, being the major contributors of IFN γ , NKT, B- and professional antigen presenting cells (APCs) have also been reported to secrete the cytokine (Schroder et al., 2004).

Interferons engage with specific receptors present on the cell surfaces (Figure 1) leading to activation of the associated kinases JAK1, JAK2 and TYK2 which in turn phosphorylate and thereby activate transcription factors STAT1 and STAT2. STAT1 and STAT2 translocate into the nucleus and bind to GAS elements in the promoter regions driving expression of IFN-regulated genes. Some of those genes encode transcription factors (IRF) mediating the next waves of the transcription events from the promoter ISRE elements (Schroder et al., 2004; Borden et al., 2007).

It is now appreciated that interferons, acting in autocrine and paracrine fashion, induce multiple processes such as stimulation of intracellular and extracellular networks, regulation of resistance to infections, amplification of innate and acquired immune response, modulation of survival and death of normal and tumor cells (Schroder et al., 2004; Borden et al., 2007).

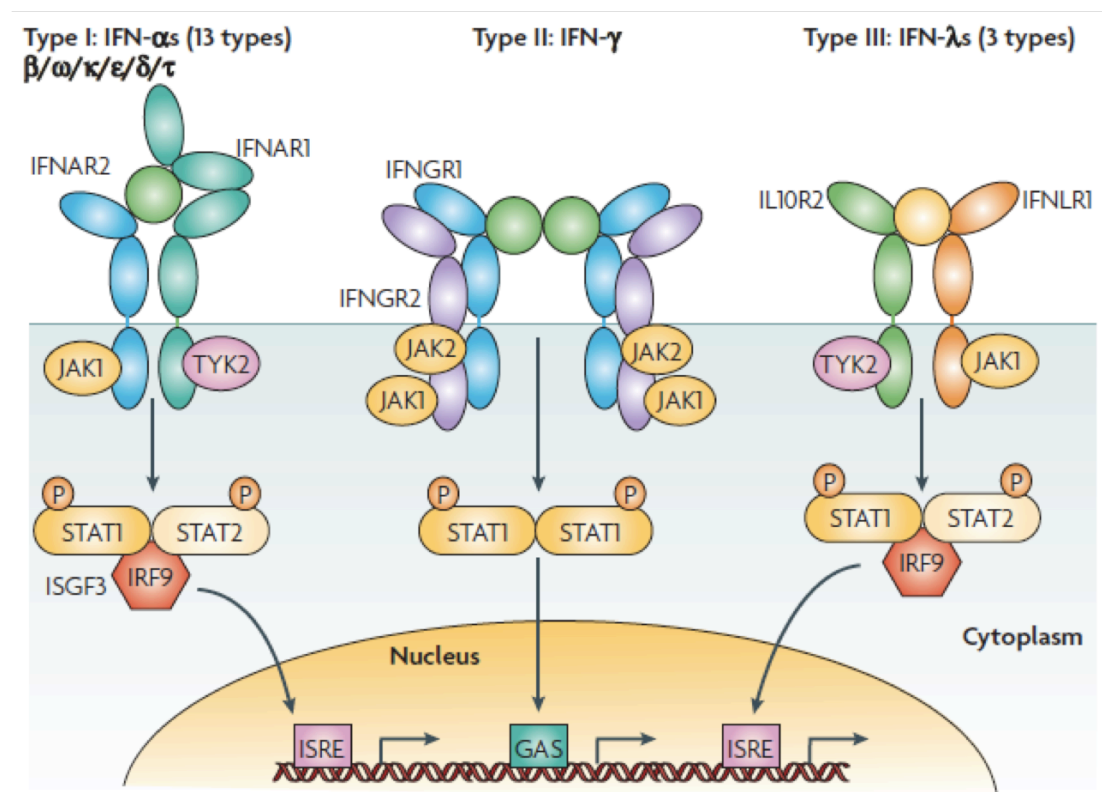


Figure 1 Receptor activation or ligand–receptor complex assembled by type I, type II or type III interferons.

Type I interferons (α , β , ω , κ , ϵ , δ , τ) interact with IFN (α , β and ω) receptor 1 (IFNAR1) and IFNAR2; type II IFN γ with IFN γ receptor 1 (IFNGR1) and IFNGR2; and type III IFN λ s with IFN λ receptor 1 (IFNLR1; also known as IL28RA) and interleukin 10 receptor 2 (IL10R2; also known as IL10RB). Type II IFN γ is an antiparallel homodimer exhibiting a two-fold axis of symmetry. It binds two IFNGR1 receptor chains, assembling a complex that is stabilized by two IFNGR2 chains. These receptors are associated with two kinases from the JAK family: JAK1 and TYK2 for type I and III IFNs; JAK1 and JAK2 for type II IFN. IFNAR2, IFNLR1, IL10R2, IFNGR1 and IFNGR2 are classical representatives of this family, while IFNAR1 is atypical as its extracellular domain is duplicated. GAS, IFN γ -activated site; IRF9, IFN regulatory factor 9; ISGF3, IFN-stimulated gene factor 3, refers to the STAT1–STAT2–IRF9 complex; ISRE, IFN-stimulated response element; P, phosphate; STAT1/2, signal transducers and activators of transcription $\frac{1}{2}$ (Borden et al., 2007).

Interferons regulate cell-autonomous response to pathogens. Cell-autonomous immunity designates the ability of a cell to cope with infection within the boundaries of the cell and without involvement of the ambient cellular environment. Because interferons are derived from outside of the cells to engage with the specific plasma membrane receptors in order to arm the cells with mechanisms of defense against

invasion, this type of immunity could not be referred to as entirely autonomous.

1.3 Cellular responses to interferons

Interferons increase cellular concentration of proteins, many of which have proved to be resistance factors and have been implicated in innate and adaptive components of the immune system. The examples of immunity-related proteins regulated by interferons are numerous and their list is constantly growing (Boehm et al., 1997).

Expression of MHC class I and class II molecules and other components of the antigen presentation system of the antigen-presenting cells (APCs) is increased upon induction with interferons. Furthermore, these cytokines are involved in generation of reactive oxygen and nitrogen species by enhancing intracellular activities of the corresponding enzymes (e.g. gp91-phox and nitric oxide synthase (iNOS)). In macrophages, natural resistance-associated macrophage protein 1 (NRAMP1), a mediator of the natural resistance against intracellular pathogens, is constitutively expressed and, additionally, could be strongly upregulated by IFN γ and LPS. Double-stranded RNA activated protein kinase (PKR), oligoadenylate synthetase (OAS) and specific adenosine deaminase (dsRAD), enzymes upregulated by interferons, exert a characteristic direct antiviral effects at the cell-autonomous level (Boehm et al., 1997; Schroder et al., 2004; Borden et al., 2007). Depletion of the cellular sources of tryptophan, mediated by the enzymes indoleamin 2,3-dioxygenase (IDO) and tryptophan 2,3-dioxygenase (TDO), has been reported to execute the antimicrobial and immunomodulatory function of the interferons (Pfefferkorn, 1984; Boehm et al., 1997; Munn et al., 1999; Schmidt et al., 2009).

Mx proteins, induced strictly by type I interferons, are potent antiviral factors, which are believed to directly bind to the virion components (e.g. influenza, Thogoto virus) and interfere with the viral trafficking, assembly or replication (Lindenmann, Lane, and Hobson, 1963; Lindenmann et al., 1978; Kochs et al., 1998; Kochs and Haller, 1999a; Kochs and Haller, 1999b; Haller and Kochs, 2002). Mx proteins are 70-80 kDa homologous to dynamin GTPases (present in all vertebrates, Mx1 and Mx2 in mice, MxA and MxB in humans), displaying some dynamin-like properties, such as GTP-dependent oligomerisation and micromolar affinities for GTP and GDP (Richter et al., 1995; Hinshaw, 2000; Kochs et al., 2002; Song and Schmid, 2003).

The family of guanylate-binding proteins (GBPs) is represented by 65-67 kDa

interferon inducible GTPases (present in all vertebrates, 10 members in mice, 7 in humans) (Degrandi et al., 2007; Olszewski, Gray, and Vestal, 2006; Robertsen et al., 2006). Resembling dynamins, GBP proteins bind nucleotides with micromolar affinity and demonstrate di- or tetramerisation and cooperative hydrolysis of GTP (Praefcke and McMahon, 2004). In contrast to Mx proteins, GBPs are strongly induced by IFN γ whereas type I interferons, TNF α and IL-1 β have only a slight effect on the protein expression (Nantais et al., 1996; Boehm et al., 1998; Guenzi et al., 2001; Guenzi et al., 2003). GBPs have been implicated in resistance against vesicular stomatitis (VSV), Encephalomyocarditis (ECMV) and Hepatitis C viruses (Anderson et al., 1999; Carter, Gorbacheva, and Vestal, 2005; Itsui et al., 2009) as well as in regulation of vasculogenesis and cell proliferation (Guenzi et al., 2001; Gorbacheva et al., 2002; Guenzi et al., 2003). Interestingly, recent localisation and overexpression studies of GBP proteins suggested their role in resistance against *T. gondii* (Degrandi et al., 2007) and *Chlamydia trachomatis* (Tietzel, El-Haibi, and Carabeo, 2009).

Very large inducible GTPases (VLIGs) are 280 kDa proteins induced in mouse cells by IFN γ and to some extent by IFN β . The G domain of VLIGs displays some homology to Mx proteins and GBPs, but the functions of the VLIGs in resistance are still to be clarified (Klamp et al., 2003).

Autophagy (macroautophagy) is a conserved cellular degradation system, specialized in removal of damaged organelles, clearance of aggregated proteins or turnover of any part of the cell cytoplasm (Mizushima, 2002; Xie and Klionsky, 2007; Mizushima et al., 2008). In addition to starvation, microorganisms, protein aggregates and numerous drugs, IFN γ has been reported to induce autophagy (Gutierrez et al., 2004; Deretic, 2005; Deretic, 2006). Atg1-27 proteins (defined in yeasts, but most of the proteins have homologs in mammals) orchestrate the process of the phagophore formation around the target, its conversion into autophagosome and fusion with the lysosomal compartment to give rise to autolysosomes (Figure 2) (Deretic, 2005). Interestingly, an Atg5/Atg7-independent pathway of autophagy has been recently reported (Nishida et al., 2009). Autophagy has been implicated in direct elimination of intracellular pathogens such as *Mycobacterium tuberculosis*, *Listeria monocytogenes*, *Shigella flexneri* etc. (Deretic, 2005), however certain pathogens (e.g. *Francisella tularensis*, *Staphylococcus aureus*) exploit the process of autophagy in order to survive and replicate (Checroun et al., 2006; Schnaith et al., 2007).

Autophagy may lead to death of the cell, designated as programmed cell death type II (Golstein and Kroemer, 2007), characterized by massive accumulations of autophagic vesicles in the cytosol (Levine, 2005; Pyo et al., 2005; Feng et al., 2008b; Kroemer and Levine, 2008). Apoptosis (programmed cell death type I) carries features of chromatic condensation and fragmentation, shrinkage and blebbing of the plasma membrane and formation of apoptotic bodies (Golstein and Kroemer, 2007). Interferons have been shown to induce expression of death-associated proteins (e.g. TNF α -related apoptosis inducing ligand (TRAIL/Apo2L), caspase-4 and caspase-8) and in certain models stimulate apoptotic cell death (Boehm et al., 1997; Chin et al., 1997; Bernabei et al., 2001; Inagaki et al., 2002; Chawla-Sarkar et al., 2003). Necrosis (or programmed cell death type III) is defined by rupture and dilatation of cytoplasmic organelles and the plasma membrane (Golstein and Kroemer, 2007). Necrotic cell death has been recently reported to occur upon infection of IFN γ -stimulated mouse cells with avirulent *T. gondii* (Zhao et al., 2009b).

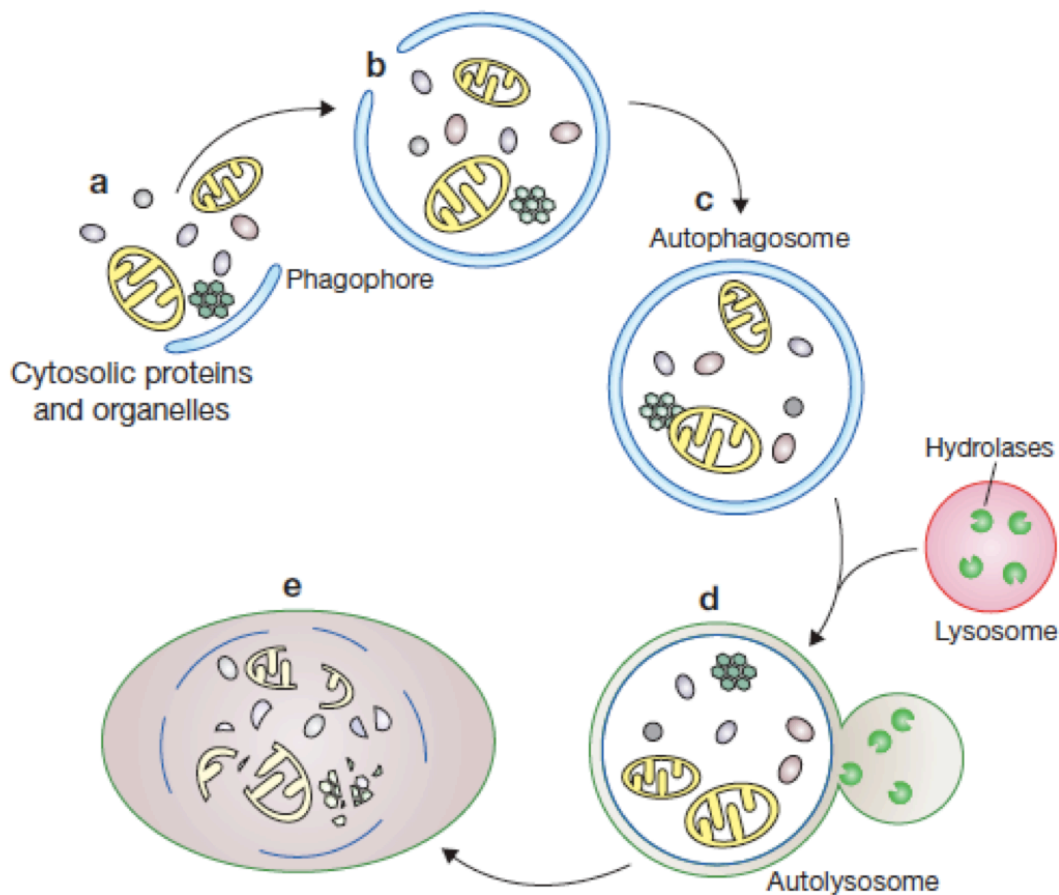


Figure 2 Schematic depiction of autophagy.

(A and B) Cytosolic material is sequestered by an expanding membrane sac, the phagophore (C)

resulting in the formation of a double-membrane vesicle, an autophagosome; **(D)** the outer membrane of the autophagosome subsequently fuses with a lysosome, exposing the inner single membrane of the autophagosome to lysosomal hydrolases; **(E)** the cargo-containing membrane compartment is then lysed, and the contents are degraded (Xie and Klionsky, 2007).

1.4 Immunity-related GTPases

1.4.1 Nomenclature and expression

The families of GBP and IRG proteins (immunity-related or p47 GTPases) have been found to dominate during cellular response to IFN γ (Boehm et al., 1998). Within the last decade IRG genes and their products have been extensively studied leading to the accumulation of a great amount of information (Taylor, 2004; MacMicking, 2005; Martens and Howard, 2006; Taylor, 2007). The homologs of the IRG genes have been identified in various species including amphioxus, fish, dog, mouse, rat and man (Bekpen et al., 2005; Li et al., 2009). In C57BL/6 mice the IRG family is represented by 21 genes located on chromosomes 7, 11, 18 and is divided on phylogenetic principles into Irga, Irgb, Irgc, Irgd and Irgm subgroups (Bekpen et al., 2005). The best-characterized members of the family are Irgb6 (TGTP/Mg21), Irga6 (IIGP1), Irgd (IRG-47), Irgm1 (LRG-47), Irgm2 (GTPI), Irgm3 (IGTP) and Irgb10. Irgm1, Irgm2 and Irgm3 have a GX₄GMS sequence within the canonical G1 motif of the GTP-binding domain and are therefore designated as GMS proteins whereas the rest of the family harbors GX₄GKS and is called GKS proteins (Bekpen et al., 2005; Boehm et al., 1998). The GMS subgroup of IRG proteins stands out from the rest of the family not only structurally but also functionally, since they have been implicated in regulation of GKS proteins in IFN γ -induced mouse cells (Hunn et al., 2008; Papic et al., 2008).

Due to the presence of GAS and ISRE sites in promoters of the IRG genes (with exception of Irgc), their expression is strongly upregulated by IFN γ and to some extent by IFN α/β and LPS in a STAT1-dependent manner (Taylor et al., 1996; Boehm et al., 1998; Collazo et al., 2002; Zerrahn et al., 2002; MacMicking, Taylor, and McKinney, 2003; Bekpen et al., 2005; Lapaque et al., 2006). Other cytokines elevate the protein levels relatively inefficiently (Lafuse et al., 1995; Boehm et al., 1998). Additionally, Irga6 is constitutively expressed in mouse liver, driven by a tissue-specific promoter (Zeng, Parvanova, and Howard, 2009).

IRGC and IRGM, found on chromosomes 5 and 19, respectively, are the only transcribed IRG genes present in humans (Bekpen et al., 2005). Neither of the human

IRG sequences is regulated by interferons. Irgc is highly conserved in all mammals and expressed specifically in haploid spermatids during spermatogenesis in testis (Bekpen et al., 2005; Rohde, 2007). The G domain of human IRGM is truncated, and expression of IRGM is driven by an ERV9 repetitive element. Thus in contrast to mice, humans possess no functional IFN γ -inducible IRG system indicating the marked disparities in immune mechanisms between these species (Bekpen et al., 2005; Coers, Starnbach, and Howard, 2009).

1.4.2 Biochemical properties of IRG proteins

Cells are equipped with GTPases involved in various physiological processes like membrane trafficking (e.g. dynamin), cell signaling (e.g. Ras, G-proteins), and translation during protein synthesis (e.g. EF-Tu) (Leipe et al., 2002). These proteins have a common GTP-binding fold. Conformational changes in two flexible switch regions signal the rest of the protein to render the GTPases active or inactive when bound to GTP or GDP, respectively (Vetter and Wittinghofer, 2001). Guanine-nucleotide exchange factors (GEF) activate the GTPases by catalyzing the release of GDP from the G domain while GTPase activating proteins (GAPs) accelerate GTP hydrolysis and thereby inactivate the proteins. Guanine-nucleotide dissociation inhibitors (GDI) bind the GDP-form of the enzymes and keep them in an inactive state (Vetter and Wittinghofer, 2001; Martens and Howard, 2006).

Irga6 is the only member of the IRG GTPase family, that has been crystallized so far, and its structure currently serves as a model for the other IRG proteins (Figure 3) (Ghosh et al., 2004). The structure shows a classical globular Ras-like G domain, inserted between N- and C-terminal helical regions. The GTP-binding domain includes universally conserved G1 (GX₄GKS), G3 (DXXG) and G4 (N(T/Q)KXD) motifs (Ghosh et al., 2004; Martens and Howard, 2006). Bacterially expressed and purified Irga6 showed micromolar affinities for the nucleotides with affinity for GDP about 10 times higher than for GTP. Additionally, recombinant Irga6 shows GTP-dependent oligomerisation and cooperativity during GTP hydrolysis (Uthaiyah et al., 2003).

Mutational analysis of the Irga6 molecule revealed the pattern of surface residues forming the putative interface (catalytic interface) essential for oligomerisation and GTP hydrolysis *in vitro* (Pawlowski et al., in preparation). The ability to hydrolyse

GTP has also been shown for Irgb6, Irgd, Irgm1 and Irgm3 proteins (Taylor et al., 1996; Carlow, Teh, and Teh, 1998; Pawlowski, 2009; Tiwari et al., 2009). Oligomerisation of Irga6 *in vitro* accelerates GTP hydrolysis, and a catalytic mechanism based on activation *in trans* between two G domains has been proposed. GKS proteins are subjected to the regulation by GMS proteins *in vivo* preventing the former from spontaneous activation and aggregation on intracellular membranes (Hunn et al., 2008; Papic et al., 2008). Thus, the GMS subgroup of the IRG proteins serves as GDIs, keeping the GKS proteins in inactive GDP-bound state.

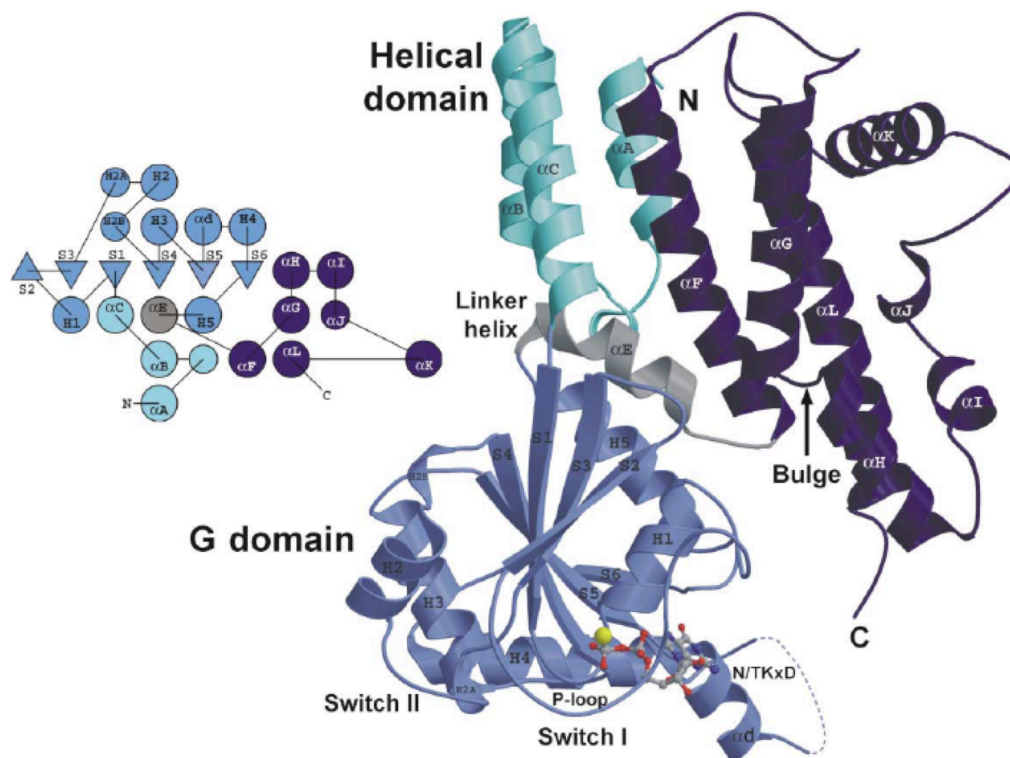


Figure 3 3D structure of Irga6.

Ribbon presentation of one Irga6 molecule of the Irga6-GDP dimer is shown with the G domain (S1-H5) colored in light-blue and the N- and C-terminal helical regions colored in cyan (aA-aC) and dark-blue (aF-aL). The linker helix aE connecting the G domain and C-terminal helical region is shown in gray. GDP and Mg²⁺ are shown as atomic stick figure and yellow sphere. The topology is shown schematically using the same color code (Ghosh et al., 2004).

1.4.3 Cellular localisation of IRG proteins

In IFN γ -induced mouse cells IRG proteins distribute among distinct cellular compartments, Irgm1 to the Golgi (Martens et al., 2004) and the endolysosomal compartments (Zhao et al., 2010), Irgm2 to the Golgi (Hunn et al., 2008; Martens and Howard, 2006), Irgm3 (Taylor et al., 1997) and Irga6 (Martens et al., 2004; Zerrahn et al., 2002) to the endoplasmic reticulum. Irga6 and Irgb6 (Boehm et al., 1998; Martens et al., 2004; Martens and Howard, 2006) as well as Irgb10 have large cytosolic pools

of proteins whereas Irgm proteins are predominantly membrane bound ((Martens and Howard, 2006) and unpublished data).

After infection of IFN γ -induced cells with avirulent *T. gondii* 6 IRG proteins (Irgb6, Irga6, Irgd, Irgm2, Irgm3 and Irgb10) have been found in high density on the parasitophorous vacuole membrane (PVM) (Martens et al., 2005; Khaminets et al., 2010). Irgm1 has never been reported on the PVM, but accumulates on phagocytic cups and phagosomes in cells phagocytosing *M. tuberculosis* or latex beads (Butcher et al., 2005a; Martens et al., 2005; Shenoy et al., 2007). Additionally, Irgm1 has been reported to colocalise with autophagosome markers monodansylcadaverine (MDC) and microtubule-associated protein 1 light chain 3 (LC3) suggesting a role in autophagy (Gutierrez et al., 2004; Singh et al., 2006). Furthermore Irgb10 is targeted to the inclusions of *Chlamydia trachomatis* but not of *Chlamydia muridarum* in infected mouse fibroblasts (Coers et al., 2008).

To date it is not explicitly clear what mediates targeting of most of IRG proteins to the subcellular compartments. It has been reported that Irgm1 localises to Golgi via amphipathic helix α K (Martens et al., 2004; Tiwari et al., 2009) and myristoylation of Irga6 is partially dispensable for targeting to the ER but is required for efficient loading onto the *T. gondii* PV ((Martens et al., 2004; Papic et al., 2008) and unpublished data).

1.4.4 Roles of IRG proteins in immunity

IRG proteins have been implicated in resistance to various pathogens (Table 1) (Martens and Howard, 2006; Taylor, 2007). Mice, deficient in the following members of the family, were susceptible to distinct bacterial and protozoan pathogens: Irgm1 to *T. gondii* (Collazo et al., 2001), *Leishmania major* (Taylor, 2004), *Trypanosoma cruzi* (Santiago et al., 2005), *Listeria monocytogenes* (Collazo et al., 2001), *Mycobacterium tuberculosis* (MacMicking, Taylor, and McKinney, 2003), *Mycobacterium avium* (Feng et al., 2004), *Salmonella typhimurium* (Henry et al., 2007), *Chlamydia trachomatis* (Coers et al., 2008); Irgm3 to *T. gondii* (Taylor et al., 2000), *Leishmania major* (Taylor, 2004), *Chlamydia trachomatis* (Coers et al., 2008); Irgd to *T. gondii* (Collazo et al., 2001), Irgb10 to *Chlamydia trachomatis* (Bernstein-Hanley et al., 2006). In many cases loss of resistance to the parasites *in vivo* correlated with inability to control infection in cell culture. The role in cell-autonomous immunity

against the pathogens was demonstrated for Irgm1 (MacMicking, Taylor, and McKinney, 2003; Butcher et al., 2005a; Santiago et al., 2005; Coers et al., 2008), Irgm2 (Miyairi et al., 2007), Irgm3 (Butcher et al., 2005a; Ling et al., 2006; Coers et al., 2008), Irga6 (Martens et al., 2005; Nelson et al., 2005), Irgb6 (Zhao et al., 2009b) and Irgd (Koga et al., 2006).

IRG protein standard/ original designation	Defined role in host resistance		
	<i>In vivo</i>	In cultured cells	Possible mechanism(s)
Irgm1/LRG-47	<i>T. gondii</i> (Collazo et al., 2001), <i>L. major</i> , <i>T. cruzi</i> (Santiago et al., 2005), <i>L. monocytogenes</i> (Collazo et al., 2001), <i>M. tuberculosis</i> (MacMicking et al., 2003), <i>M. avium</i> (Feng et al., 2004), <i>S. typhimurium</i>	<i>T. gondii</i> (Butcher et al., 2005), <i>T. cruzi</i> (Santiago et al., 2005), <i>M. tuberculosis</i> (MacMicking et al., 2003), <i>S. typhimurium</i>	Lysosome fusion (MacMicking et al., 2003), autophagy (Gutierrez et al., 2004), haematopoiesis
Irgm3/IGTP	<i>T. gondii</i> (Taylor et al., 2000), <i>L. major</i>	<i>T. gondii</i> (Ling et al., 2006; Butcher et al., 2005), <i>C. trachomatis</i> (Bernstein-Hanley et al., 2006)	Vacuole vesiculation (Ling et al., 2006), lysosome fusion (Ling et al., 2006), autophagy (Ling et al., 2006)
Irga6/IIGP1		<i>T. gondii</i> (Martens et al., 2004), <i>C. trachomatis</i> (Nelson et al., 2005)	Vacuole vesiculation (Martens et al., 2004), membrane trafficking (Nelson et al., 2005)
Irgd/IRG-47 Irgb10	<i>T. gondii</i> (chronic) (Collazo et al., 2001)	<i>T. cruzi</i> (Koga et al., 2006) <i>C. trachomatis</i> (Bernstein-Hanley et al., 2006)	

Table 1 Summary of the evidence supporting the role of IRG proteins in host resistance (Taylor, 2007).

Several models of the mechanism of IRG protein function in elimination of intracellular parasites have been proposed (Martens and Howard, 2006; Taylor, 2007): (1) disruption of the pathogen containing vacuoles, in a manner similar to the vesiculating action of dynamins, which leads to death of the enclosed parasite (Martens et al., 2005; Ling et al., 2006; Melzer et al., 2008; Zhao et al., 2009b); (2) initiation of autophagy, which either directly kills or disposes of the already dead parasite following disruption of the parasite-containing vacuole (Ling et al., 2006); (3) maturation of the pathogen-containing vacuoles via promotion of acidification (MacMicking, Taylor, and McKinney, 2003; Shenoy et al., 2007); (4) direct stimulation of autophagy of the pathogenic vacuoles followed by fusion with the lysosomal compartment for degradation (Gutierrez et al., 2004; Deretic, 2005). Additionally, IRG proteins were proposed to regulate haematopoiesis (Feng et al., 2004; Feng et al., 2008a), macrophage motility (Henry et al., 2007; Henry et al., 2010) and antigen presentation (Bougneres et al., 2009), however, it is currently unclear how these processes are affected by the absence of single IRG GTPases and therefore these hypotheses require deeper analysis (Hunn and Howard, 2010). Recent genome-wide association studies in humans have linked sequence polymorphism of

the human IRGM locus with increased risk for Crohn's disease (Parkes et al., 2007; Fisher et al., 2008). Overexpression of *Irgb6* and *Irgm2* in various cellular systems has suggested anti-viral function of the proteins in combating VSV virus (Carlow, Teh, and Teh, 1998) and coxsackie virus (Zhang et al., 2003), respectively.

1.5 *Toxoplasma gondii* as a model pathogen to study human and mouse cell-autonomous response

T. gondii is an obligate protozoan parasite assigned to the phylum Apicomplexa along with the causative agents of malaria (Dubey, 1977). Infections in humans are typically asymptomatic but may be lethal for immunocompromised individuals (Frenkel, 1988; Luft and Remington, 1988) and can lead to severe congenital defects during pregnancy (Wilson et al., 1980). In organisms with a healthy immune system *T. gondii* avoids complete elimination by entering the dormant state (cysts) in tissues like brain and muscles where it waits to be reactivated. The parasite has a complex life cycle (Figure 4).

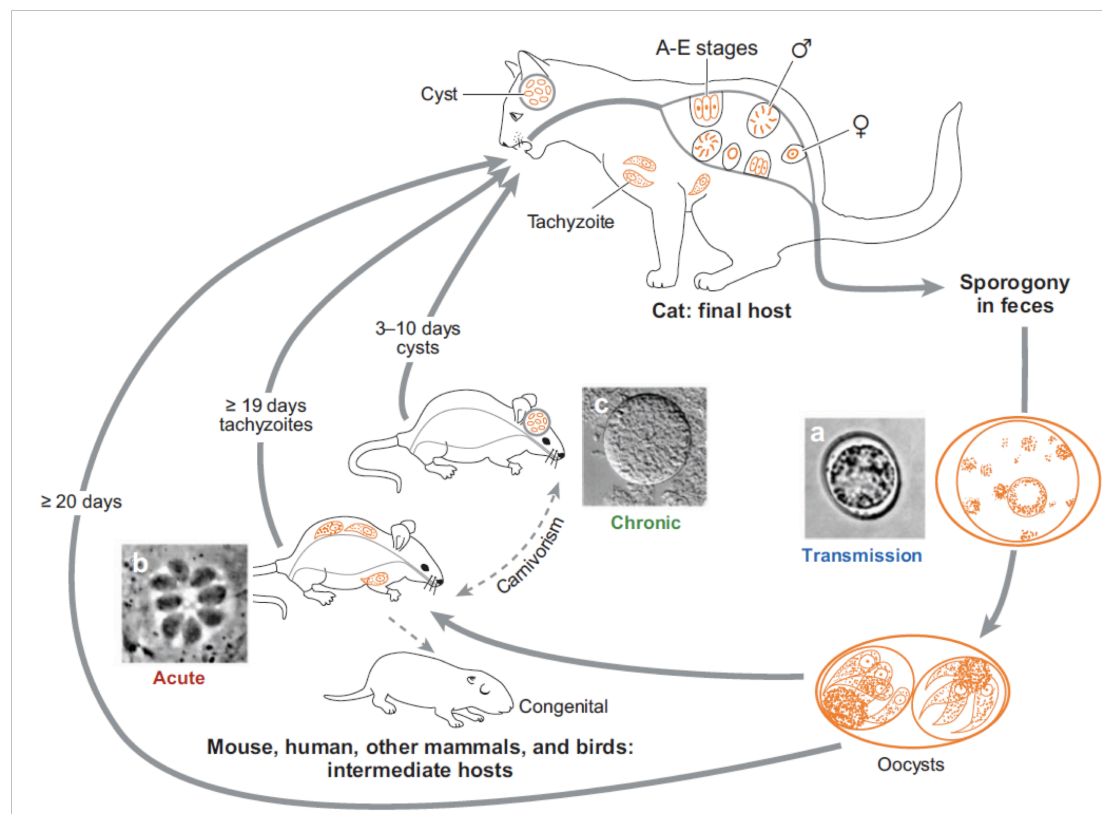


Figure 4 Life cycle of *Toxoplasma gondii*, depicting stages and modes of transmission of the parasite.

Members of the cat family serve as definitive hosts, and sexual development only occurs within the small intestine, where micro- and macrogametes form within enterocytes following a round of mitotic replication (A-E stages). Fusion of the gametes yields a diploid zygote that is shed as a resistant spore (oocyst) in the feces. Meiosis occurs within the environment, yielding eight haploid progeny.

Transmission (image *a* shows an unsporulated oocyst) occurs when oocysts contaminate food or water. Ingestion by a variety of warm-blooded hosts leads to acute infection, typified by fast-growing tachyzoites (image *b* shows a single vacuole with eight haploid parasites). Development of tissue cysts results in long-lasting chronic infection (image *c* shows a tissue cyst from mouse brain), which can also be transmitted by carnivorous feeding or scavenging (Sibley and Ajioka, 2008).

Acute toxoplasmosis is marked by rapid replication of tachyzoites in any infected non-feline vertebrate host. As mentioned above, the immune system attempts to eliminate infection, and this causes the pathogen to convert into the persistent state, called bradyzoite. Sexual stage of the cycle occurs in the members of Felidae (definitive host). Ingested by cats, bradyzoites infect intestinal epithelial cells and proceed through the stages of gametogenesis, gamete fusion and mitotic division to give rise to oocysts, each containing 8 sporozoites. These are distributed in the environment in the faeces. When eaten by any vertebrate, oocysts or bradyzoites turn into tachyzoites to multiply and disseminate throughout the host (Pfefferkorn, 1990).

T. gondii is able to infect virtually all nucleated cells. The process of infection involves attachment of the parasite onto the cell surface followed by active penetration driven by a motility system present in the pathogen (Figure 5) (Joiner et al., 1990; Joiner and Dubremetz, 1993; Dobrowolski and Sibley, 1997).

Invading parasites become covered and eventually enclosed by the host plasma membrane, which forms the parasitophorous vacuole membrane (PVM) (Suss-Toby, Zimmerberg, and Ward, 1996). Secretory organelles, micronemes, rhoptries and dense granules are sequentially secreted at consecutive steps during invasion to ensure successful establishment of the intracellular niche (Dubremetz et al., 1993; Dubremetz and Schwartzman, 1993; Carruthers and Sibley, 1997). The PVM is largely devoid of host cell proteins which are actively excluded by the parasite to render the organelle nonfusogenic with the lysosomal compartment of the cell (Sibley, Weidner, and Krahenbuhl, 1985; Joiner et al., 1990; Dubremetz and Schwartzman, 1993; Mordue et al., 1999). Furthermore, the PVM mediates interaction with endoplasmic reticulum and mitochondria (Sinai, Webster, and Joiner, 1997). Thus, survival and multiplication of *T. gondii* strictly depends on the PV, isolating the parasite from the cytosolic environment and mediating nutrient acquisition (Moulder, 1985; Pfefferkorn, 1990; Schwab, Beckers, and Joiner, 1994).

The outcome of infection in mice, the major intermediate host, is dependent on virulence of the infecting *T. gondii*. Phylogenetic analysis of the North American and European *T. gondii* isolates initially grouped the parasites into 3 clonal lineages: type

I, type II and type III (Howe and Sibley, 1995; Su et al., 2003; Sibley and Ajioka, 2008). However, the genetic diversity of the parasite populations proved to be much greater, in particular after isolation of the South American *T. gondii* strains (Lehmann et al., 2006; Khan et al., 2007; Sibley and Ajioka, 2008). Genetically different strains displayed distinct virulence phenotypes, primarily measured by the amount of tachyzoites required to kill laboratory mice. Type I *T. gondii* strains are acutely virulent with 100% lethality following infection with a single parasite (LD_{100} 1) whereas type II and type III strains have been designated as avirulent (LD_{50} 10^4 - 10^5) (Sibley and Boothroyd, 1992; Saeij, Boyle, and Boothroyd, 2005). Several rhoptry proteins, ROP5, ROP16 and ROP18, secreted upon invasion into the host cell, have been found to be major virulence determinants of *T. gondii*. The precise functions and mechanisms of action of these virulence factors are still under debate (El Hajj et al., 2006; Taylor et al., 2006; Saeij et al., 2006; El Hajj et al., 2007; Saeij et al., 2007).

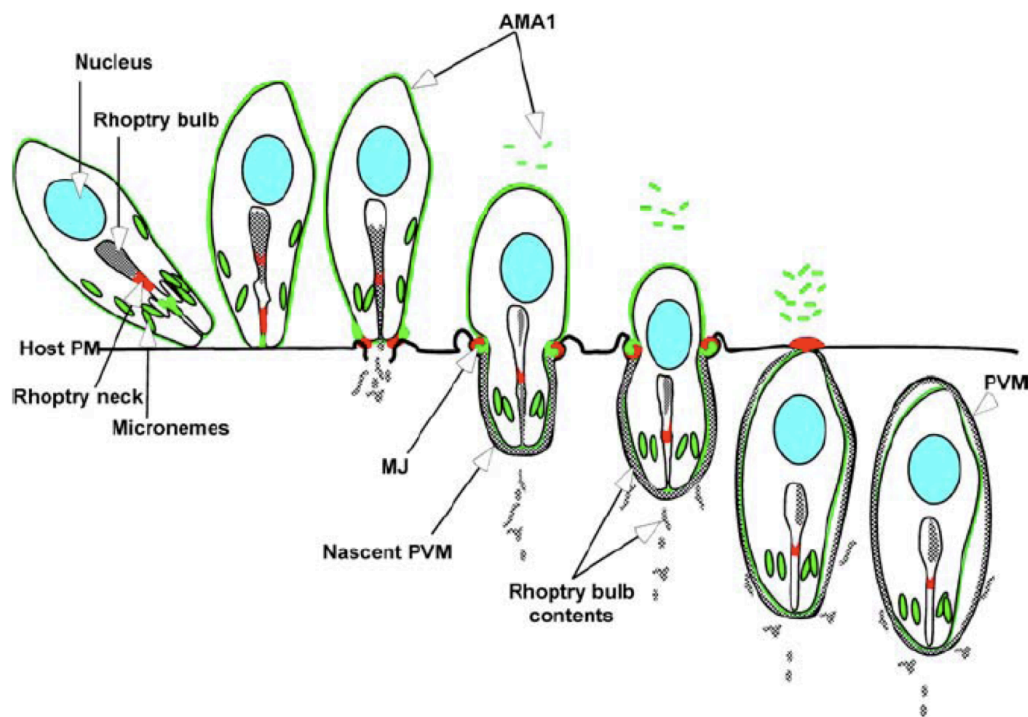


Figure 5 Schematic representation of host cell infection with *T. gondii*.

Attachment of the parasite to the cell surface and secretion of the microneme content (proteins essential for invasion, e.g. TgAMA1 (green)) form the moving junction (MJ) that begins at the anterior end of the parasite and then migrates posteriorly. Rhoptries are then discharged to deliver other essential components of the invasion system into the host cell (RON and ROP proteins). The resulting invagination of host plasma membrane creates a parasitophorous vacuole membrane (PVM) that completely envelops intracellular parasite (Alexander et al., 2005).

$IFN\gamma$ is indispensable for survival of mice during infection with *T. gondii*

(Remington and Merigan, 1968; Suzuki et al., 1988; Schariton-Kersten et al., 1996). Recognition of *T. gondii*-associated molecular patterns triggers IL-12 production by dendritic cells, neutrophils and macrophages (Johnson and Sayles, 1997; Scanga et al., 2002; Aliberti et al., 2003; Sher et al., 2003; Yarovinsky and Sher, 2006). IL-12, in turn, stimulates IFN γ secretion by T- and NK cells to activate an immune response to the parasite (Gazzinelli et al., 1994a; Gazzinelli et al., 1994b; Hunter et al., 1995; Denkers, 2003). In a STAT1-dependent manner IFN γ regulates cell-autonomous immunity to *T. gondii* by upregulating cellular concentrations of resistance proteins (Boehm et al., 1998; Collazo et al., 2002). To date, in mouse system, several IRG proteins (Irgm1, Irgm3, Irga6, Irgb6 and Irgd) have been implicated in resistance to *T. gondii*, analysed *in vivo* and in cell culture (Martens and Howard, 2006; Taylor, 2007). In IFN γ -stimulated mouse cells, IRG proteins bind to the PV and actively participate in its disruption, presumably by vesiculation of the vacuolar membrane. This leads to demise of the parasite and necrotic death of the infected cell (Martens et al., 2005; Melzer et al., 2008; Zhao et al., 2009b). It was also proposed that, in activated macrophages, disruption of the *T. gondii* PVM mediates recognition of the parasite by the autophagic machinery resulting in killing or degrading of already dead pathogens in infected cells (Ling et al., 2006). In another report a toxoplasmacidal effect was achieved independently of IFN γ by autophagy-mediated fusion of PVs with lysosomes in CD40-induced macrophages (Andrade et al., 2006; Subauste and Wessendarp, 2006). However, this paradigm has later been confronted by the group of Yap in the report that emphasized the primary role of IFN γ in resistance to *T. gondii* (Zhao et al., 2007).

Association of IRG proteins with *T. gondii* PVs appears to be crucial in IFN γ -mediated parasite elimination but till now the process of protein loading onto the parasite-containing vacuoles has not been subjected to comprehensive analysis.

In contrast to mouse, in human cells resistance to the parasite has been considered essentially dependent on tryptophan depletion by IDO since growth of *T. gondii* could be completely restored by addition of excess tryptophan to the cells or by pharmacological IDO inhibition prior to infection (Pfefferkorn, 1984; Habara-Ohkubo et al., 1993; Daubener et al., 2001; Bekpen et al., 2005; Könen-Waisman and Howard, 2007; Heseler et al., 2008). However, in human endothelial cells and macrophages *T. gondii* growth restriction has been shown to be mediated independently of IDO via

unclarified mechanisms (Woodman, Dimier, and Bout, 1991; MacKenzie et al., 1999). It was also reported that human leukocytes could spontaneously eliminate *T. gondii* by phagocytosis of the viable parasites (Wilson and Remington, 1979). Oxygen and nitrogen species (Murray and Cohn, 1979; Adams et al., 1990; Aline, Bout, and Dimier-Poisson, 2002) and iron depletion (Dimier and Bout, 1998) are the other mechanisms that could contribute to resistance to *T. gondii*.

T. gondii interferes with the immune response at nearly every step of development of resistance to infection (Lang et al., 2006; Plattner and Soldati-Favre, 2008). Infection by the parasite is associated with dysregulation and decreased production of the major proinflammatory cytokines IL-12 and IFN γ (Butcher et al., 2001; Sher et al., 2003; Butcher et al., 2005b; Lee et al., 2008); *T. gondii* also triggers generation of anti-inflammatory cytokines, such as IL-10, TGF- β to antagonize the IL-12/IFN γ -mediated Th1 response (Bermudez, Covaro, and Remington, 1993; Khan et al., 1997; Langermans et al., 2001; Yamamoto et al., 2009). It has been reported that infection with the parasite blocks translocation of STAT1 into the nucleus (Luder et al., 2001), modifies NF κ B (Gazzinelli et al., 1996; Butcher and Denkers, 2002; Denkers, 2003; Molestina and Sinai, 2005a; Molestina and Sinai, 2005b; Shapira et al., 2005) and PI3 kinase signaling (Kim and Denkers, 2006), protects the cells from apoptosis (Goebel, Gross, and Luder, 2001; Keller et al., 2006; Carmen and Sinai, 2007), inhibits production of reactive nitrogen and oxygen species (Luder et al., 2003; Ding et al., 2004; Denkers and Butcher, 2005) and impede antigen presentation (Luder et al., 1998; McKee et al., 2004). Finally, it was suggested that virulent *T. gondii* strains were able to attenuate the immune response by interfering with the process of IRG protein loading onto the PV (Hunn, 2007; Zhao et al., 2008; Zhao et al., 2009a; Zhao et al., 2009c; Khaminets et al., 2010).

1.6 Aims of the study

Experiments in mice and cell culture demonstrated that IRG proteins are the key factors mediating IFN γ -regulated resistance to *T. gondii* (Martens and Howard, 2006; Taylor, 2007). At the single-cell level IRG proteins accumulate on the parasite-containing vacuoles and participate in disruption of the PVM leading to elimination of the pathogen and necrotic death of the cell (Martens et al., 2005; Ling et al., 2006; Melzer et al., 2008; Zhao et al., 2008; Zhao et al., 2009b). Therefore, association of

IRG GTPases with *T. gondii* PVs appears to be central in resistance to the parasite in cells and determines the outcome of the infection *in vivo*. Despite the fundamental importance of the process to date there has been a gap of knowledge in understanding various aspects of the mechanism of vacuolar loading.

In the first part of this work I attempt to document the dynamics of the process of multiple IRG protein loading onto *T. gondii* PVs; to understand if the process of GTPase association with the vacuoles is carried out in passive or active fashion; to analyse loading of IRG proteins onto the vacuoles of *T. gondii* strains of different virulence and to study the involvement of host cell autophagic regulator Atg5 and major *T. gondii* virulence determinants ROP5, ROP16 and ROP18 in the process of loading. In addition, using various cellular models displaying deficiency in the process of loading I set out to provide the evidence linking IRG protein association with *T. gondii* PVs to elimination of the parasite in infected IFN γ -stimulated cells.

Tryptophan depletion by IDO has been reported to play a pivotal role in restricting *T. gondii* growth in IFN γ -stimulated human cells (Pfefferkorn, 1984; Daubener et al., 2001). However, based on published data (Woodman, Dimier, and Bout, 1991; MacKenzie et al., 1999) and knowledge of the colossal variability of IFN γ -mediated programs (Boehm et al., 1997; Schroder et al., 2004; Borden et al., 2007), alternative mechanisms of resistance to *T. gondii* are conceivable, providing the impetus for further research.

In the second part of this study the possible existence of an IDO-independent immunity mechanism to *T. gondii* functioning in human cells is tested. Furthermore, to get an insight into the IDO-independent mechanisms in human cells I envisage and test a two-step scenario documented for the mouse system (Zhao et al., 2009b): disruption of the parasite-containing vacuole followed by the death of infected cell.

2 Material and Methods

2.1 Reagents and cells

2.1.1 *Chemicals, reagents and accessories*

All chemicals were purchased from Aldrich (Steinheim), Amersham-Pharmacia (Freiburg), Applichem (Darmstadt), Baker (Deventer, Netherlands), Boehringer Mannheim (Mannheim), Fluka (Neu-Ulm), GERBU (Gaiberg), Merck (Darmstadt), Pharma-Waldhof (Düsseldorf), Qiagen (Hilden), Riedel de Haen (Seelze), Roth (Karlsruhe), Serva (Heidelberg), Sigma-Aldrich (Deisenhofen) or ICN biochemicals, Oxoid, (Hampshire UK). Developing and fixing solutions for Western Blot detection were from Amersham Pharmacia (Freiburg), Luminol from Sigma Aldrich (Deisenhofen), Coumaric acid from Fluka (Neu-Ulm). Deionised and sterile water (Seral TM) was used for all the buffers and solutions, ultra pure water derived from Beta 75/delta UV/UF from USF Seral Reinstwassersysteme GmbH, (Baumbach) equipped with UV (185/254 nm) and ultrafiltration (5x10³ kDa cut off), or from Milli-QSynthesis (Millipore).

2.1.2 *Equipment*

Centrifuges used were: Biofuge 13, Heraeus; Sigma 204; Sigma 3K10; Labofuge 400R, Heraeus; Sorvall RC-5B, Du Pont instruments; Optima TLX Ultracentrifuge, Beckmann and Avanti J-20 XP, Beckman. BioRAD Gel dryer, Model-583; BioRad Power pack 300 or 3000; electrophoresis chambers from FMC Bioproducts (Rockland Maine US); Gel Electrophoresis Chamber, Cambridge electrophoresis; Biorad Mini Protean II; PTC-100, MJ Research Inc.; ÄKTA P-920, OPC-900, Frac-950, Amersham; Centrifuge tubes 15ml, TPP Switzerland; 50ml Falcon, BectonDickenson; Zeiss AxioPlan II microscope equipped with AxioCam MRm camera (Zeiss); Zeiss Axiovert 200M motorized microscope equipped with AxioCam MRm camera (Zeiss). ELISA reader (Vmax, Molecular Devices), Harvester Filtermate 196 (Packard), Direct Beta Counter Matrix 9600 (Packard), Typhoon TRIO Variable Mode Imager (GE Healthcare).

2.1.3 *Materials*

Sterile filters FP 030/3 0.2 µm and ME 24 0.2 µm (Schleicher und Schüll, Dassel); Nitrocellulose transfer membrane PROTRAN (Schleicher und Schüll, Dassel); 3MM

Whatmann Paper (purchased via LaboMedic); 100 Sterican 0.50 x 16 mm hypodermic needles (Braun AG, Melsungen); 0.2 μm and 0.45 μm sterile filters (Schleicher und Schuell, Dassel); X-OMAT LS and AR X-ray films, Kodak. All plastic ware for cell culture was from Sarstedt (Nuümbrecht) or Greiner (Solingen), Glass Fiber Filters (Packard 6005412, Groningen, Netherlands), phosphorimaging plates (BAS-1000, FUJIFILM Europe GmbH), staurosporine (STO, Sigma).

2.1.4 Enzymes and proteins

Restriction enzymes (New England Biolabs); *Pyrococcus furiosus* (Pfu) DNA Polymerase (Promega, Mannheim); T4 DNA ligase (New England Biolabs); RNase A (Sigma); shrimp alkaline phosphatase (SAP) (USB, Amersham); PageRuler™ Prestained Protein Ladder (Fermentas); PageRuler™ Protein Ladder (Fermentas); SigmaMarker™ Wide Range (Sigma); GeneRuler™ DNA Ladder Mix (Fermentas).

2.1.5 Kits

Plasmid Maxi and Midi kit (Qiagen, Hilden), Terminator-cycle Sequencing kit version 3 (ABI), QuikChange™ Site directed mutagenesis kit (Stratagen), Rapid PCR product purification Kit (Roche, Mannheim).

2.1.6 Vectors and constructs used in the present study

pGW1H (British Biotech), pEGFP-N3 (Clontech), pmDsRed-N3, pCherry-N3 (both from (Zhao et al., 2009b)), pGW1H-Irga6-cTag1 (Papic et al., 2008), pGW1H-Irgb6-FLAG, pGW1H-Irgb6-K69A-FLAG and pGW1H-Irgd-ctag1 (all from (Hunn et al., 2008)).

2.1.7 Cell lines, bacterial and protozoan strains

Mouse embryonic fibroblasts (MEFs) derived from C57BL/6 mice, L929 (ATCC CCL-1), *Atg5*^{-/-} and the corresponding wt control immortalised mouse fibroblasts ((Kuma et al., 2004), kindly provided by Martin Krönke and Noboru Mizushima), *MyD88*^{-/-} MEFs ((Adachi et al., 1998), kindly provided by Manolis Pasparakis), human cervix carcinoma HeLa (ATCC CCL-2, kindly provided by Gerrit Praefcke), human embryonic kidney cell line HEK 293T (ATCC CRL-11268), human breast

adenocarcinoma MCF-7 (ATCC HTB-22, kindly provided by Hamid Kashkar) and human keratinocyte cell line HaCaT ((Boukamp et al., 1988), kindly provided by Dagmar Knebel-Mörsdorf) were cultured in DMEM (Gibco BRL and PAA) supplemented with 10% FCS (Biochrom AG, Berlin), 2 mM L-Glutamine, 1 mM sodium pyruvate, 1x non-essential amino acids, 100 U/ml penicillin and 100 µg/ml streptomycin (all from Gibco BRL). Human foreskin fibroblasts (Hs27, ATCC CRL-1634) and human skin fibroblasts (HSF, kindly provided by Günter Schwarz) were cultured in IMDM (Gibco or PAA) supplemented with 5% FCS and 2 mM L-glutamine. Human lymphoma U937 (ATCC CRL-1593, kindly provided by Hamid Kashkar) was cultured in RPMI 1640 (PAA) supplemented with 5% FCS and 2mM L-glutamine; cell line differentiation was induced by 48-h incubation with 100 nM PMA (phorbol-12-myristate-13-acetate, Sigma-Aldrich). Sterile trypsin/EDTA solution in PBS (10xtrypsin/ EDTA solution: 0.05% (w/v) trypsin (1:250, Gibco BRL)/ 17 mM EDTA/ 145 mM NaCl) was used to detach adherent cells from culture flasks.

Escherichia coli DH5 α : 80dlacZ Δ M15, recA1, endA1, gyrA96, thi-1, hsdR17 (rB-, mB+), supE44, relA1, deoR, Δ (lacZYA-argF)U169 was cultured in Luria Bertani (LB) medium: 10 grams bacto tryptone, 5 grams yeast extract, 10 grams NaCl, distilled water to 1L. LB plate medium: 10 grams bacto tryptone, 5 grams yeast extract, 10 grams NaCl, 15 grams agar, distilled water to 1L.

Toxoplasma gondii: type I strains RH (Lecomte et al., 1992), RH-YFP (Gubbels, Li, and Striepen, 2003), BK (Winsser, Verlinde, and et al., 1948), RH- Δ rop16 (kindly provided by John Boothroyd) in which the ROP16 locus has been deleted through double homologous recombination using HXGPRT for selection and PCR for confirmation of the deletion, as previously described (Saeij, Arrizabalaga, and Boothroyd, 2008); type II strains ME49 (Guo, Gross, and Johnson, 1997), NTE (Gross et al., 1991), Pru, expressing GFP ((Donald and Roos, 1998), kindly provided by Dominique Soldati-Favre); avirulent recombinant *T. gondii* strains S22 (Saeij et al., 2006), and S22-LC37 (both kindly provided by John Boothroyd and Jon Boyle), the latter harbouring a cosmid containing four ROP5 genes (ROP5A-D) along with two adjacent genes (annotated gene models TGME49_108070 and

TGME49_108060) from the RH strain and introduced using bleomycin selection.

2.1.8 Serological reagents

Primary antibodies and antisera are listed in Table 2.

name	immunogen	type	concentration and dilution	source
165	Recombinant Irga6	Rabbit polyclonal	IF1:8000 WB1:25000	(Martens et al., 2004)
10D7	Recombinant Irga6	Mouse monoclonal	4.3 mg/ml IF1:1000 WB1:2000	(Zerrahn et al., 2002; Papic et al., 2008)
10E7	Recombinant Irga6	Mouse monoclonal	3.7 mg/ml IF1:1000 WB1:2000	(Zerrahn et al., 2002; Papic et al., 2008)
A20	N-terminal peptide of mouse Irgb6	Goat polyclonal	IF1:100 WB1:500	Santa Cruz Biotechnology sc11079
B34	Recombinant Irgb6	Mouse monoclonal	3.4 mg/ml IF1:2000 WB1:4000	(Carlow, Teh, and Teh, 1998)
α -IGTP clone7	Mouse Irgm3 amino acids 283-423	Mouse monoclonal	0.25 mg/ml IF1:250 WB1:2000	BD Transduction Laboratories 610881
H53	Mouse Irgm2 N-terminal peptide MEEAVESPEVKEFEY	Rabbit polyclonal	IF1:500 WB1:1000	Eurogentec
L115	Mouse Irgm1 peptides QTGSSRLPEVSRSTE, NESLKNLSGVRDDD	Rabbit polyclonal	WB1:2000	Eurogentec

2078	Mouse Irgd peptides CKTPYQHPKYPKVIF, CDAKHLRLKIETVNVA	Rabbit polyclonal	WB1:1000	Eurogentec
2600	cTag1 peptide CLKLGRLERPHRD	Rabbit polyclonal	IF1:5000 WB1:12000	Eurogentec
M2	FLAG peptide DTKDDDDK	Mouse monoclonal	4.9 mg/ml IF1:4000	Sigma Aldrich
081	Recombinant Irgd	Rabbit polyclonal	IF1:8000	(Khaminets et al., 2010)
α - <i>Toxoplasma</i>	<i>T. gondii</i> (strain C56)	Rabbit polyclonal	IF1:1000	BioGenex
5-241-178 α -GRA7	<i>T. gondii</i> (strain TS4)	Mouse monoclonal	IF1:1000	(Bonhomme et al., 1998)
TxE2 α -GRA7	<i>T. gondii</i> (strain BK)	Mouse monoclonal	IF1:100	(Fischer et al., 1998)
SPA-865	Canine calnexin N-terminal peptide	Rabbit polyclonal	WB1:4000	StressGene
α -Cytochrome C	Rat cytochrome C	Mouse monoclonal	0.5 mg/ml IF1:1000	BD PharMingen 556432
α PARP1	Peptide corresponding to the caspase cleavage site	Rabbit polyclonal	WB1:1000	Cell Signaling Technology 9542
α HMGB1	C-terminal 150 amino acids of human HMGB1	Rabbit polyclonal	WB1:250	Abcam 18256
α -tubulin	Filaments from sea urchin sperm axonemes	Mouse monoclonal	2 mg/ml IF1:400	Sigma Aldrich T6074
BB2	Purified yeast virus-like particle MA-5620 (Ty1); recognizes the peptide EVHTNQDPLD	Mouse monoclonal	9.2 mg/ml IF1:2000	(Brookman et al., 1995; Bastin et al., 1996)

1D4B	Mouse LAMP1	Rat monoclonal	IF1:1000	DSHB, Iowa
α -Akt	C-terminal peptide of mouse Akt	Rabbit polyclonal	WB1:1000	Cell Signaling Technology 9272
a-phospho- Akt	Phosphopeptide surrounding Ser473 of mouse Akt	Rabbit polyclonal	WB1:1000	Cell Signaling Technology 9271

Table 2 Primary immunoreagents. (WB: Western blot; IF: immunofluorescence).

Secondary antibodies and antisera.

The following secondary immunoreagents were used: goat anti-mouse Alexa 488 and 546, goat anti-rabbit Alexa 488 and 546, goat anti-rat Alexa 555, donkey anti-rat Alexa 488, donkey anti-goat Alexa 350, 488, 546 and 647, donkey anti-mouse Alexa 488, 555 and 647, donkey anti-rabbit Alexa 488, 555 and 647 (Molecular Probes; all used 1:1000 for immunofluorescence). Donkey anti-rabbit HRP (Amersham), donkey anti-goat HRP (Santa Cruz) and goat anti-mouse HRP (PIERCE) (all horse radish peroxidase (HRP)-coupled sera were used 1:5000 for immunodetection of Western blots). 4', 6-Diamidino-2'-phenylindole dihydrochloride (DAPI, Invitrogen) was used for nuclear counterstaining at a final concentration of 0.5 μ g/ml.

2.2 Molecular Biology

2.2.1 Agarose gel electrophoresis

DNA was analysed by agarose gel electrophoresis (1x TAE; 0.04 M Tris, 0.5 mM EDTA, pH adjusted to 7.5 with acetic acid). The DNA was stained with ethidium bromide (0.3 μ g/ml), a fluorescent dye which intercalates between nucleotide bases, and the migration of the DNA molecules was visualized using bromophenol blue.

2.2.2 Generation of the expression constructs

pmDsRed-N3-Irgb6-FLAG was made via PCR amplification of Irgb6-FLAG from pGW1H-Irgb6-FLAG construct using primers listed below and insertion into pmDsRed-N3 following Sall digestion.

forward 5'-ccccccccgtcgaccaccatggcttggcctccagc-3'

reverse 5'-ccccccccgctgaccttgatcgtcgtccttgtaatc-3'

pEGFP-N3-Irgb6-FLAG was generated by subcloning Irgb6-FLAG fragment from pmDsRed-N3-Irgb6-FLAG into pEGFP-N3 (Clontech) using Sall digestion.

pmCherry-N3-Irgd-cTag1 was generated by PCR amplification of Irgd-cTag1 from pGW1H-Irgd-cTag1 using primers listed below and by cloning it into pmCherry-N3

forward 5'-ccccccgctgaccaccatggatcagttcatctcagcc-3'

reverse 5'-ccccccgctgacgtcacgatgcgccgctcgagtcgg-3'

pGW1H-unROP18 ME49 and pGW1H-unROP18 RH-YFP containing the unprocessed forms of ROP18 were generated by PCR amplification from the template genomic DNA of ME49 (cell lysate) and RH-YFP *T. gondii* strains using primers listed below and subsequent cloning into the Sall site of pGW1H (British Biotech).

forward 5'-ccccccgctgaccaccatgttttcggtacagcggcc -3'

reverse 5'-ccccccgctgacttagtcaagtggatcctggttagtagtgacaccttctgtgtggagatgttctgc-3'

The C-terminally Ty-tagged mature forms of ROP18 were amplified from pGW1H-unROP18 ME49 and pGW1H-unROP18 RH-YFP using primers listed below and cloned into pGW1H by Sall digestion.

forward 5'-ccccccgctgaccaccatggaaaggctcaacaccgggta-3'

reverse 5'-ccccccgctgacttagtcaagtggatcctggttagtagtgacaccttctgtgtggagatgttctgc-3'

Following mutations were introduced in pGW1H-Irga6-cTag1 construct by site-directed mutagenesis using a pair of specific primers; 5'- 3' sequences of the forward primers are listed below; 5'- 3' sequences of backward primers are equivalent to reverse complement sequences of forward primers.

E77A 5'- gctcaatgttgctgtcaccggggcgacgggatcaggggaagtcc - 3'

G103R 5'- ggaatgaagaagaaggtgcagctaaaactagggtggtggaggtaacatggaaagacatc - 3'

S132R 5'- gggacctgcctgggattggaaggacaaattcccacaaac - 3'

R159E 5'- cattattatttcggccacagaattcaagaaaaatgatatag - 3'

K161E 5'- cggccacacgcttcgagaaaaatgatatagac - 3'

K162E 5'- gccacacgcttcaaggaaaatgatatagacattgc - 3'
D164A 5'- cggccacacgcttcaagaaaaatgctatagacattgccaaagcaatcagc - 3'
E106R 5'- gctaaaactggggtggtgctgggtaaccatggaaag - 3'
K196D 5'- gaagcagatggcgaccctcaaacctttgac - 3'
R31E-K32E 5'- gggtattttaagaaatataacgggagaagaaatcatttctcaagagatcctcaatttg - 3'
K169E 5'- gaaaaatgatatagacattgccgaagcaatcagcatgatg - 3'
K176E 5'- gcaatcagcatgatgaaggaggaattctacttcgtg - 3'
R210E 5'- gacaaagaaaaggctctgcaggacatcgagcttaactgtgtgaacacctttaggg - 3'
K246E 5'- ctatgactccccgctctgatggacgagctgataagtaccccttatctac - 3'

2.2.3 Cloning of PCR amplification products

Amplified PCR products were purified using the rapid PCR purification Kit (Roche) and eluted with 100 µl 10 mM Tris, pH 8.5. DNA yield was monitored by agarose gel electrophoresis and DNA fragments were digested with the appropriate restriction endonuclease (New England Biolabs) according to the suppliers' protocol. Restriction enzymes were used at a 5-10 fold over-digestion. Following restriction, DNA fragments were again column purified using the rapid PCR purification Kit (Roche) and DNA yield was monitored by agarose gel electrophoresis.

2.2.4 Purification of DNA fragments from agarose gels

DNA fragments were loaded on agarose gels after incubation with appropriate restriction endonucleases. After proper separation of the fragments, DNA was visualized under a low energy UV source and cut out of the gel using a clean blade. DNA fragments were eluted from the gel with the rapid PCR purification Kit (Roche) according to the manufactures protocol. Purity and yield of the DNA was determined by agarose gel electrophoresis and UV spectroscopy.

2.2.5 Ligation

The appropriate cloning vector was cut with the respective restriction enzyme(s) (10 U/ 1 µg DNA) for 1 h according to the restriction enzyme suppliers' protocol. Subsequently, the same amount of restriction enzyme and 0.1 U of shrimp alkaline phosphatase were added to the reaction followed by 1.5-h incubation. Following restriction, DNA fragments were column purified using the rapid PCR purification

Kit (Roche) and DNA yield was monitored by agarose gel electrophoresis. Vector and the appropriate insert were mixed at a ratio of 1:3 and ligated with T4-DNA ligase in a total volume of 10 μ l at 16°C over-night according to the manufactures protocol. As control, the same reaction without insert was carried out which should not yield any colonies after transformation into competent DH5 α .

2.2.6 Preparation of competent cells

A single colony from a particular *E. coli* strain was grown over-night in 2 ml LB medium with 0.02 M MgSO₄/ 0.01 M KCl with vigorous shaking (~300 rpm). It was then diluted 1:10 into fresh medium with the same constituents and grown for 90 min, at 37°C to an OD₆₀₀ of 0.45. Cultures were incubated on ice for 10 min after which the cells were pelleted by centrifugation at 4000 g at 4°C for 5 min. Cells were resuspended in TFB I (30 ml/ 100 ml culture), incubated 5 min on ice, pelleted again by centrifugation at 4000 g at 4°C for 5 min and finally resuspended in TFB II (4 ml per 100 ml culture). 100 μ l aliquots of the competent bacteria were frozen at -80°C.

Composition of the buffers:

TFB I (30 mM KOAc/ 50 mM MnCl₂/ 100 mM RbCl₂/ 10 mM CaCl₂/ 15% w/v glycerin, pH 5.8)

TFBII (10 mM MOPS, pH 7.5/ 75 mM CaCl₂/ 100 mM RbCl₂/ 15% w/v glycerin)

Solutions were sterilized and stored at 4°C.

2.2.7 Transformation of competent bacteria

100 μ l of competent bacteria were thawed on ice and gently mixed 3-4 times. 5 μ l of the ligation reaction was added to the cells followed by incubation for 20 min on ice. Cells were then heat-shocked for 45 sec at 42°C followed by a further incubation on ice for 2 min. Antibiotic free LB medium was added to a total volume of 1 ml and cells were rolled at 37°C for 1 h. The culture was spun at 8000 g for 2 min and 800 μ l of the supernatant was removed. The cell pellet was resuspended in the remaining 200 μ l medium in the 1.5 ml reaction tube and plated on a LB agar plate supplemented with the appropriate antibiotics.

2.2.8 Plasmid isolation

For screening a large number of cultures for clones containing the desired insert, 4

ml LB cultures with the appropriate antibiotics were inoculated with single colonies picked from a ligation plate and grown over-night at 37°C, 100 g. All following steps were performed at room temperature. 1.5 ml of the cultures was transferred into a 1.5 ml reaction tube and pelleted by centrifugation at 23000 g for 5 min. The supernatant was discarded and pellet resuspended in 100 µl P1 (50 mM Tris, pH 8.0/ 10 mM EDTA/ 100µg/ml RNase A). After addition of 100 µl P2 (200mM NaOH/ 1% SDS) the reaction was gently mixed and incubated for 5 min. 140 µl of P3 (3M potassium acetate, pH 5.5) was added and the reaction was spun for 15 min at 23000 g. The supernatant (~340 µl) was transferred into a new tube and 700 µl of 100% ethanol was added. After mixing, the reaction was spun for 15 min at 23000 g and the supernatant was removed. The pellet was washed by addition of 700 µl of 70% ethanol and spun at 23000 g. After removal of the supernatant the pellet was air-dried and resuspended in 50 µl 10mM Tris pH 8.0. 5 µl of the plasmid preparation was cut with the appropriate restriction enzyme(s) in a total volume of 50 µl for 1 h and 10 µl of the reactions were subjected to agarose gel electrophoresis to identify insert-containing clones. For preparation of large amounts of plasmid, the Qiagen Midi and Maxi Plasmid Preparation Kits were used according to the manufactures instructions.

2.2.9 Determination of the concentration of DNA

The concentration of DNA was measured using a spectrophotometer at 260 nm. The purity of the DNA solution was determined using the ratio of OD readings at 260 nm and 280 nm. Pure preparations of DNA have an OD₂₆₀/OD₂₈₀ ratio of 1.8. The concentration was calculated according to the following equation. Conc. = A₂₆₀ x 50 µg/ml x dilution factor.

2.2.10 Site-directed mutagenesis

Site directed mutagenesis was carried out using a modified protocol supplied with “Quik-Change™ XL Site-Directed Mutagenesis” Kit from Stratagene. The amplification was carried out using 20 ng plasmid as template, 125 ng of the sense and antisense oligonucleotide as primers and 2.5 U of Pfu-polymerase (Promega) in a total volume of 50 µl. The following program was used: 1. 95°C, 30 sec; 2. 95°C, 30 sec; 3. 55°C, 60 sec; 4. 68°C, 15 to 20 min (back to step 2., 15 to 18 times); 5. 68°C, 15 min. After amplification 1 µl *DpnI* (20 U, New England Biolabs) was added to the

reaction and incubated for 1.5 h at 37°C. 5 µl of the reaction was used to transform 200 µl competent DH5α. As control the whole procedure was carried out without addition of Pfu-polymerase. Ideally no colonies are found on the final LB agar plate for the control reaction.

2.2.11 DNA sequencing

All constructs generated were verified by sequencing. DNA was sequenced using the *ABI Prism[®] BigDye[™] Terminator Cycle Sequencing Ready Reaction Kit* (PE Applied Biosystems), using fluorescently labeled dideoxynucleotides based on the dideoxy-chain termination. Template DNA (0.5 µg), the respective primer (10 pmole) and 2 µl *Big Dye[™] terminator ready reaction mix* (ABI) were combined in a total volume of 10 µl and the sequencing reaction was carried out as follows: 25x (96°C, 30 sec; 50°C, 15 sec; 60°C, 4 min). Sequencing was done on an automated sequencer (ABI 373A).

2.3 Cell biology

2.3.1 Transfection

Cells were transiently transfected for 24 h at 37°C using FuGENE 6 Transfection Reagent (Roche) according to the manufacturer's protocol with DNA (µg): FuGENE6 (µl) ratio 1:3. For transfection of cells in 6 well plates dish 1-2 µg of the plasmid DNA was used.

2.3.2 Immunocytochemistry

Cells were grown on coverslips, fixed with PBS/ 3% paraformaldehyde (PFA) for 20 min and subsequently washed three times with PBS. Cells were permeabilized with PBS/0.1% saponin (washing buffer) followed by a blocking step with PBS/0.1% saponin/1% BSA (fractionV, Roth) (blocking buffer) for 1 h. Coverslips were incubated with primary antibodies (diluted in blocking buffer) in a humid chamber for 1 h at RT and subsequently washed 3x 5 min with washing buffer. Incubation with secondary antibodies was done as described for primary antibodies for 30 min at RT and washed 3x as described above. Coverslips were mounted on slides with ProLong[®] Gold antifade reagent (Invitrogen), sealed with nail polish and cleaned with deionized water. DAPI, used to stain DNA (300 nM), was added to the secondary antibody

solution. Images were taken with a Zeiss Axioplan II fluorescence microscope equipped with an AxioCam MRm camera (Zeiss). Images were processed with Axiovision 4.6 software (Zeiss).

2.3.3 *In vitro* passage of *T. gondii*

Tachyzoites of various *T. gondii* strains were maintained by serial passage in confluent monolayer of human foreskin fibroblasts (Hs27, ATCC number CRL-1634). RH-YFP and Pru, expressing YFP, parasites were propagated in presence of chloramphenicol (3.2 µg/ml, Sigma-Aldrich); RH-Δrop16 was maintained in presence of mycophenolic acid (25 µg/ml, Sigma-Aldrich) and xanthine (50 µg/ml, Sigma-Aldrich). Extracellular parasites were harvested from the supernatant and purified from host cell debris by differential centrifugation (5 minutes at 100 g, 15 minutes at 500 g). The parasites were resuspended in medium, counted using a Neubauer chamber and immediately used for the infection of the host cells.

2.3.4 Infection of cells with *T. gondii* for immunocytochemistry

To assay IRG protein association with the *T. gondii* PV or other aspects of the cellular response to the parasite, cells were handled as described in each experiment. Tachyzoites, purified as described in section 2.3.3, were inoculated into the 1-2 ml of the medium contained in each well of 6-well plate. Parasites were sedimented by centrifugation of the plates for 2 min at 550 g. Whenever specified, after indicated infection time free parasites were removed by repeated washing with medium until no free parasites could be detected microscopically. Cells were subsequently washed with PBS and fixed in PBS/3% paraformaldehyde.

2.3.5 *T. gondii* lysis

Tachyzoites of ME49 and RH-YFP *T. gondii* strains were harvested, resuspended in PBS and inactivated by immediate freezing in dry ice. Samples were thawed and incubated with proteinase K (PTC-100, MJ Research, United States) (70 ng/µl) for 50 min at 55°C, followed by a proteinase K deactivation step for 10 min at 95°C. *T. gondii* lysates were further used for PCR (Müllenbeck, 2007).

2.3.6 Live cell imaging

The live cell imaging experiments were performed using μ -slide I (Ibidi, München). Cells were incubated in phenol-red-free DMEM supplemented with 10% FCS, 20 mM HEPES pH 7.4, 2 mM L-glutamine, 1 mM sodium pyruvate, 1x non-essential amino acids, 100 U/ml penicillin, and 100 μ g/ml streptomycin. 10000/100 μ l MEFs were seeded in the channel of the μ -slide I and 500 μ l medium was then added to each of the reservoirs. For transfection experiments, 1 μ g DNA/3 μ l Fugene6 in 100 μ l FCS-free medium was prepared and 50 μ l of the transfection reagent was added to the channel of one μ -slide I. The cells were simultaneously stimulated with 200 U/ml IFN γ for 24 h. To visualize mitochondria and lysosomes, IFN γ -stimulated cells were preloaded with 200 nM MitoTracker Red and 50 nM LysoTracker Red (both from Invitrogen), respectively, for 30 min and subsequently washed with the medium. After infection with *T. gondii*, the cells were observed under the Zeiss Axiovert 200M motorized microscope with the objective EC “Plan-Neofluar” 40°—/1.30 Oil Ph3 (Zeiss). The time-lapse images were obtained and processed by Axiovision 4.6 software (Zeiss).

2.3.7 Inhibition of signalling pathways and microtubule polymerisation

To block PI3 kinase and G protein-coupled receptors overnight FCS-starved C57BL/6 MEFs were pretreated with wortmannin (0.5 μ M), LY294002 (2-(4-morpholinyl)-8-phenyl-4H-1-benzopyran-4-one) (25 μ M) and pertussis toxin (200 ng/ml) for 6 h (all reagents were derived from Sigma-Aldrich and handled according to the manufacturers protocol). The extent of inhibition was tested by monitoring the level of phospho-Akt (pAkt) after 10 min stimulation with EGF (epidermal growth factor) (100 ng/ml) in Western blot (Peprotech). To block caspase activity MEFs were pretreated with z-VAD-fmk (benzyloxycarbonyl-Val-Ala-Asp fluoromethyl ketone) pan-caspase inhibitor (100 μ M) (Alexis Biochemicals, 260-020-M005) for 2 h and the degree of blockade was analysed by monitoring the processing of PARP1 (poly-ADP ribose polymerase 1) 6 h after TNF α (40 ng/ml) (Peprotech) plus cycloheximide (Chx) (10 μ g/ml) stimulation in Western blot. Inhibition of microtubule polymerisation was achieved by incubating MEFs in 10 μ M nocodazole in DMSO (Sigma-Aldrich) for 1 h and was monitored microscopically after performing immunostaining using anti- α -tubulin mouse monoclonal antibody.

2.3.8 Synchronisation of *T. gondii* infection

Toxoplasma infection of MEFs was synchronised as described previously (Kafsack, Beckers, and Carruthers, 2004; Kafsack, Carruthers, and Pineda, 2007). The parasites were resuspended to 5×10^6 parasites/ml in invasion non-permissive Endo buffer (44.7 mM K_2SO_4 / 10 mM $MgSO_4$ / 106 mM sucrose/ 5 mM glucose/ 20 mM Tris- H_2SO_4 / 3.5 mg/ml BSA, pH 8.2). 1 ml of tachyzoite suspension was added to each well on the 6-well plate, the plates centrifuged at 500 g for 2 min and then placed in the incubator. The infection was synchronised by replacing the Endo buffer by permissive medium (IMDM+10 mM HEPES buffer, pH 7.4, and 5% FCS) for 2 minutes. Free parasites were subsequently removed by repeated washing with medium until no free parasites could be detected microscopically. At various times after infection, cells were washed with PBS and fixed in PBS/3% paraformaldehyde. Non-synchronised cells were handled throughout the experiment in IMDM/5% FCS, parasites were added at time zero and the cells were examined at various times thereafter after washing and fixation.

2.3.9 *T. gondii* proliferation assay

3H -uracil incorporation assay was used to analyse growth of *T. gondii* (Pfefferkorn and Guyre, 1984). Human cells were seeded (in triplicates) in 96-well plates and induced for 24 h (or indicated periods of time) with $IFN\gamma$ (Peprotech, 200 U/ml unless specified). 1-methyl-tryptophan (1-MT) (1.5 mM, Sigma) was added to the cells to inhibit IDO at the time of $IFN\gamma$ stimulation. The culture medium was then supplemented with L-tryptophan (L-Trp) (0.5 mM, Sigma) and the cells were infected with *T. gondii* strain, resuspended in L-Trp-free DMEM (PAA), for the specified time at MOI 1 (calculated from the seeded amount of cells) unless noted. The cultures were further labelled with 0.3 μCi /well of 3H -uracil (3HU , Harmann Analytic) for 24 h and then frozen at $-20^\circ C$. The content of the thawed 96-well plates was harvested onto the Glass Fiber Filters (Packard). The amount of radioactivity incorporated into the proliferating parasites was determined in a β -scintillation spectrometer. The data is shown in radioactive counts, which are proportional to the parasite growth.

2.3.10 Quantification of IRG protein signal intensity at *T. gondii* PV

The signal intensities for the specific IRG proteins on the *T. gondii* parasitophorous vacuoles were quantified using the ImageJ software (rsb.info.nih.gov/ij/). The images are processed in 16-bit (Zeiss Axioplan II microscope) or 12 bit (Zeiss Axiovert 200M motorized microscope) gray-scale TIFF format. To measure the intensity of fluorescent signal on a labelled PVM, two lines were drawn at right angles across the long and short axes of the vacuole, and pixel intensity profiles obtained for each line (Figure 6). The first and last values for each line provided 4 estimates of “background” signal, while the 4 peaks where each line crossed the margins of the PVM gave 4 independent values for the signal strength at the vacuole. The signal intensity for the vacuole was given as the mean of the 4 peak values minus the mean of the 4 background values.

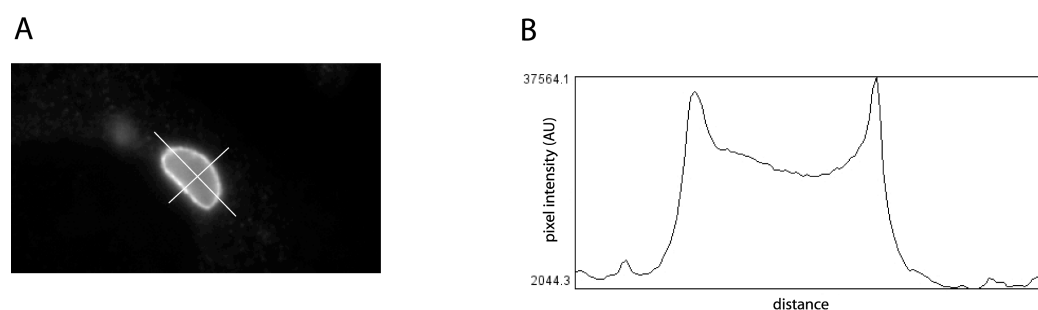


Figure 6 Analysis of IRG pixel intensity on *T. gondii* PVs.

To measure the intensity of IRG signal on *T. gondii* PVs two lines were drawn approximately at right angles across each vacuole (A). Each line thus crossed the “margin” of the vacuole twice, giving a total of 4 values for each vacuole using the Image J software. The pixel intensity of each vacuole was defined as the mean of these 4 values after background subtraction (B).

2.3.11 Western blotting

After SDS-PAGE, proteins were transferred to nitrocellulose transfer membranes (Schleicher&Schuell) by electroblotting. The gel was placed in contact to a nitrocellulose transfer membrane, and was sandwiched between four sheets of 3 mm Whatmann paper, two porous pads, and two plastic supports on either side, soaked in a transfer buffer containing 25 mM Tris/ 190 mM glycine. The sandwich was then placed between platinum plate electrodes, with the nitrocellulose membrane facing the anode, and the transfer was carried out at RT for 1 h with a current of 0.5 V. Ponceau S staining was used to visualize proteins (0.1% (w/v) Ponceau S (Sigma) in 5% (v/v) acetic acid) after Western blotting. Membranes were blocked with PBS/ 5% milk powder/ 0.1% Tween 20 or Western Blotting Blocking Reagent (Roche) at room temperature for 1 h or over-night at 4°C. Antisera/ antibodies were diluted in PBS/ 5% FCS/0.1% Tween 20 or PBS/ 5% Western Blotting Blocking Reagent. Bands

were visualized with enhanced chemiluminescence (ECL) substrate.

2.3.12 Colorimetric cell viability assay

Specified amounts of cells were seeded in 96-well plates and stimulated with IFN γ (200 U/ml) for the indicated periods of time. Whenever needed, 1-MT (1.5 mM) was added to the cells at the time of IFN γ stimulation or the medium was supplemented with L-Trp (0.5 mM) just before infection. The cells were then infected with *T. gondii* for the variable periods of time. The amount of viable cells was evaluated by the CellTiter 96 AQueous non-radioactive cell proliferation assay (Promega) according to the manufacturer's instructions. The absorption of the bio-reduced form (formazan) of a substrate (MTS) generated by metabolically active cells during incubation at 37°C for 2-4 h was measured in an ELISA reader (Molecular Devices) at 490 nm. The quantity of formazan product is directly proportional to the number of live cells in culture.

2.3.13 Propidium iodide staining

10⁵ Hs27 cells were seeded in 60 μ -Dishes (Ibidi, München) in phenol-red-free DMEM supplemented with 10% FCS, 20 mM HEPES pH 7.4, 2 mM L-glutamine, 1 mM sodium pyruvate, 1x non-essential amino acids, 100 U/ml penicillin, and 100 μ g/ml streptomycin and stimulated with 200 U/ml IFN γ for 72 h. Cell cultures were further supplemented with L-Tryptophan (0.5 mM) (Sigma) and then infected with ME49 *T. gondii* (at MOI 5), resuspended in L-Trp-free DMEM (PAA) for 24 h. Propidium iodide (1.5 mM) (Invitrogen) was added to the cells and after 15 min incubation the cells were observed under the Zeiss Axiovert 200M motorized microscope with the objective EC "A-Plan" 10°—/0.25 Ph1 (Zeiss). The images of random fields were obtained and processed by Axiovision 4.6 (Zeiss) and Image J (Wayne Rasband, NIH) software.

2.3.14 Pulse-chase analysis

Wt and Atg5^{-/-} fibroblasts (5x10⁵/dish) were seeded in 6 cm dishes and stimulated for 24 h with IFN γ (200 U/ml). The cells were then starved in methionine, serine and FCS-free DMEM (PAA) supplemented with 2 mM L-glutamine, 1 mM sodium pyruvate, 1x non-essential amino acids, 100 U/ml penicillin, and 100 μ g/ml

streptomycin for 1 h followed by the 1 h pulse with Met-³⁵S-label (containing ³⁵S-labelled L-Methionine, L-Serine and miscellaneous amino acids) (Hartmann Analytic). Cells were thoroughly washed and chased in complete DMEM containing 10% FCS, 2 mM L-glutamine, 1 mM sodium pyruvate, 1x non-essential amino acids, 100 U/ml penicillin and 100 µg/ml streptomycin for 24 h. The samples after 0, 1, 3, 6, 12, 24 h of chase were taken and subjected to Irgb6 immunoprecipitation, SDS-PAGE, and analysis by autoradiography. Evaluation of bands at each time point was conducted using phosphorimager plates (FUJIFILM), Typhoon scanner and ImageQuant software (Amersham).

2.3.15 Immunoprecipitation

Wt and Atg5^{-/-} fibroblasts (5x10⁵/6 cm dish) were washed with cold PBS and harvested by scraping. Cells were lysed in 500 µl of lysis buffer 0.5% NP-40/ 5 mM MgCl₂/ 20 mM Tris-HCl/ 140 mM NaCl “CompleteMini protease inhibitor cocktail without EDTA” (Roche) per sample by incubation for 1 h on ice. To the supernatants, collected after 18000 g 30 min spin (4°C), 2 ml of B34 mAb (3.4 mg/ml stock) were added; samples were rotated o/n at 4°C. 50 µl of wet Protein A Sepharose™ CL-4B (Amersham) bead suspension (25 ml of dry beads and 25 ml of to lysis buffer) were combined with each sample and further rotated at 4°C for 3 h. The beads were subsequently collected by 1 min centrifugation at 2000 g and washed 2 times in 1 ml 5 mM MgCl₂/ 20 mM Tris-HCl/ 140 mM NaCl. Finally, the beads were boiled for 2 min in 1x Sample buffer (80 mM Tris-HCl pH 6.8/ 5 mM EDTA/ 34% sucrose/ bromophenol blue/ 40 mM DTT); the buffer was then collected and subjected to SDS-PAGE.

3 Results I

3.1 Time-course of endogenous IRG protein loading onto avirulent ME49 *T. gondii* vacuoles in mouse fibroblasts

6 IRG proteins (Irgb6, Irgb10, Irga6, Irgd, Irgm2 and Irgm3) have been shown to associate with avirulent *T. gondii* PVM (Martens et al., 2005; Khaminets et al., 2010). In order to understand fully how IRG proteins load onto *T. gondii* vacuoles, the time course of avirulent ME49 *T. gondii* infection of MEFs was conducted. Cells were infected with the parasite for indicated periods of time, fixed and processed for immunofluorescence. To increase the sensitivity and thereby detect even a weak IRG protein signal on *T. gondii* PVs, samples were stained for both Irga6 and Irgb6 with immunoreagents detected by secondary antibodies coupled to the fluorochrome with the same emission spectrum. IRG (Irga6+Irgb6) positive PVs were enumerated from 1000 cells (judged by DAPI staining) and plotted as a percentage of maximum (Figure 7A). Strikingly, IRG positive vacuoles were already detected at 2.5 min after infection (pi or post infection, indicates the time after addition of parasites to the cultures). The numbers rose rapidly for 30-40 min before reaching a plateau at 60-120 min pi. Dynamics of loading of Irgb6 alone onto *T. gondii* ME49 PVs was analysed as a proportion of Irgb6 positive PVs to intracellular parasites (detected by the characteristic staining of *T. gondii* PV protein GRA7). The results (Figure 7B) are consistent with the kinetics of Irga6 and Irgb6 analysed together (Figure 7A), although it is evident that estimation of IRG positive PVs out of intracellular parasite gives a more accurate picture of the loading process. In particular, it was observed that some vacuoles failed to bind IRG proteins, demonstrating that the process of IRG association with *T. gondii* is not absolute and could perhaps be actively hampered.

The increase in frequency of IRG positive *T. gondii* vacuoles with infection time was accompanied by an increase in intensity of the protein signal on the PVs (Figure 7C and D) measured as described in Material and Methods. Remarkable heterogeneity of IRG protein signal intensity on *T. gondii* PVs was observed in each experiment (Figures 7C and D) with vacuoles spanning from almost completely unloaded (4×10^3 - 6×10^3 AU) to very intensely loaded with IRG proteins (4×10^4 - $6,5 \times 10^4$ AU). The heterogeneity was not merely a result of the technical failure to accurately measure the protein signal intensity but was indeed true heterogeneity (Khaminets et al., 2010), documenting one of the features of cellular behavior of IRG proteins in the context of

T. gondii infection. A possible explanation for the wide distribution of IRG protein vacuolar intensity would be asynchrony in infection (see results 3.2). To examine the impact of the delayed infection on the heterogeneity of IRG signal on *T. gondii* PVs, vigorous washing step was introduced after 15 min pi to get rid of free parasites. Another approach was synchronised infection (as described in Material and Methods) followed by vigorous washing as in the previous procedure. Figures 7C and D demonstrate that neither method eliminated the striking heterogeneity of IRG protein intensity on *T. gondii* PVs indicating that the loading process is also dependent on other factors, some of which are documented in this work.

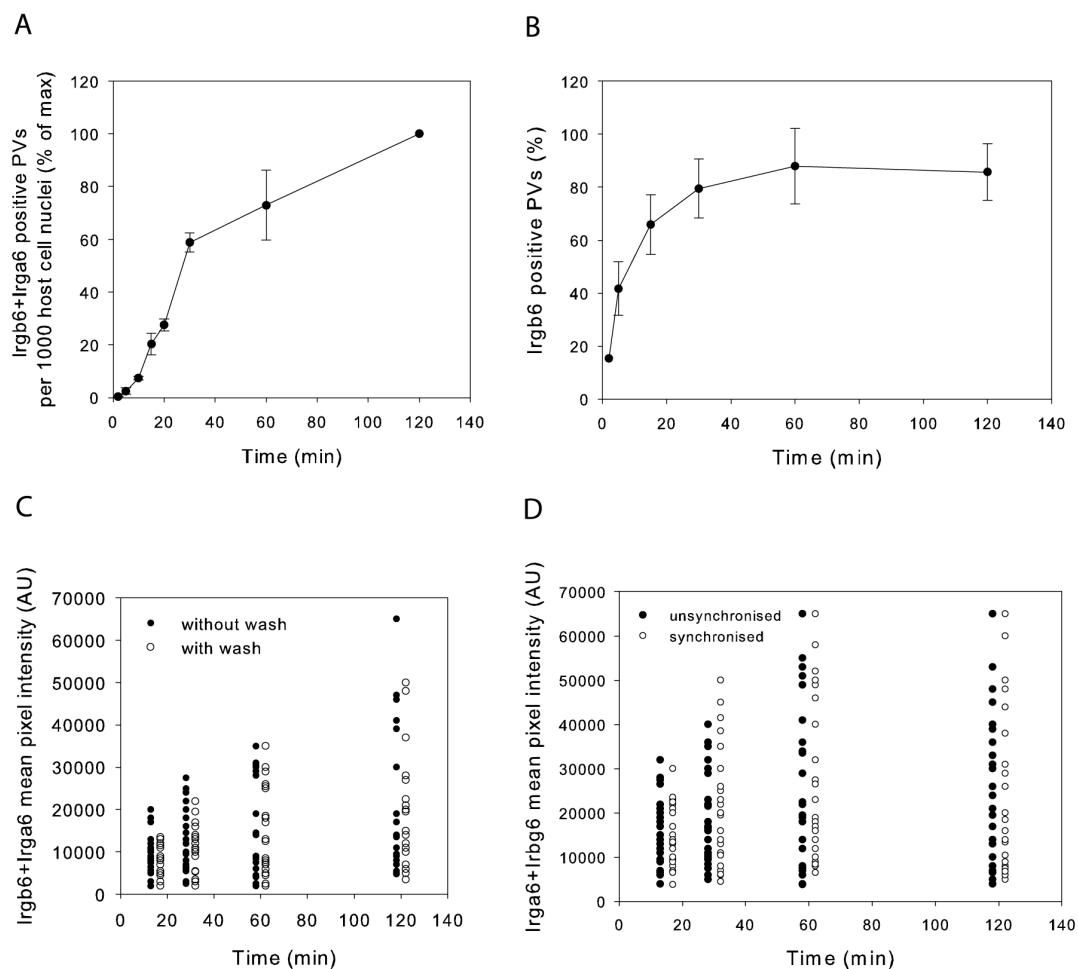


Figure 7 Time-course of IRG protein association with *T. gondii* ME49 PVs.

IFN γ -induced C57BL/6 MEFs were infected with *T. gondii* ME49 strain as described in Material and Methods. At intervals from 2.5 minutes to 2 h after infection slides were prepared for staining simultaneously with antibody reagents against Irga6 (mAb 10D7) and Irgb6 (serum A20) using secondary antibodies coupled with the same fluorochrome to enhance the visible signal (**A**, **C** and **D**) or for staining against Irgb6 alone (serum A20) and GRA7 (mAb aGRA7) (**B**). DAPI was used to stain the nuclei. (**A**) Loading of IRG proteins begins early after infection. Vacuoles with visible accumulations of IRG proteins on the PVM were counted per 1000 host cell nuclei at each time point and presented as a percentage of maximum. The mean of 2 independent repetitions and the range between them are shown. (**B**) The frequency of Irgb6 positive vacuoles increased with time after infection. In two independent experiments Irgb6 positive PVs were counted out of 12-100 intracellular

parasites at different time points after infection. Means and ranges are given. The two-minute time point was assayed in only one experiment. **(C and D)** IRG signal intensity at the PVM increased with time after infection. Fluorescent signal intensities of IRG protein (Irgb6 plus Irga6) on individual vacuoles were measured as described in Material and Methods at the times indicated. Neither signal intensities nor heterogeneity were detectably affected by washing off the parasites after 15 min of infection (**C**, open circles: free parasites were washed off; closed circles: free parasites were not washed off after inoculation) or synchronised infection (as described in Material and Methods) and thorough removal of free parasites by washing (**D**, open circles: infection was synchronised and free parasites were washed off; closed circles: infection was not synchronised and free parasites were not washed off after inoculation). 25 positive vacuoles were measured at each time point.

3.2 Time-course of ectopically expressed IRG protein loading onto avirulent ME49 *T. gondii* vacuoles in mouse fibroblasts

To get a better insight into kinetics of the loading process, live cell imaging in combination with fluorescent-tagged IRG proteins was employed. MEFs were stimulated by IFN γ , transfected with the construct expressing Irgb6-FLAG-EGFP and subsequently infected with ME49 *T. gondii* as described in Material and Methods and subjected to live-cell microscopy. Figures 8A and B display a series of consecutive frames from 2 independent movies showing Irgb6-FLAG-EGFP association with the *T. gondii* vacuoles. The mean pixel intensities of Irgb6 on *T. gondii* PVs from the frames were quantified and presented on Figure 8C. The parasites infected the cells 40 min (Figure 8A, start of the movie) and 4 min (Figure 8B) after inoculation, respectively, indicating that asynchrony of infection indeed took place and therefore could influence the heterogeneity of the IRG protein signal on *T. gondii* PVs. Strikingly, Irgb6-FLAG-EGFP signal became visible as early as 1 min (Figure 8B) and approximately 5 min (Figure 8A) after invasion and then continued to rise before reaching saturation of the camera. Thus, consistent with loading of endogenous proteins, ectopically expressed Irgb6-FLAG-EGFP could be detected on the *T. gondii* PVs minutes after invasion followed by swift intensification of the protein signal.

The delay between invasion and initiation of loading shown here (1 and 5 min) and elsewhere (Zhao, 2008; Khaminets et al., 2010) requires a comprehensive understanding since it may represent one of the strategies used by *T. gondii* to attenuate the IRG-mediated cell-autonomous response against to the parasite. Similar tendency of loading onto avirulent *T. gondii* PVs by ectopically expressed Irga6-cTag1-EGFP has been previously reported (Zhao, 2008).

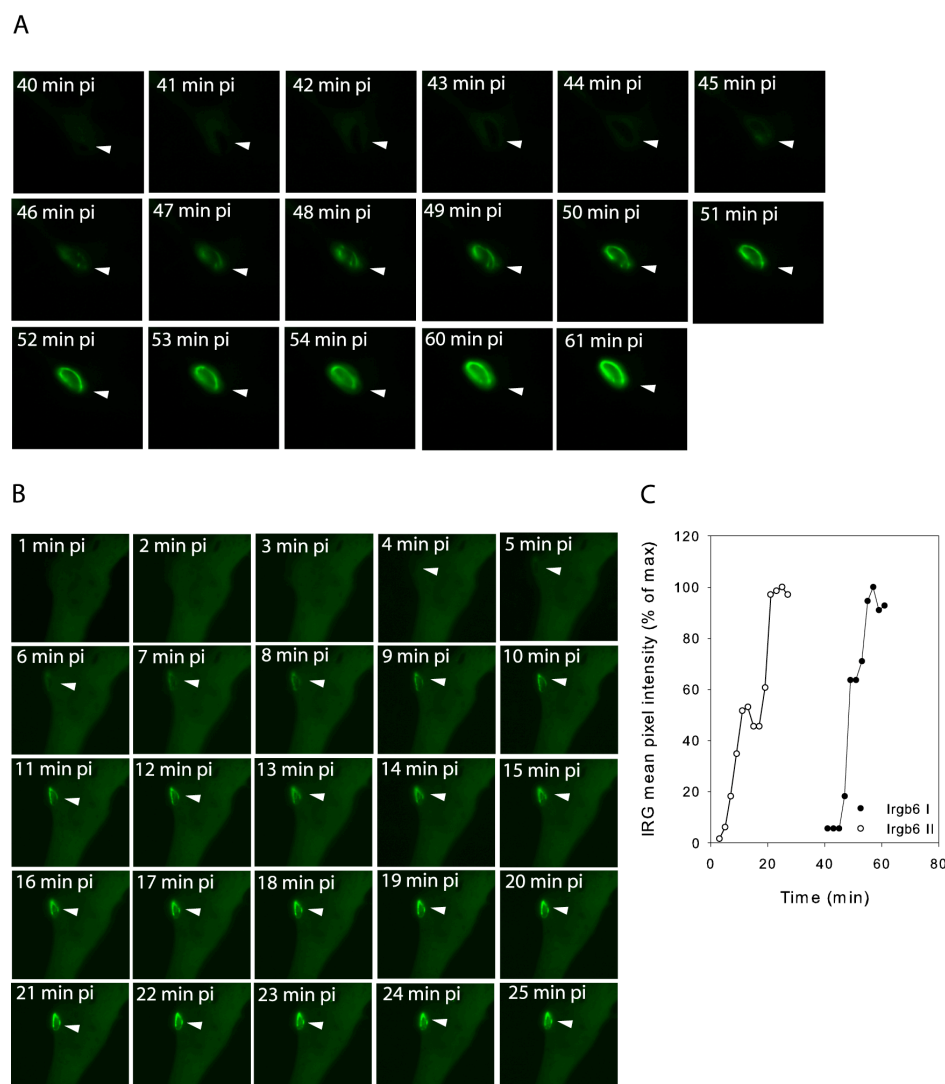


Figure 8 Loading of individual vacuoles by Irgb6-FLAG-EGFP observed by time-lapse microscopy.

MEFs were transfected with the expression plasmid pEGFP-N3-Irgb6-FLAG and simultaneously induced with IFN γ . After 24 h, the cells were infected with *T. gondii* ME49 strain in microscope slide chambers as described in Material and Methods and monitored continuously in order to document the entry of individual parasites and the subsequent accumulation of Irgb6-FLAG-EGFP on the PV. (**A and B**) The frames of two time-lapse videos of Irgb6-FLAG-EGFP loading on ME49 *T. gondii* PV. Arrowheads indicate the location of the analysed *T. gondii* PVs. Note that the frames in (**A**) from 54 min pi till 60 min pi are not included because they were out of focus. (**C**) Mean pixel intensities of Irgb6 at the PVM were measured from the vacuoles shown in Fig. 8A and Fig. 8B (Irgb6 I and Irgb6 II respectively) and plotted as percentage of the maximum intensity. The origin on the time axis is the time of addition of *T. gondii* to the cells. The first symbol of each plot gives the time when the observed parasite was seen to enter the cell. In the case of the Irgb6 II movie the protein signal slightly decreased after 13 min due to focus drift on the 15 and 17 min frames and resumed its rise after correction.

3.3 Sequential loading of multiple IRG proteins on to the PV of avirulent ME49 *T. gondii*

Various IRG proteins accumulate on a certain proportion of vacuoles (Khaminets et al., 2010). To analyse and compare the loading of individual IRG proteins on to *T.*

gondii PVs in time, IFN γ -stimulated MEFs were pulsed with *T. gondii* ME49 for 2, 5, 10 and 20 min before fixation. Specific reagents were used to detect Irgb6 and Irga6 and the protein intensities on PVs were quantified as described in Material and Methods. Figure 9A shows that at 2 and 5 min after infection Irgb6 was more intense than Irga6 measured on the same vacuoles. However, at 10 and 20 min after infection Irgb6 and Irga6 loaded onto the *T. gondii* vacuoles to almost the same extent. To compare vacuolar loading of Irgb6 and Irgd onto PVs, live-imaging microscopy was employed. MEFs were stimulated with IFN γ , cotransfected with the constructs expressing Irgb6-FLAG-EGFP and Irgd-cTag1-Cherry and subsequently infected with ME49 *T. gondii* for live microscopy as described in Material and Methods to document loading of IRG proteins onto the PVs. Figure 9B illustrates consecutive frames from the movie showing a 5 min delay in loading of Irgd-cTag1-Cherry relative to Irgb6-FLAG-EGFP which starts to accumulate at 10 min pi. In another movie (Zhao, 2008; Khaminets et al., 2010) Irga6-cTag1-EGFP accumulated on the ME49 *T. gondii* PV minutes earlier than Irgd-cTag1-Cherry co-expressed in IFN γ -stimulated MEFs providing another example of sequential loading of IRG proteins.

These differences in time of loading initiation between members of IRG protein family lead to the organized spatial distribution of IRG positive vacuoles at a given time after infection. In other words, the proteins, which arrive later, are predominantly found on the *T. gondii* vacuoles already occupied by other earlier associated proteins. Accordingly, IRG proteins load onto the *T. gondii* PV in hierarchical manner (or in “inclusion relationship”) with Irgb6 and Irgb10 as pioneers occupying the majority of vacuoles, followed by Irga6, Irgd and Irgm2. IRG proteins that arrive at the vacuole first could provide the binding sites and thereby may be required for efficient loading of the subsequent GTPases. Notably, removal of Irga6 from the cells did not affect the loading of the “downstream” members of the hierarchy, Irgd and Irgm2, indicating of redundancy in building a loading platform for the analysed IRG proteins (Khaminets et al., 2010). Alternatively, binding of IRG proteins to *T. gondii* PVs may not be regulated by the heterotypic interactions within IRG family but by the other factors, proteins or lipids, which are still to be discovered. It is plausible, that these two models are not mutually exclusive, and future studies will help elucidate the precise mechanism of the loading process.

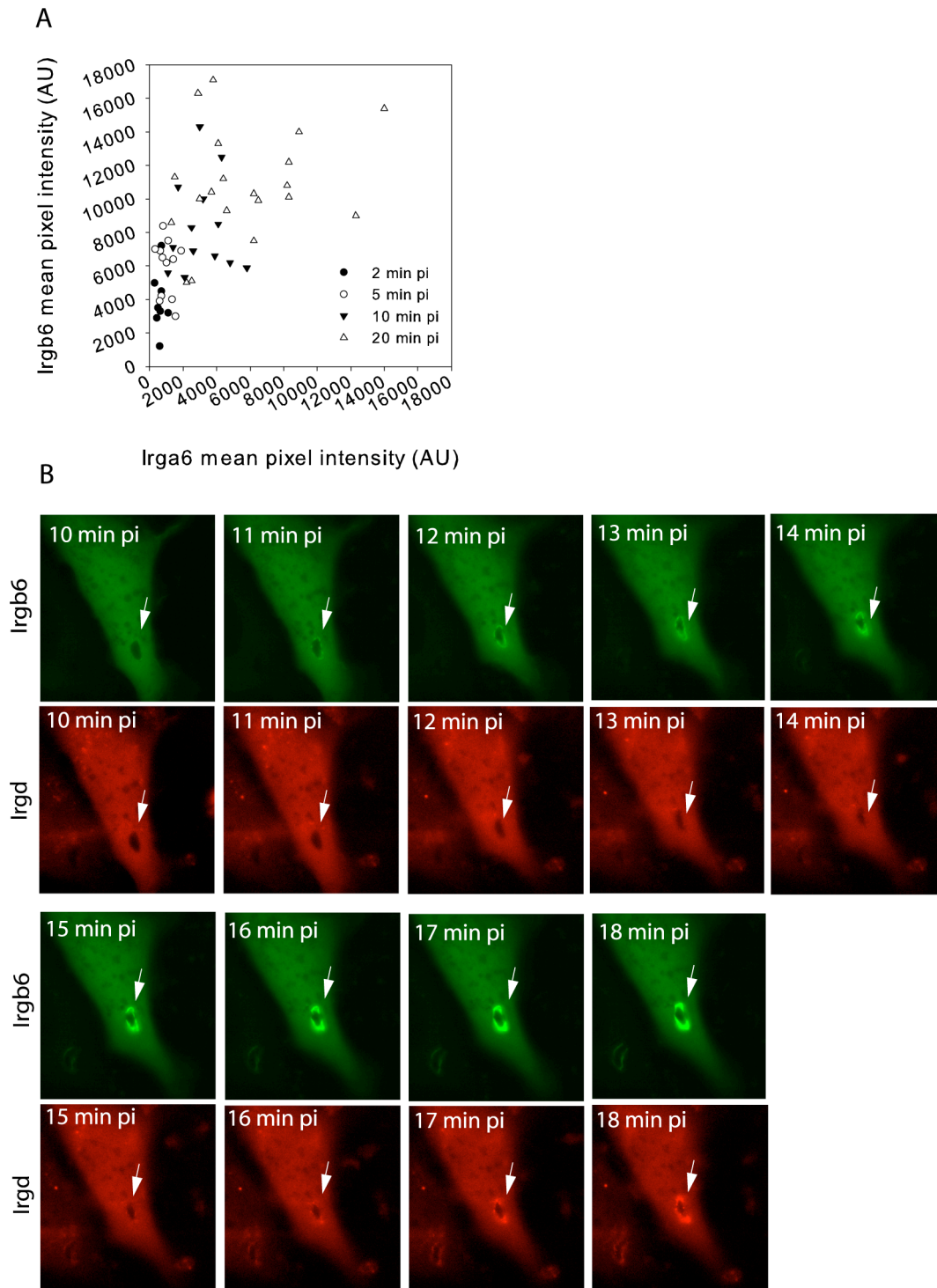


Figure 9 Sequential loading of multiple IRG proteins on to PV of ME49 *T. gondii*.

(A) Irgb6 loads more heavily than Irga6 onto *T. gondii* vacuoles at early time points after infection. MEFs were induced with IFN γ and infected with *T. gondii* ME49 strain. At indicated times after infection Irgb6 and Irga6 vacuole loading intensities were analysed simultaneously with specific primary antibodies (Irgb6, serum A20; Irga6, mAb 10D7) detected with secondary antibodies labelled with different fluorochromes. (B) Irgb6 loads before Irgd on PV of ME49 *T. gondii*. MEFs were induced with IFN γ and transfected simultaneously with the constructs expressing Irgb6-FLAG-EGFP and Irgd-ctag1-Cherry. After 24 h, cells were infected with *T. gondii* ME49 strain in microscope slide chambers and accumulation of IRG proteins was documented by the time-lapse microscopy. Successive one-minute frames from one vacuole show Irgb6-FLAG-EGFP loading several minutes before Irgd-ctag1-Cherry.

3.4 Vacuolar loading with IRG proteins is independent of major signalling systems and microtubules

T. gondii PVM was shown to be occupied by the active GTP-bound form of Irga6 (Papic et al., 2008) while the rest of the cytoplasmic protein was predominantly in an inactive GDP-bound state, inhibited by the GMS subset of IRG protein family (Hunn et al., 2008). This suggests that transition from GDP- into GTP-bound conformation of IRG proteins during infection with *T. gondii* may be triggered by any form of posttranslational modification from the cellular signalling pathways activated by the parasite. Via disruption of several signalling systems I tested their involvement in loading of the *T. gondii* PV with IRG proteins in IFN γ -stimulated MEFs.

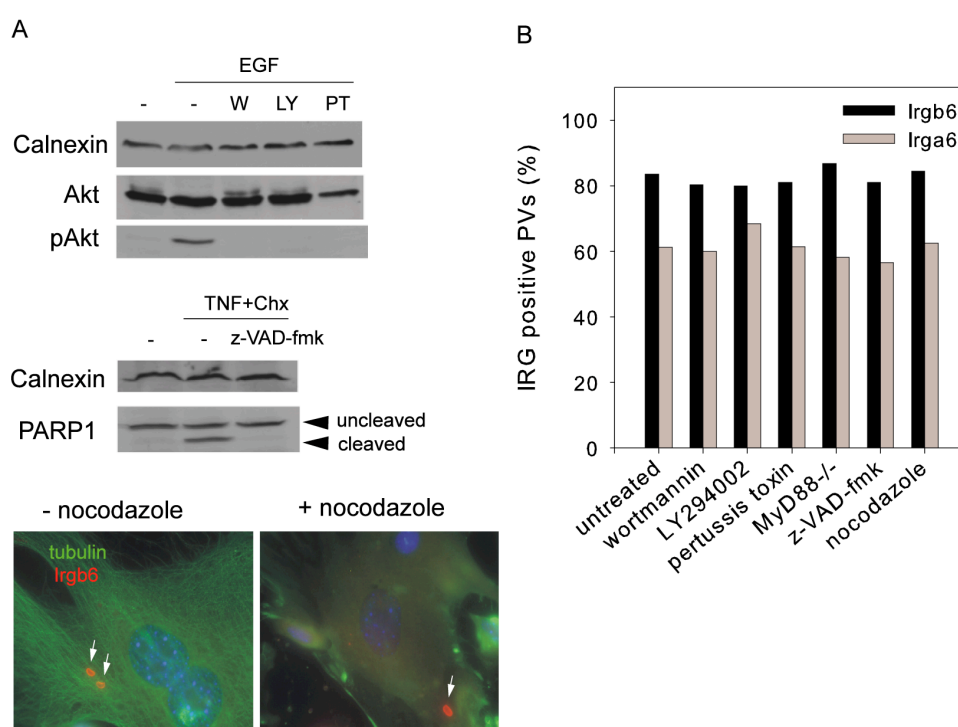


Figure 10 Vacuolar loading of IRG proteins is independent of major signalling systems and microtubules.

(A) Inhibition of major signalling pathways and microtubule polymerisation. The blockade of PI3 kinase and G protein-coupled receptors was demonstrated by Western blot for phospho-Akt (pAkt). MEFs were treated with wortmannin (W), LY294002 (LY) or pertussis toxin (PT) for 6 h as described in Material and Methods. Inhibited cells were stimulated by EGF for 10 min to induce Akt phosphorylation. Calnexin and total Akt served as a loading control. To inhibit caspases, MEFs were treated with z-VAD-fmk for 2 h followed by stimulation with TNF α for 6 h in the presence of cycloheximide (Chx), as described in Material and Methods. The amount of PARP1 processing by caspases was analysed by Western blot. Calnexin served as a loading control. Inhibition of microtubule polymerisation was monitored microscopically by immunostaining with an anti- α -tubulin mAb. MEFs were induced with IFN γ for 24 h and treated with nocodazole, or DMSO as control, for 1 h, as described in Material and Methods. Treated cells were infected with *T. gondii* ME49 strain and loading of parasite PVs was monitored 2 h after infection by immunostaining for Irgb6 (serum A20). (B) MEFs were induced with IFN γ and treated as described in (A) with inhibitors of PI3-kinase (wortmannin and LY294002), G-protein-coupled receptors (pertussis toxin), caspases (z-VAD-fmk) and microtubule polymerisation (nocodazole). Multiple TLR-mediated signals were excluded in IFN γ -induced MEFs

from MyD88-deficient mice. Untreated, treated and MyD88-deficient cells were infected with *T. gondii* ME49 strain for 2 h and stained separately with antibody reagents against Irga6 (mAb 10D7) and Irgb6 (serum A20). The frequency of vacuoles detectably positive for Irga6 and Irgb6 was calculated as a percentage from 200-400 intracellular parasites.

Wortmannin and LY293002 were used to inhibit PI3 kinase, pertussis toxin was employed to dysregulate G protein-coupled receptors, involvement of TLR signalling was tested in MyD88^{-/-} MEFs (TLR2, TLR4 and TLR11 activated by *T. gondii* use MyD88^{-/-} adaptor molecule for signal propagation (Egan et al., 2009)) and z-VAD-fmk was used to inhibit caspases. Controls for efficient inhibition of the pathways are presented in Figure 10A. Surprisingly, disruption of the analysed pathways had no effect on the IRG protein loading process (Figure 10B).

Hook3, a microtubule-associated protein, has been reported to interact with Irga6 (Kaiser, Kaufmann, and Zerrahn, 2004), thus, raising the possibility of microtubule involvement in loading of *T. gondii* PVs with IRG proteins. However nocodazole-mediated inhibition of microtubule polymerisation did not influence the frequency of IRG protein loaded PVs (Figure 10A and B). This result suggests that IRG proteins most likely access *T. gondii* vacuoles via passive diffusion from the cytoplasmic pools of these proteins (Martens and Howard, 2006) followed by the spontaneous activation on the membrane as described elsewhere ((Hunn et al., 2008; Papic et al., 2008; Khaminets et al., 2010) and section 5.4).

3.5 Vacuolar loading with IRG proteins is dependent on autophagic regulator Atg5

Mouse fibroblasts lacking the autophagic regulator Atg5 are starkly deficient in restricting growth of avirulent *T. gondii* (Könen-Waisman and Howard, 2007). Moreover, it has been reported that Irga6 virtually fails to load onto avirulent PTG *T. gondii* PVs in Atg5^{-/-} macrophages (Zhao et al., 2008). Therefore, IFN γ -stimulated immortalised mouse wt and Atg5^{-/-} fibroblasts were examined in more detail to analyse the influence of Atg5 on loading of *T. gondii* PVs with IRG proteins (in collaboration with Steffi Könen-Waisman). As reported earlier (Zhao et al., 2008), Irga6 association with avirulent (ME49 was used in this study) *T. gondii* PVs in Atg5^{-/-} cells was reduced (Figure 11A), although the difference between wt and Atg5^{-/-} was not as large as for Zhao et al (Zhao et al., 2008).

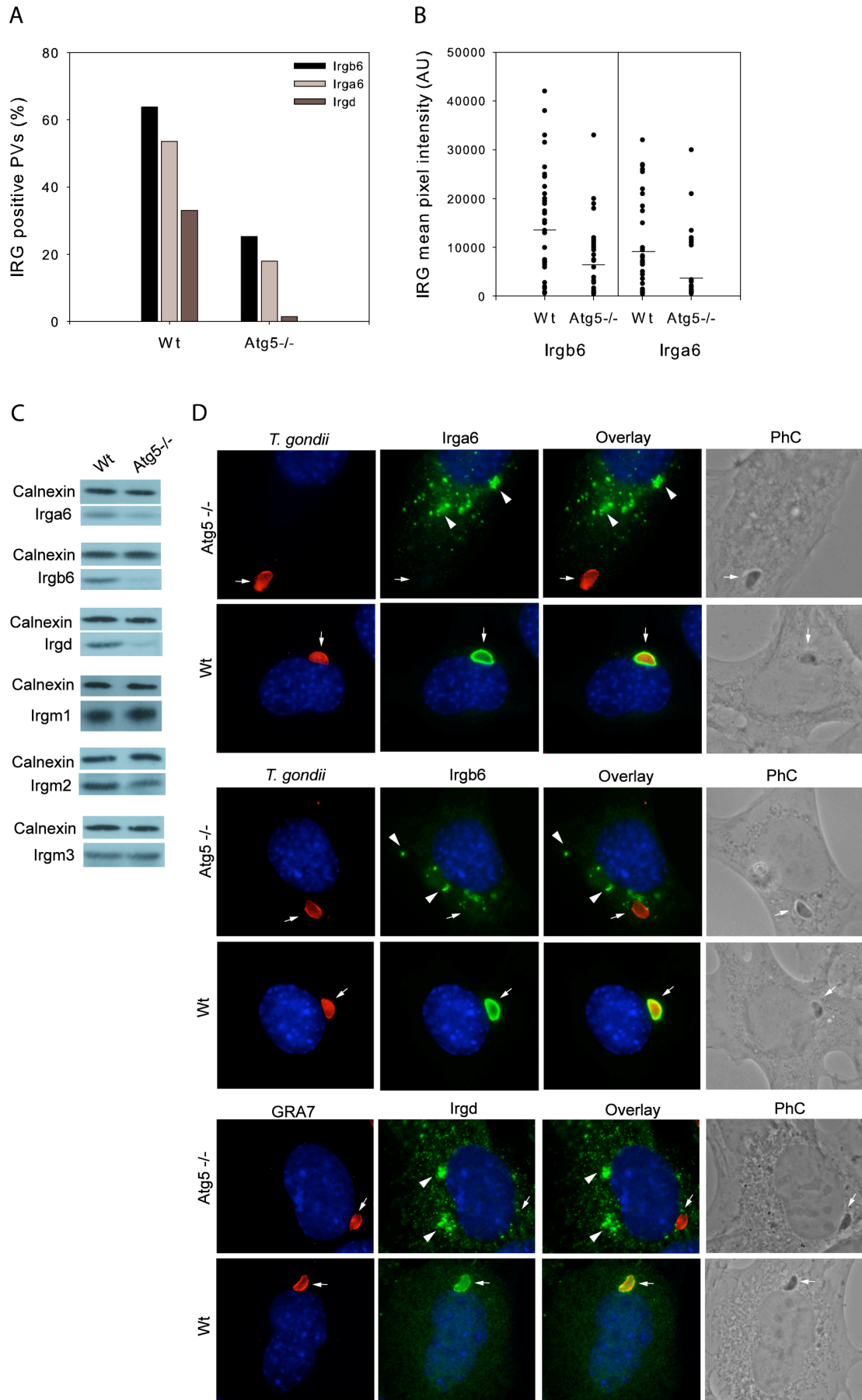


Figure 11 Atg5 influences loading of IRG proteins onto *T. gondii* PVs.

(A) IRG protein association with *T. gondii* ME49 PVs is reduced in Atg5^{-/-} fibroblasts. Wt and Atg5^{-/-} fibroblasts were induced for 24 h with IFN γ and infected with *T. gondii* ME49 strain for 2 h. Irga6, Irgb6 and Irgd positive vacuoles were detected by staining with mAb 10D7, serum A20 and serum 081/1 respectively. 400-700 intracellular parasites were scored for each IRG protein in each cell line in 2-3 independent experiments and pooled. (B) The intensity of Irgb6 and Irga6 vacuolar loading is reduced in Atg5^{-/-} cells. Loading intensity was measured as described in Material and Methods on at least 40 vacuoles from the experiment shown in Figure 11A. Horizontal bars represent the arithmetic mean values. (C) Irga6, Irgb6, Irgd and Irgm2 protein levels are reduced in Atg5^{-/-} MEFs while Irgm1 and Irgm3 are unaffected. Wt and Atg5^{-/-} fibroblasts were induced with IFN γ for 24 h and analysed by Western blot with antibody reagents detecting the following IRG proteins: Irga6 (mAb 10D7), Irgb6 (mAb B34), Irgd (serum 2078/3), Irgm2 (serum H53/3), Irgm1 (serum L115 BO) and Irgm3 (mAb anti-IGTP). (D) IRG proteins form aggregates in IFN γ -induced Atg5^{-/-} MEFs. Cells were induced with IFN γ , infected with *T. gondii* ME49 strain and processed for microscopical analysis as described in Figure 11A. Rabbit anti-*Toxoplasma* serum (upper and middle panels) or anti-GRA7 (lower panels) monoclonal antibody was used to identify the pathogen. Arrows indicate intracellular parasites. PhC: phase contrast. The arrowheads indicate the IRG protein aggregates.

Importantly, reduction in loading was not seen only for Irga6 but also for Irgb6 and Irgd (Figure 11A) indicating that the lesion was not specific for one protein but at least for two more GKS proteins of the IRG GTPase family.

Decrease in frequency of IRG protein positive avirulent *T. gondii* vacuoles in Atg5^{-/-} cells was accompanied by reduction in intensity of IRG proteins loaded onto individual *T. gondii* PVs (Figure 11B). In contrast to Zhao et al (Zhao et al., 2008), a prominent reduction in the IRG protein levels in IFN γ -stimulated Atg5^{-/-} fibroblasts was observed as compared to the wt cells (Figure 11C). The half-life of the Irgb6 was reduced from about 17 h in wt to 3 h in Atg5^{-/-} cells analysed by pulse-chase (Figure 12) indicating that IRG proteins stability is severely compromised in cells lacking Atg5.

Irga6 protein aggregates observed by Zhao et al (Zhao et al., 2008) in Atg5^{-/-} macrophages were apparent in Atg5^{-/-} mouse fibroblasts and, interestingly, were positive for the antibody 10D7 (Figure 11D) specific for the GTP-bound state of the protein (Papic et al., 2008). Irgb6 and Irgd were also found aggregated in Atg5^{-/-} fibroblasts (Figure 11D). It is noteworthy that aggregated proteins were evident in cells infected with *T. gondii* as well as in uninfected cells (Figure 13B). Contrary to Zhao et al (Zhao et al., 2008), neither proximity nor colocalisation of IRG protein aggregates with lysosomes (stained by the antibody detecting LAMP1) was seen in Atg5^{-/-} fibroblasts (Figure 13).

Taken together, absence of Atg5 in IFN γ -stimulated mouse fibroblasts leads to aggregation and decreased stability of IRG proteins followed by their degradation by an unidentified cellular proteolytic system.

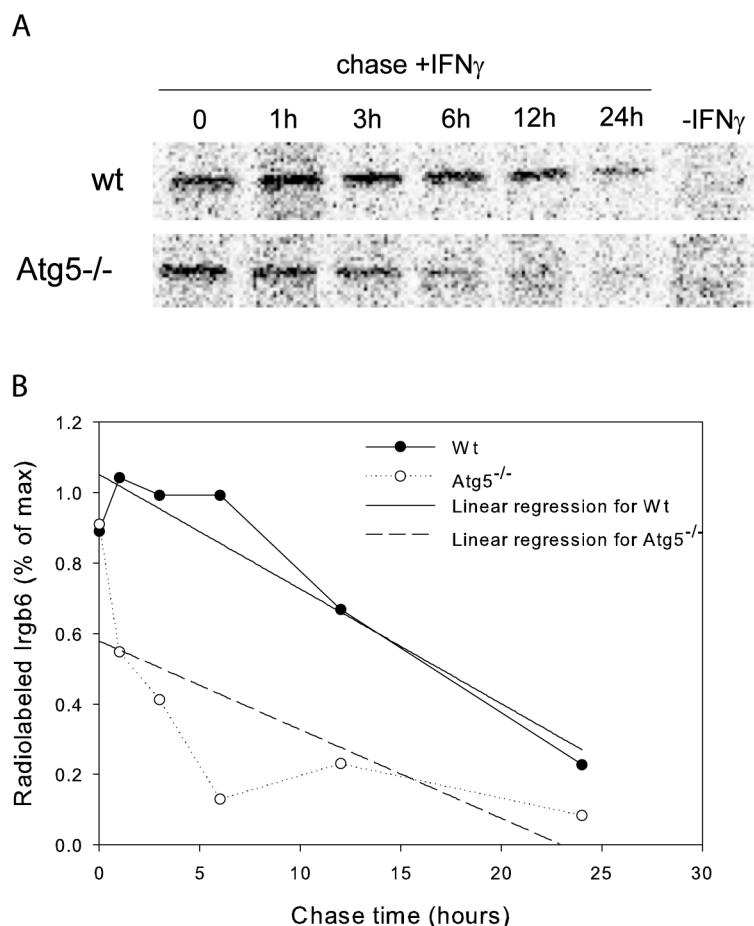


Figure 12 Enhanced degradation of Irgb6 in Atg5^{-/-} fibroblasts compared to the protein turnover in wt cells.

IFN γ -stimulated wt and Atg5^{-/-} fibroblasts were starved in methionine, serine and FCS-free medium for 1 h followed by 1 h pulse with Met-³⁵S-label (containing ³⁵S-labelled L-Methionine, L-Serine and miscellaneous amino acids). The cells were subsequently washed with medium followed by the 24-h chase in complete medium (0 h time point indicates start of the chase). Samples at indicated time points were taken and subjected to Irgb6 immunoprecipitation (with mAb B34 as described in Material and Methods), SDS-PAGE, and autoradiography. **(A)** Autoradiographic analysis of Irgb6 stability in IFN γ -stimulated wt and Atg5^{-/-} fibroblasts using PhosphorImager. **(B)** Quantification of bands and at each time point using Typhoon scanner and ImageQuant software. Linear regressions for each curve were calculated using Sigma Plot which yielded reduction of Irgb6 half-life from approximately 17 h in wt to 3 h in Atg5^{-/-} cells.

Atg5 most likely plays an indirect role in the process of IRG protein loading onto *T. gondii* PVs since the general behaviour of the proteins is disturbed in uninfected resting cells. In the absence of Atg5, Irga6 aggregates, found in GTP-bound state, may indicate a possible function of Atg5 in regulating the transition of the protein form inactive GDP-bound into active GTP-bound conformation of the protein or vice versa. Alternatively, Atg5 could act upstream of GMS proteins, preventing spontaneous activation of GKS proteins, or downstream, regulating degradation of the aggregates spontaneously formed in the cytoplasm of IFN γ -stimulated cells.

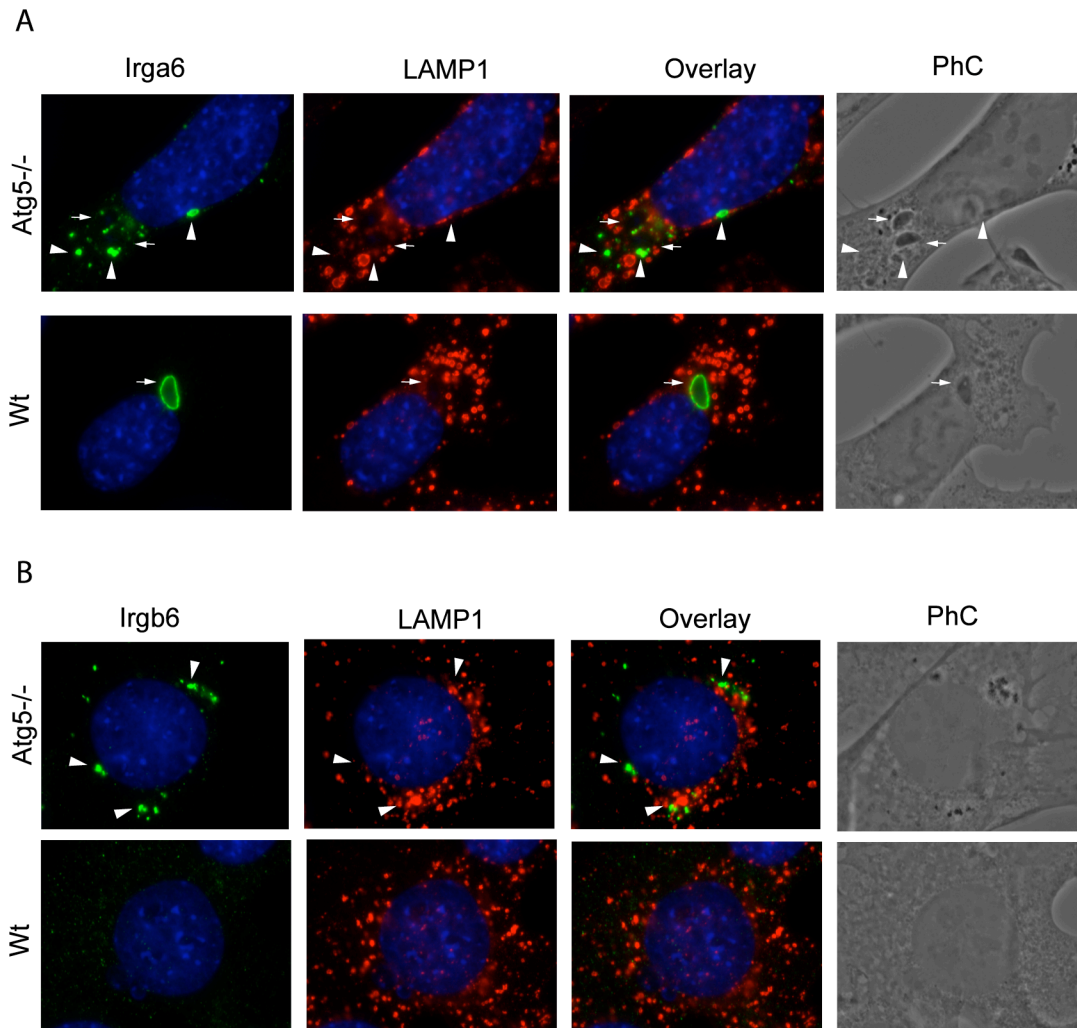


Figure 13 Irga6 and Irgb6 aggregates do not co-localise with lysosomal marker LAMP1 in Atg5^{-/-} fibroblasts.

Wt and Atg5^{-/-} fibroblasts were induced for 24 h with IFN γ and infected with *T. gondii* ME49 strain for 2 h and immunostained for Irga6 (mAb 10D7) (**A**) or Irga6 (mAb B34) (**B**) and LAMP1 (mAb 1D4B). No obvious co-localisation of Irga6 (upper panels) and Irgb6 (lower panels) with LAMP1 in wt and Atg5^{-/-} fibroblasts was observed. Arrows indicate intracellular parasites identified by phase contrast (PhC) and arrowheads indicate Irga6 and Irgb6 aggregates. The cells shown in (**B**) were not infected.

3.6 Reduced loading of IRG proteins onto the PVM of virulent *T. gondii* strains

All the data presented so far were obtained using avirulent ME49 strain of *T. gondii*. The vacuoles containing type I virulent parasites (BK and RH) were much less loaded with Irgb6, typically the most abundant IRG protein, than the vacuoles of type II avirulent (ME49, NTE and Pru) (Figure 14A and B) and type III *T. gondii* (Khaminets et al., 2010). Zhao et al obtained similar results in macrophages and MEFs (Zhao et al., 2009a). The frequency of Irga6-loaded vacuoles was not considerably reduced (by 14%) in case of virulent RH-YFP compared to avirulent ME49 strain of *T. gondii* (Figure 14C). However, protein signal intensity of both Irgb6 and Irga6 on virulent (RH-YFP) vacuoles was clearly diminished compared to

the normal distributions of the IRG protein signal intensities on the avirulent (ME49) *T. gondii* vacuoles (Figure 14D). In rare cases (up to 8% of virulent *T. gondii* vacuoles) single vacuoles of the virulent parasites showed strong IRG protein intensity (one vacuole with Irgb6 intensity of 3×10^4 AU in Figure 14D, (Hunn, 2007; Khaminets et al., 2010)) indicating that a certain proportion of virulent parasites fail to inhibit initiation of IRG protein loading onto the PV, and when initiation is fulfilled loading proceeds very rapidly.

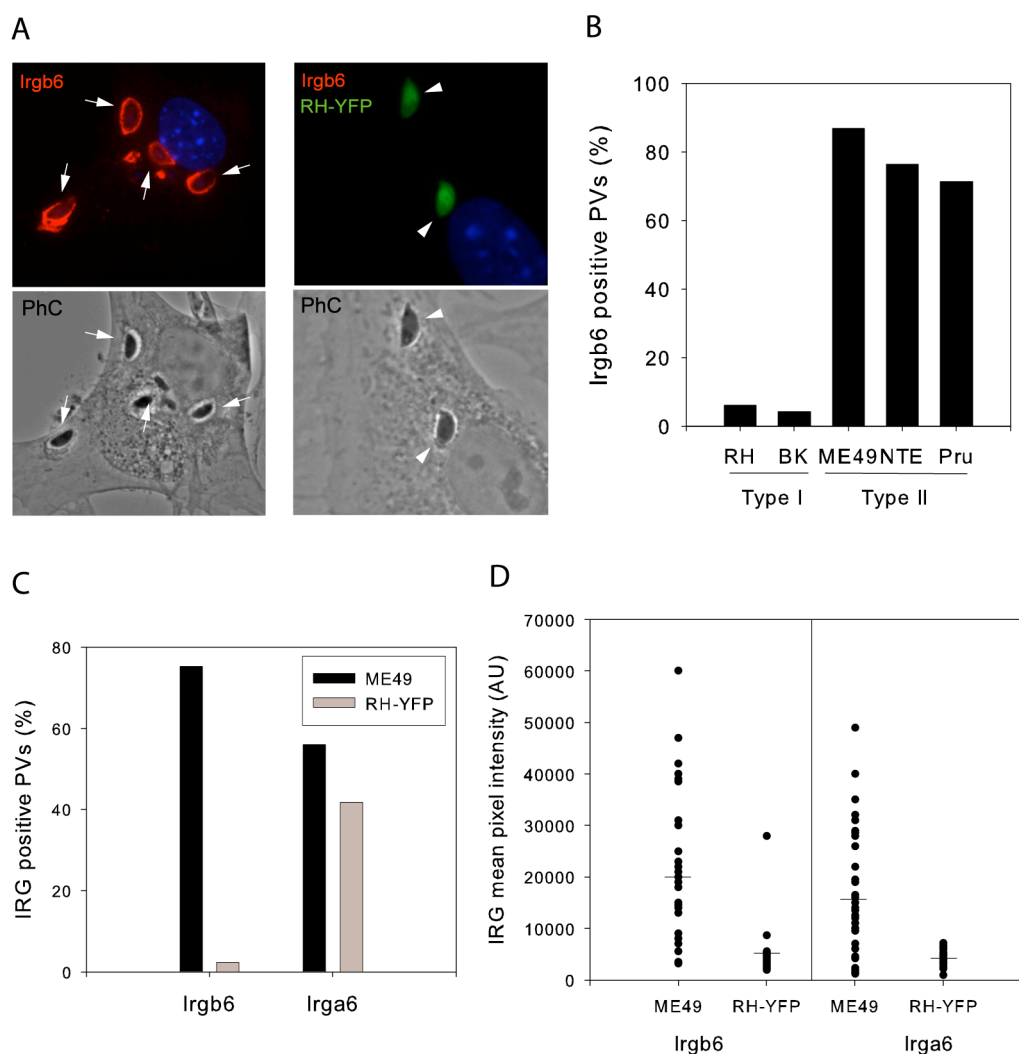


Figure 14 Accumulation of IRG proteins on the PVM is reduced during virulent *T. gondii* infection.

(A) PVs with virulent RH-YFP *T. gondii* are not detectably loaded with Irgb6. IFN γ -induced MEFs were infected for 2 h with *T. gondii* ME49 strain (indicated by arrows) or RH-YFP strain (indicated by arrowheads) and stained for Irgb6 (serum A20). (B) IFN γ -induced MEFs were infected for 2 h with type I virulent (RH and BK) and type II avirulent (ME49, NTE and Pru) *T. gondii* strains and assayed microscopically for Irgb6-positive vacuoles (serum A20). Irgb6 positive PVs were counted for each parasite strain from 350-600 intracellular parasites in 2 independent experiments and pooled. (C) MEFs were induced with IFN γ and infected with *T. gondii* ME49 strain (black bars) or RH-YFP strain (grey bars). The numbers of Irgb6 and Irga6 positive PVs were counted in 2 experiments out of approximately 1000 intracellular parasites and pooled. (D) MEFs were induced with IFN γ and infected with either ME49 or RH-YFP *T. gondii* strains. Mean fluorescence intensities of Irga6 (mAb 10D7)

and Irgb6 (serum A20) signals at the PVM were quantified as described in and Material and Methods. 30-35 PVs per data set were quantified.

It is clear that Irgb6 and Irgb10, the pioneer IRG proteins in terms of loading onto *T. gondii* PV in C57BL/6 MEFs, are inhibited to a greater extent than the other so far studied members of the family (Figure 14C and (Khaminets et al., 2010)), whereas Irga6 is mainly reduced in protein amount loaded on the individual vacuoles (Figure 14C and D). These results suggest that Irgb6 and Irgb10 could be the primary targets of the virulent *T. gondii* and the absence of the pioneer IRG proteins causes attenuation of vacuolar accumulation of the following IRG proteins (e.g. Irga6 and Irgd).

3.7 Coinfection of mouse fibroblasts with *T. gondii* of different virulence and virulence-associated *T. gondii* proteins ROP18, ROP16 and ROP5 do not affect loading of PVM with IRG proteins

Virulent *T. gondii*, in contrast to avirulent strains of the parasite, efficiently evades targeting action of IRG proteins by interfering with the process of loading onto PVM (Figure 14 and (Zhao et al., 2009a; Zhao et al., 2009b; Khaminets et al., 2010)). To examine loading of virulent and avirulent *T. gondii* PVs in coinfecting cells, IFN γ -stimulated MEFs were simultaneously infected with YFP-expressing virulent (RH-YFP) and unlabelled ME49 parasites. Interestingly, RH-YFP vacuoles remained essentially unloaded and ME49 vacuoles showed strong Irgb6 and Irga6 accumulations in coinfecting cells (Figure 15A and B) comparable to the protein intensity on ME49 vacuoles in avirulent parasite singly infected cells. This result could imply that the blockade of IRG protein loading by the virulent *T. gondii* is not mediated by a diffusible factor secreted during infection. Similar conclusions were reported by Zhao et al (Zhao et al., 2009a).

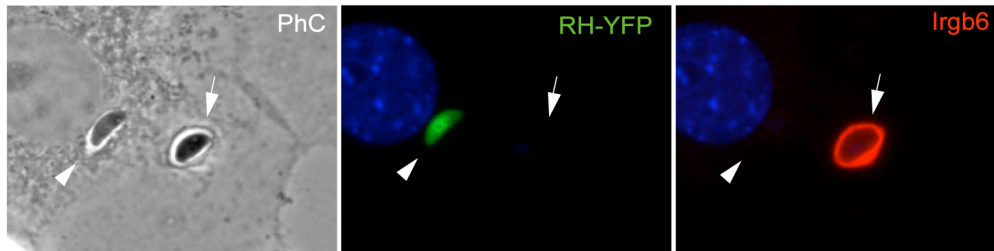
Rhoptry kinases ROP18, ROP16 and pseudokinases ROP5 of the ROP2 family, secreted by *T. gondii* during early stages of invasion, have been reported to be the major virulence determinants of the parasite studied in mice and in cell culture (Carruthers and Sibley, 1997; El Hajj et al., 2007; Saeij et al., 2006; Saeij et al., 2007; Taylor et al., 2006). ROP18 is an active kinase, highly polymorphic between virulent type I and avirulent type II *T. gondii* strains and is expressed at very low levels in avirulent type III parasites (El Hajj et al., 2007; Khan et al., 2009; Saeij et al., 2006;

Taylor et al., 2006). ROP18 is discharged from invading parasites into the host cell cytosol and minutes later found associated with the nascent PVM. Ectopically expressed tagged ROP18 displayed similar properties and behaved like wt protein in cell culture (El Hajj et al., 2007). ROP16 is secreted by the parasite into host cell cytoplasm and, additionally, translocates into the nucleus (Saeij et al., 2007). Moreover, it has been demonstrated that ROP16 directly phosphorylated host cell STAT3/6 transcription factors and thereby modulated inflammatory response *in vivo* and in cell culture (Saeij et al., 2007; Yamamoto et al., 2009). The locus containing closely linked ROP5 genes has been implicated in virulence of *T. gondii* shown by genetic crosses of types II and type III parasites (Saeij et al., 2006). Taken together, *T. gondii* ROP proteins are essential determinants of the parasite virulence and therefore should be considered in the context of loading of IRG proteins onto the *T. gondii* PVs.

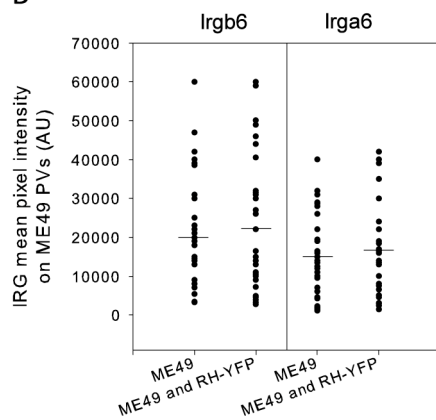
In one approach to study the involvement of virulence determinants in the loading process, the constructs, expressing mature forms of C-terminally Ty-tagged ROP18 from virulent (RH) and avirulent (ME49) *T. gondii* and Cherry as a control, were transfected into IFN γ -stimulated L929 fibroblasts followed by infection with avirulent ME49 *T. gondii* and analysis of the frequency of Irgb6 positive vacuoles. Figure 15C illustrates that there was no effect of virulent or avirulent ROP18 on loading of IRG proteins onto avirulent PVs relative to the IRG protein accumulation in Cherry-expressing cells. Similar results were obtained by Zhao et al using transgenic strains of *T. gondii* (Zhao et al., 2009a). To investigate the role of ROP16 and ROP5 in the loading process type I parasite deficient in ROP16 gene (RH Δ rop16) and type II *T. gondii* transgenic for cosmid LC37 (S22-LC37) carrying a segment of the RH genome encompassing ROP5A-D as well as two other predicted gene sequences (TGME49_108070 and TGME49_108060) accompanied by the parental control strains were assayed (in collaboration with Steffi Könen-Waisman). The numbers of Irgb6 positive vacuoles were comparable between RH Δ rop16, S22-LC37 and their respective controls (Figure 15D). Additionally, growth of transgenic *T. gondii* strains was controlled normally in IFN γ -stimulated MEFs (Khaminets et al., 2010). Taken together, the data shown here and elsewhere (Zhao et al., 2009a; Khaminets et al., 2010) suggest that there is no apparent function of individual *T. gondii* virulence determinants, ROP18, ROP16 and ROP5, in loading of *T. gondii* vacuoles with IRG

proteins and argue against their role in modulating the IFN γ -mediated cell-autonomous immunity to the parasite (see section 5.5).

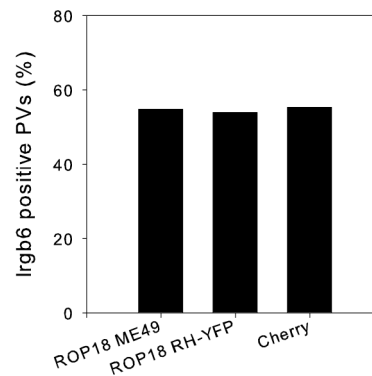
A



B



C



D

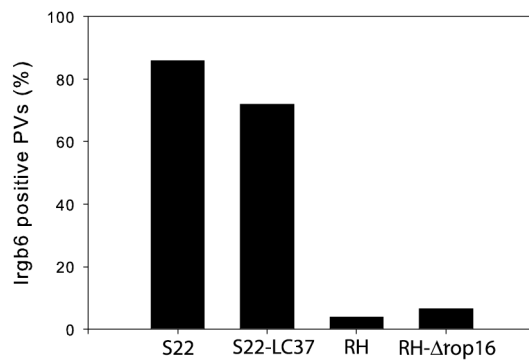


Figure 15 Coinfection of MEFs with *T. gondii* of differential virulence and ROP18, ROP16 and ROP5 virulence-associated *T. gondii* proteins do not affect loading of PVs with IRG proteins. (A) IFN γ -stimulated MEF are shown 2 h after double infection with ME49 strain (indicated by arrow) and RH-YFP strain *T. gondii* (green, indicated by arrowhead). The ME49 strain parasite shows intense Irgb6 (serum A20, red) accumulation at the PV while the RH-YFP in the same cell has no Irgb6 on the PV. (B) The loading of Irga6 and Irgb6 onto PVs of avirulent ME49 strain *T. gondii* was unaffected by the presence of virulent RH-YFP in the same cells. IFN γ -stimulated MEFs were infected with *T. gondii* ME49 strain alone or simultaneously with ME49 and RH-YFP strains. Irgb6 (detected by serum A20) and Irga6 (detected by mAb 10D7) fluorescence intensities were measured on at least 30 ME49 PVs in singly and doubly infected cells. ME49 and RH-YFP were discriminated by the YFP signal in virulent RH-YFP. The arithmetic means are given as horizontal lines. (C) Ectopically expressed Ty-tagged ROP18 does not affect loading of *T. gondii* ME49 PVs with Irgb6 in infected L929 cells. L929 cells were induced with IFN γ , transfected with pGW1H expression plasmids encoding the mature form of ROP18 from either ME49 or RH-YFP *T. gondii* strains, or pmCherry-N3 as a transfection control and infected for 2 h with *T. gondii* ME49 strain. Cells were stained for Irgb6 (serum A20) and for Ty-tag to

identify the transfected cells. Irgb6 positive vacuoles in ROP18-Ty-tag and Cherry positive cells were enumerated. A total of approximately 700 vacuoles were scored in two independent experiments. **(D)** ROP16 and ROP5A-D do not affect Irgb6 loading onto *T. gondii* PV. IFN γ -stimulated MEFs were infected with S22-LC37 *T. gondii* strain expressing virulent 4 ROP5 and 2 other genes (see also Material and Methods and main text), RH- Δ rop16 and control parental strains S22 and RH for 2 h. Irgb6 positive PVs (stained with serum 141/1) were quantified from 350-500 intracellular parasites. The results shown are pooled from two independent experiments.

3.8 IRG complex formation is required for efficient loading onto *T. gondii* PV

IRG proteins are able to form homo- and heterotypic interactions within the family in cells (Hunn et al., 2008; Papic et al., 2008). GMS proteins of IRG GTPase family (Irgm1, Irgm2 and Irgm3), predominantly localised to intracellular membranes, regulate the correct localisation of proteins of the GKS subset (e.g. Irgb6, Irgb10, Irga6, Irgd) to ensure translocation of GKS proteins onto *T. gondii* PVM during infection (Hunn et al., 2008). Provided that GMS proteins are present in cells, Irga6 associates at a certain frequency with the vacuoles of avirulent *T. gondii*. However the amounts of Irga6 on the PVs could be significantly increased by ectopic expression of an extra GKS protein (Irgb6 or Irgd) (Khaminets et al., 2010). This result demonstrates that multiple IRG proteins load onto the *T. gondii* PV in a cooperative manner possibly achieved via protein-protein interactions between them (Hunn et al., 2008; Khaminets et al., 2010). Recombinant Irga6 displayed cooperative GTP hydrolysis and nucleotide-dependent oligomerisation *in vitro* (Uthaiyah et al., 2003). A number of amino acid residues of the Irga6 molecule, mutations in which essentially abrogated oligomerisation and GTP hydrolysis *in vitro* (E77A, G103R, S132R, R159E, K161E, K162E, D164A, N191R, E106R, K196D), clustered together on the surface of the protein and were called the “catalytic interface” (Figure 16A and (Pawlowski et al., in preparation)). Mutations in several other Irga6 residues, scattered all over the protein structure without forming a clear interaction surface, gave a mild defect in oligomerisation and GTP hydrolysis (R31E-K32E, K169E, K176E, R210E, K246E). The latter were branded the “secondary patch” (Figure 16A and (Pawlowski et al., in preparation)).

To investigate the role of the Irga6 catalytic interface, which could mediate homo- and possibly heterotypic interactions between IRG proteins, Irga6^{-/-} MEFs were stimulated with IFN γ and simultaneously transfected with the constructs expressing wt, catalytic interface and secondary patch mutants of Irga6-cTag1 and then infected with avirulent ME49 *T. gondii*. Photomicrographs of the typical IRG protein positive

and negative *T. gondii* vacuoles in cells expressing wt and mutant proteins are presented in Figure 16B and Appendix 6.1. Figure 16C shows that essentially all the catalytic interface mutants were impaired in loading onto *T. gondii* PV, while the secondary patch residues were dispensable. Exception was mutation of the K162 residue which was found to have only a slight effect on accumulation on *T. gondii* PVs (10% less than wt) (Figure 16C). K162 resides on the edge of the putative interface (Figure 16A) and possibly is only partially engaged in the interactions.

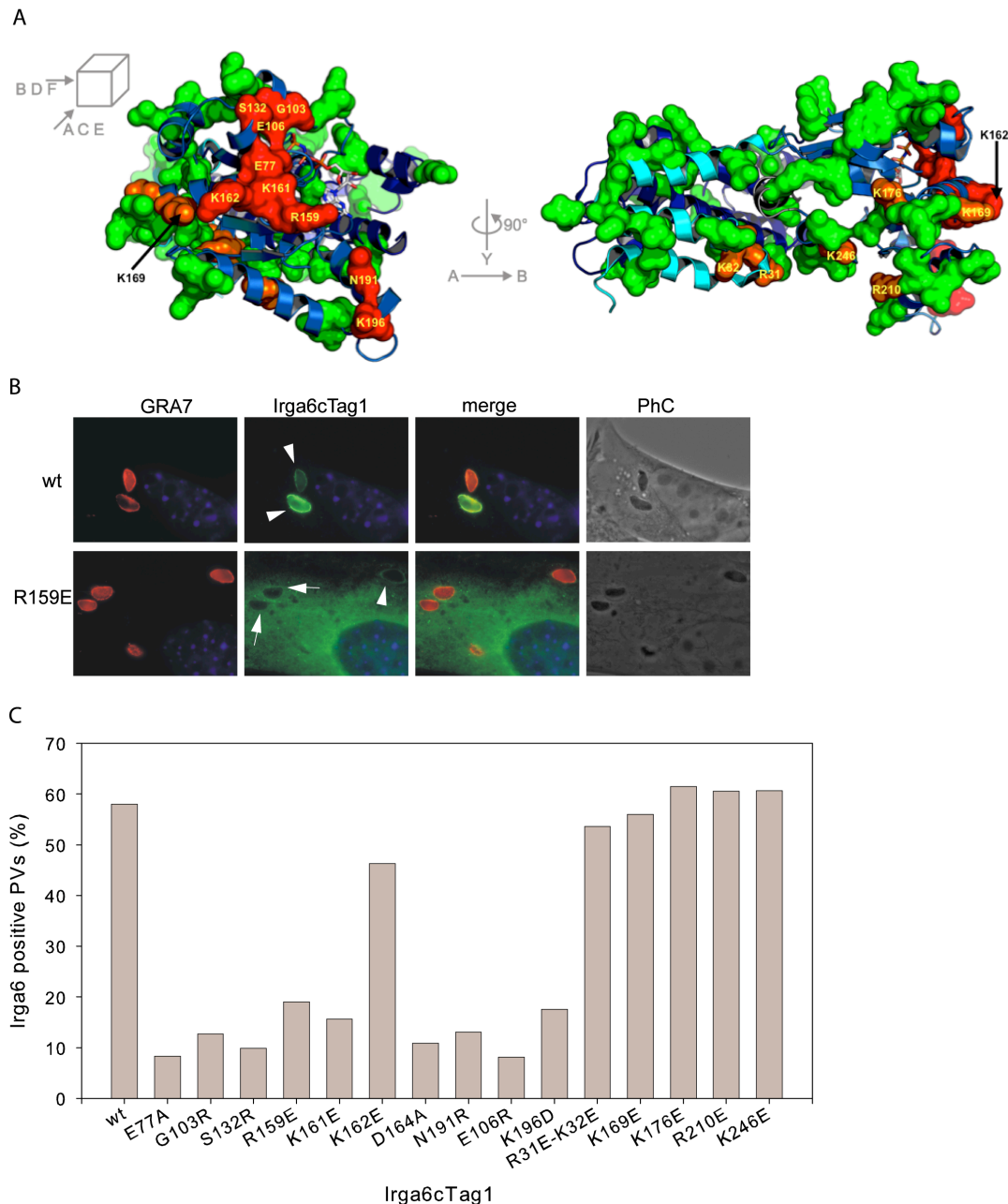


Figure 16 Catalytic interface of Irga6 is required for efficient loading on to the *T. gondii* PV.

(A) Position of the catalytic interface and the secondary patch on the crystal structure of Irga6. Irga6 (ribbon presentation) of the crystal-dimer-interface mutant M173A (PDB 1TQ6) (Ghosh et al., 2004). Residues, forming catalytic interface (E77A, G103R, S132R, R159E, K161E, K162E, D164A, N191R, E106R, K196D) are in red; secondary patch residues (R31E-K32E, K169E, K176E, R210E, K246E)

are in orange; mutated residues that had no effect on oligomerisation and GTP hydrolysis are in green (Pawlowski et al., in preparation). **(B and C)** Irga6^{-/-} MEFs were induced with IFN γ and simultaneously transfected for 24 h with pGW1H constructs expressing wt, catalytic interface and secondary patch mutants of Irga6-cTag1. The cells were subsequently infected with ME49 *T. gondii* for 2 h and stained for cTag1 (green) to identify transfected proteins and for GRA7 (red) to identify intracellular parasites. PhC is phase contrast. **(B)** Loading of wt (upper panels) and catalytic interface mutant R159E (lower panels) of Irga6-cTag1 onto ME49 *T. gondii* PVs. Arrowheads and arrows indicate Irga6 positive and Irga6 negative PVs, respectively. The representative photomicrographs of the whole set of mutants is presented in Appendix 6.1. **(C)** Quantification of wt and mutant Irga6c-Tag1 loading onto *T. gondii* PVs. cTag1 positive PVs were scored from approximately 200 intracellular parasites in cTag1 positive cells in 2 independent experiments and results were pooled. Catalytic interface mutants of Irga6-cTag1 are strongly inhibited in loading on to avirulent *T. gondii* PVs.

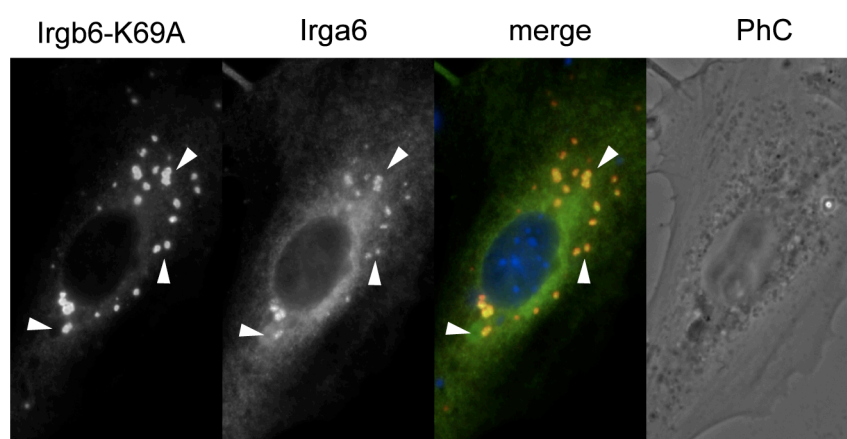
As stated above, the catalytic interface could be involved in both homo- and heterotypic interactions. Interactions with GMS proteins via this interface could lead to inhibition of GKS protein self-activation preventing aggregation (Hunn et al., 2008; Pawlowski et al., in preparation). When expressed in IFN γ -induced mouse fibroblasts several catalytic interface mutants indeed appeared to be aggregated (e.g. E106R, S132R; Appendix 6.1). However most of them displayed normal ER-like homogeneous pattern (e.g. R159E, K161E; Appendix 6.1). Future studies will determine whether GKS-GKS and GKS-GMS interactions are formed via the same or disparate interfaces between the IRG protein molecules.

3.9 Vacuolar loading with IRG proteins is required for *T. gondii* elimination

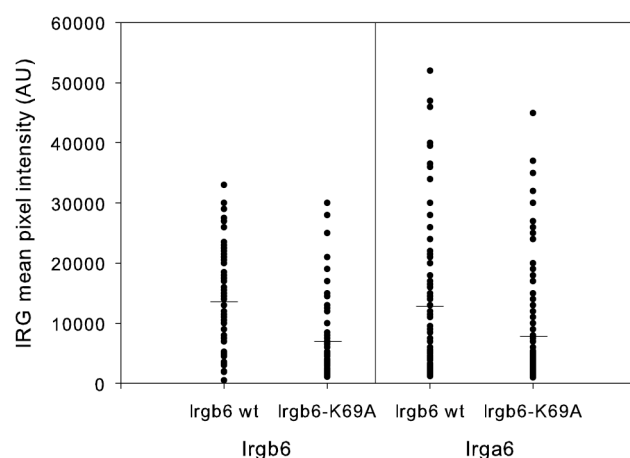
Biochemically dominant-positive and functionally dominant-negative Irga6-K82A has been previously used to study the effect of IRG protein loading onto parasite vacuoles in *T. gondii* elimination (Martens et al., 2005). In IFN γ -stimulated cells, PVs of the parasite appeared disrupted presumably as a result of vesiculation of the vacuolar membrane, and the involvement of IRG proteins in the process of intracellular parasite denudation was suggested (Martens et al., 2005; Ling et al., 2006; Zhao et al., 2008; Zhao et al., 2009b). *In vitro*, bacterially expressed and purified Irga6-K82A formed GTP-dependent oligomers which did not resolve with time in contrast to the wt protein. Moreover the mutant protein was virtually unable to hydrolyse GTP (Hunn et al., 2008). When expressed in IFN γ -stimulated cells Irga6-K82A aggregated and, through interaction with endogenous Irga6, interfered with the process of IRG protein loading onto *T. gondii* PVs (Martens et al., 2005). All these observations make the dominant-negative IRG proteins a powerful tool to study the functions of IRG GTPase in the context of infection with *T. gondii*. Two essential tools were employed to corroborate the role of vacuolar loading with IRG proteins in

the process of parasite killing. Firstly, I used the construct expressing Irgb6-K69A, an analogue of Irga6-K82A, motivated by the high frequency of Irgb6 positive *T. gondii* vacuoles relative to the other IRG proteins. Ectopically expressed Irgb6-K69A has been shown to aggregate and had a slight defect in loading onto avirulent *T. gondii* PVs (Hunn et al., 2008). I confirmed that in cells, expressing Irgb6-K69A-FLAG, endogenous Irgb6 and Irga6 proteins were significantly impaired in associating with ME49 *T. gondii* PVs (Figure 17B). Irgb6-K69A aggregates trapped endogenous proteins (Figure 17A) and prevented them from accumulating on *T. gondii* PVs.

A



B



Figures 17 Cellular aggregates of the dominant-negative Irgb6-K69A-FLAG colocalise with endogenous Irga6 and inhibit loading of endogenous Irgb6 and Irga6 onto ME49 *T. gondii* PV. (A) MEFs were stimulated with IFN γ and transfected with pGW1H plasmid expressing Irgb6-K69A-FLAG for 24 h. Cells were stained for FLAG (mAb M2) and Irga6 (serum 165). Irgb6-K69A-FLAG aggregates (indicated by arrowheads) trap endogenous Irga6. (B) MEFs were stimulated with IFN γ and transfected with pGW1H plasmids expressing Irgb6-wt-FLAG or Irgb6-K69A-FLAG for 24 h. Cells were then infected for 2 h with ME49 *T. gondii* and stained for FLAG tag (mAb m2) to identify the transfected cells, Irgb6 (serum A20) and Irga6 (serum 165). Irgb6 and Irga6 mean pixel intensities on 60-100 PVs were quantified as described in Material and Methods. Expression of Irgb6-K69A-FLAG

causes significant reduction of Irgb6 ($p < 0.001$) and Irga6 ($p = 0.0351$ by Mann-Whitney U-test) intensity on avirulent *T. gondii* PVs relative to the signal in Irgb6-wt-FLAG-expressing cells.

Secondly, to monitor *T. gondii* elimination I used the assay (Zhao et al., 2009b) based on permeabilisation of the parasite to cytoplasmic fluid proteins (EGFP, Cherry) in disrupted vacuoles (Figure 18A and Appendix 6.2). Clearly, expression of the dominant-negative Irgb6-K69A in IFN γ -stimulated MEFs reduced the number of EGFP positive parasites relative to the cells expressing wt protein (Figure 18B and C).

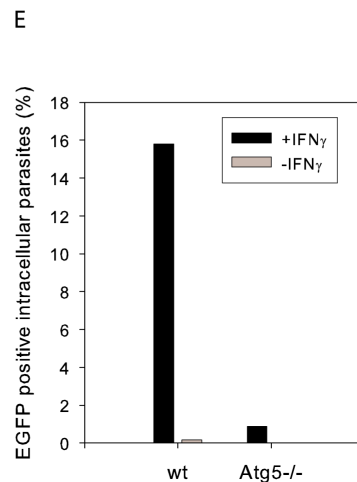
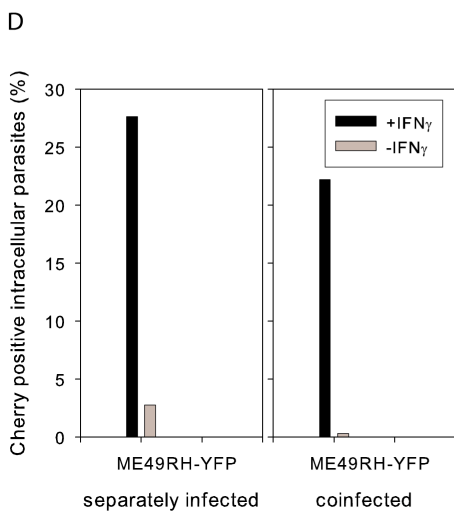
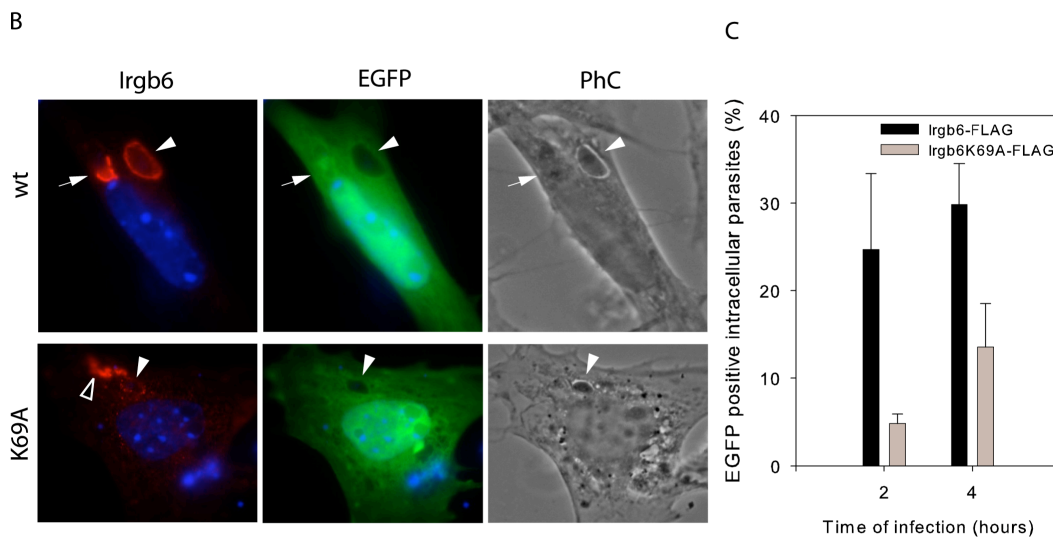
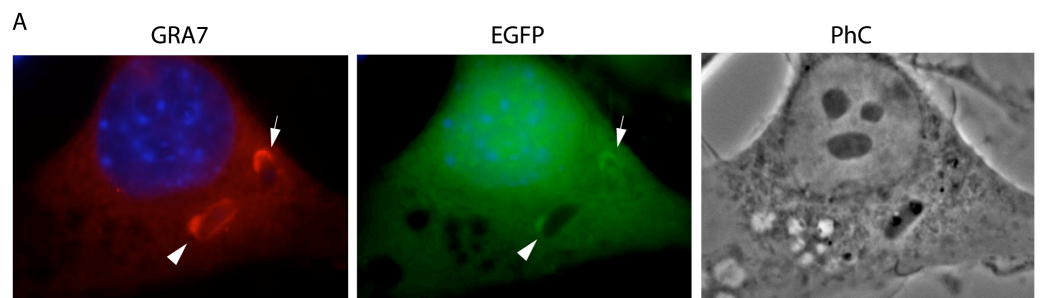


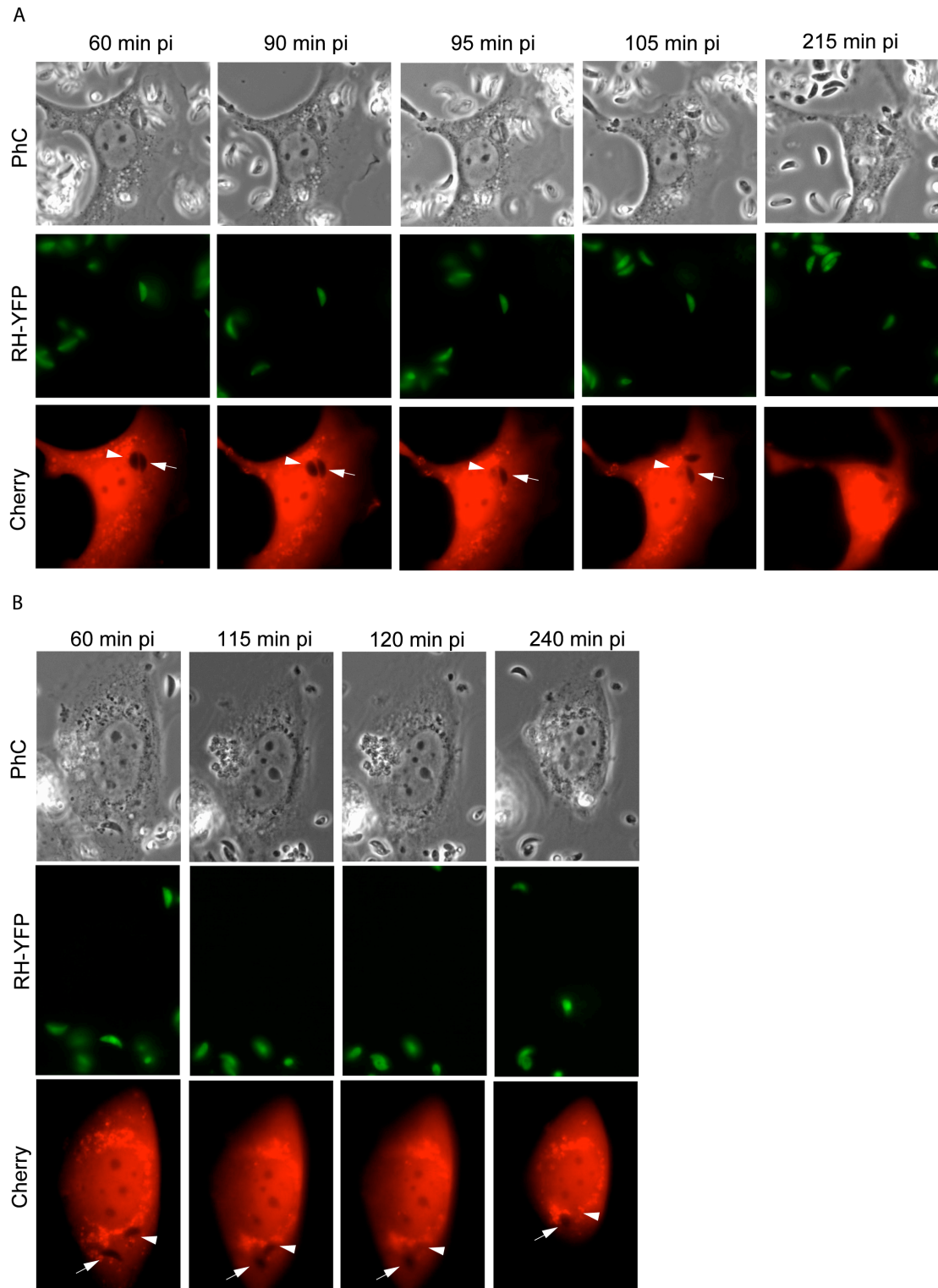
Figure 18 Loading of *T. gondii* PVs with IRG proteins determines elimination of the parasite in IFN γ -stimulated mouse fibroblasts.

(A) Killed avirulent *T. gondii* inside of disrupted PVM is permeable to cytosolic EGFP. MEFs were stimulated with IFN γ and simultaneously transfected with the construct pEGFP-N3 expressing EGFP for 24 h and then infected with ME49 *T. gondii* for 4 h. Intracellular parasites were identified by staining against GRA7 and by phase contrast (PhC). Arrows indicate the EGFP positive killed parasites and the arrowheads indicate live *T. gondii*. Note that the vacuolar membrane (identified by GRA7) of the dead parasite is disrupted and the PV protein GRA7 diffused into the cytoplasm of infected cell. (B and C) Irgb6 contributes to IFN γ -dependent killing of avirulent *T. gondii*. MEFs were stimulated with IFN γ and co-transfected with pEGFP-N3 and pGW1H plasmids coding for Irgb6-wt-FLAG (B, upper panels) or Irgb6-K69A-FLAG (B, lower panels) for 24 h. The cells were then infected for 4 h with ME49 *T. gondii* at MOI 5 and stained for FLAG tag (mAb m2) (red). Note that Irgb6-K69A-FLAG weakly associates with *T. gondii* PV and forms cytoplasmic aggregates (indicated by an empty arrowhead) as reported elsewhere (Hunn et al., 2008). Arrows indicate a permeabilised *T. gondii* in a disrupted vacuole and arrowheads indicate EGFP impermeable parasites in intact vacuoles. (C) Quantification of the permeabilised parasites at 2 and 4 h after infection of IFN γ -stimulated MEFs expressing EGFP and Irgb6-wt-FLAG or Irgb6-K69A-FLAG (as described in A and B). Intracellular parasites were identified by GRA7 staining and by phase contrast (PhC). Means and standard deviations of values from 3 experiments are shown. 50–200 PVs per data point were counted blind. (D) Avirulent *T. gondii* (ME49) is eliminated while virulent *T. gondii* (RH-YFP) is not in IFN γ -stimulated separately infected or coinfecting with both parasite strains MEFs. IFN γ -stimulated and transfected with pmCherry-N3 for 24 h MEFs were simultaneously or separately infected with ME49 and RH-YFP *T. gondii* for 4 h. Cherry positive *T. gondii* were counted from 250–350 intracellular parasites in 2 independent experiments and results were pooled. Intracellular parasites were identified by GRA7 staining and by phase contrast (PhC). Virulent parasites were distinguished from avirulent by YFP signal. (E) *T. gondii* elimination is severely impaired in Atg5^{-/-} fibroblasts. Wt and Atg5^{-/-} fibroblasts were stimulated with IFN γ and transfected with pEGFP-N3 for 24 h. The cells were then infected with ME49 *T. gondii* for 4 h and stained for GRA7. EGFP positive parasites were quantified from 400–600 intracellular parasites in 2 independent experiments and results were pooled. Intracellular parasites were identified by GRA7 staining and by phase contrast (PhC).

However, as previously reported (Martens et al., 2005; Khaminets et al., 2010), overexpression of IRG proteins of the GKS subgroup could accelerate loading of *T. gondii* vacuoles with IRG proteins and therefore GTPase overexpression itself could contribute to the parasite killing process. It is plausible, that nearly complete inability of dominant-negative IRG proteins to hydrolyse GTP, demonstrated for Irga6-K82A *in vitro*, may also have an impact on cellular functions of the IRG protein family (Hunn et al., 2008). These data, nonetheless, support the role of IRG protein loading in IFN γ -mediated control of *T. gondii*.

Virulent *T. gondii* efficiently inhibits IRG protein accumulation at the PVs and, as a result, could interfere with parasite killing (Figures 14 and 15). Figure 18D illustrates that in cells, separately infected or coinfecting with avirulent parasites, virulent *T. gondii* is resistant to the IRG-mediated elimination program, estimated by EGFP entry assay. The coinfection results were confirmed by live microscopy (Figure 19) in IFN γ -stimulated MEFs infected with unlabelled avirulent ME49 and YFP-expressing virulent RH-YFP *T. gondii* parasites. In neither of the presented videos was RH-YFP viability affected by the presence of ME49 in the same cell while ME49

parasite killing was recorded at indicated infection time (95 min pi for Figure 19A, 120 min pi for B), estimated by permeabilisation of the parasite to cytoplasmic Cherry.



Figures 19 Coinfection of MEFs with virulent and avirulent *T. gondii* does not influence *T. gondii* elimination.

MEFs were induced with IFN γ and simultaneously transfected with the expression plasmid pmCherry-N3, coding for Cherry. After 24 h the cells were coinfecting with *T. gondii* ME49 and RH-YFP strains in microscope slide chambers as described by in Material and Methods. Starting from 60 min pi, coinfecting cells were monitored continuously in order to document the fate of individual parasites. (**A and B**) Selected frames of two time-lapse videos of Cherry entry into avirulent ME49 *T. gondii* in the cells coinfecting with avirulent and virulent parasites. Arrowheads and arrows indicate the location of avirulent and virulent (distinguished YFP positive virulent parasites) *T. gondii* PVs. ME49 becomes permeable to Cherry at 95 min pi (in **A**) and 120 min pi (in **B**) while RH-YFP remains impermeable till the end of the each video (215 min pi in **A** and 240 min pi in **B**).

Hence, virulent *T. gondii* interferes with toxoplasmodicidal effects of IFN γ early during infection by inhibiting the process of vacuolar loading with IRG proteins. It is readily seen that loading of *T. gondii* PV with IRG proteins directly correlates with killing of the parasite and that these processes are tightly coupled as shown in the coinfection experiments (Zhao et al., 2009b; Khaminets et al., 2010).

IRG proteins fail to accumulate efficiently on *T. gondii* vacuoles in Atg5^{-/-} cells (Figure 11). This defect may result from mislocalisation and subsequent degradation of IRG proteins in IFN γ -stimulated cells. Consequently, Atg5^{-/-} cells were virtually unable to kill *T. gondii* demonstrated by entry of the cytoplasmic EGFP into intracellular parasites (Figure 18E). It is also not excluded, that lack of Atg5 itself or other factors malfunctioning in the absence of the autophagic regulator could deteriorate the toxoplasmodicidal process.

Taken together, these data provide a compelling evidence of the crucial role of IRG protein loading in eliminating *T. gondii* in IFN γ -stimulated mouse fibroblasts.

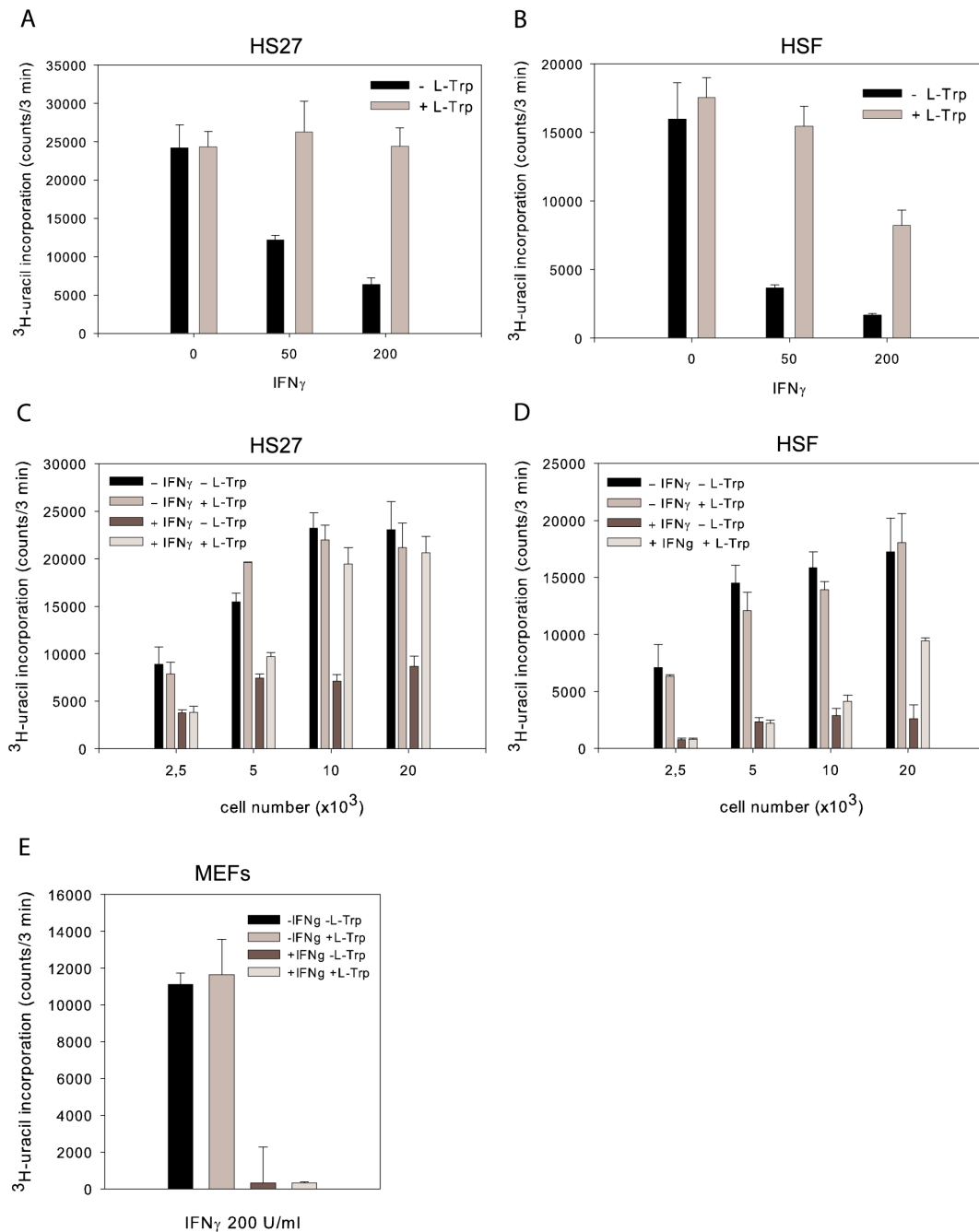
4 Results II

4.1 IDO-dependent and IDO-independent mechanisms of resistance against *T. gondii* in human cells

The field of cell-autonomous resistance to *T. gondii* in humans is mainly focused on tryptophan-depleting enzymes: IDO (Pfefferkorn, 1984; Daubener et al., 2001) and TDO (Schmidt et al., 2009). IDO efficiently protects human cells from infection by converting cellular tryptophan into N-formyl-kynurenine and thereby exhausting the source of this essential amino acid and as a result inhibiting *T. gondii* growth (Daubener et al., 2001). The action of both IDO and TDO could be overcome by addition of tryptophan surplus to the culture medium or by using pharmacological inhibitors of the enzymes such as 1-MT (1-methyl-tryptophan) (Heseler et al., 2008).

Employing one of the previously reported protocols to study *T. gondii* proliferation (Heseler et al., 2008) I was able to rescue avirulent ME49 parasite growth by adding tryptophan to IFN γ -stimulated human primary foreskin fibroblasts (Hs27) and primary skin fibroblasts (HSF) (Figure 20A and B). As reported earlier, IDO was not involved in *T. gondii* control in mouse cells and, expectedly, tryptophan addition was dispensable (Figure 20E and (Könen-Waisman and Howard, 2007)). However, it was noticed such modifications in the protocol as cell density and the period of IFN γ stimulation resulted in complete failure to restore proliferation of the parasite via addition of tryptophan to IFN γ -induced human cells (Steffi Könen-Waisman, unpublished data). To reconcile the controversy, I set out to identify the parameter varying among experimental procedures that influenced the outcome of infection. Surprisingly, the amount of cells seeded in the 96-well plates proved to be the crucial factor determining tryptophan-mediated rescue of *T. gondii* replication in IFN γ -induced primary fibroblasts (Figure 20C and D). Figure 20C and D shows that only IFN γ -induced human cell cultures of a certain density (in this case seeded at amount of 10^4 Hs27 and 2×10^4 HSF cells) allowed ME49 *T. gondii* proliferation after addition of tryptophan. Conversely, 5×10^3 Hs27 and 10^4 HSF cells (the numbers specify the amount of seeded cells) restricted *T. gondii* growth even in the presence of exogenous tryptophan. Primary human cells used in these experiments grow in a controlled manner and cease to proliferate as soon as they reach 100% confluence in the dishes. It is therefore conceivable that IDO controls *T. gondii* only in stationary nondividing

cells, and a new, still to be identified mechanism, independent of IDO, is operating in proliferating IFN γ -stimulated primary fibroblasts.



Figures 20 IDO-dependent and IDO-independent mechanisms of *T. gondii* growth restriction in IFN γ -induced primary human fibroblasts.

Proliferation of *T. gondii* was examined by ^3H -uracil incorporation assay as described in Material and Methods. (A and B) 2×10^4 Hs27 (A) and HSF (B) cells were seeded in 96-well plates and induced with IFN γ (50 or 200 U/ml) for 72 h. L-Trp was then added to wells to the final concentration of 0.55 mM and the cells were infected with ME49 *T. gondii* at MOI 1 for 48 h. The cultures were subsequently labelled with ^3H -uracil (0.33 mCi/well) and further incubated for 24 h before freezing. The amount of radioactivity incorporated into the proliferating parasites was measured and presented in counts/3 min. L-Trp restores *T. gondii* growth in IFN γ -induced nonproliferating human fibroblasts. (C and D) Indicated amounts of Hs27 (C) and HSF (D) cells were seeded in 96-well plates and induced with IFN γ (200 U/ml) for 24 h. L-Trp was then added to the wells to the final concentration of 0.55 mM and the cells were infected with ME49 *T. gondii* at MOI 1 for 48 h. The cultures were subsequently labelled

with ^3H -uracil (0.33 mCi /well) and further incubated for 24 h before freezing. The amount of radioactivity incorporated into the proliferating parasites was measured and presented in counts/3 min. Cell number affects the ability of L-Trp to restore *T. gondii* growth in IFN γ -induced human fibroblasts. **(E)** L-Trp fails to restore *T. gondii* growth in IFN γ -induced MEFs. 2×10^4 MEFs were seeded in 96-well plates and induced with IFN γ (200 U/ml) for 72 h. L-Trp was then added to wells to the final concentration of 0.55 mM. Cells were subsequently infected with ME49 *T. gondii* at MOI 1 for 48 h and further processed as described in **(A and B)**.

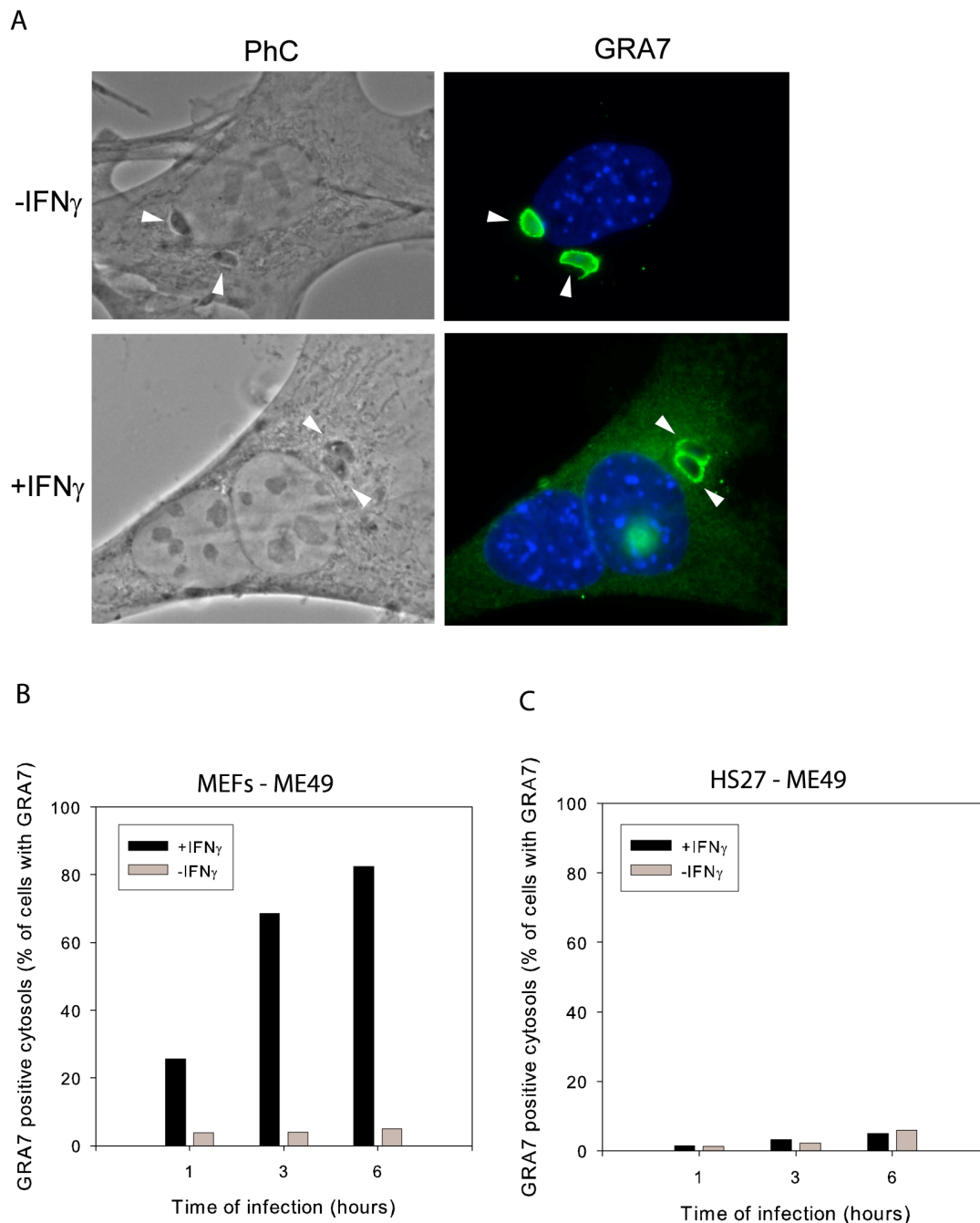
4.2 Disruption of *T. gondii* vacuoles is not apparent in IFN γ -induced primary human fibroblasts

Results presented in Figure 20 evidence the existence of a novel IDO-independent mechanism, eliminating *T. gondii* in IFN γ -induced human fibroblasts. IRG proteins determine resistance to *T. gondii* in mouse cells, triggering disruption of the PV followed by killing of the parasite and necrotic death of the host cell (Zhao et al., 2009b). However, the whole IFN γ -inducible IRG system is absent in humans (Bekpen et al., 2005), suggesting that alternative factors may functionally replace mouse IRG proteins regulating immune control of the parasite. Thus, it was interesting to examine whether an alternative mechanism of *T. gondii* elimination in human cells follows analogous steps as in mouse cells, i.e. disruption of the vacuole, killing of the pathogen and subsequent death of the infected cell (Zhao et al., 2009b).

To estimate disruption of vacuoles in IFN γ -induced human and mouse cells, I used an assay based on diffusion of the *T. gondii* protein GRA7, normally sequestered in the PV, into the cytoplasm of the infected cell. GRA7 “leakage” into the cytosol has been observed to accompany vesiculation of the vacuolar membrane in IFN γ -induced mouse cells ((Martens et al., 2005), Figure 18A and Appendix 6.2) and therefore indicated a loss of PV integrity. Figure 21A depicts GRA7 positive (lower panels) and GRA7 negative cytosols (upper panels) of IFN γ -treated and IFN γ -untreated mouse fibroblasts, respectively, infected with avirulent ME49 *T. gondii*. GRA7 positive cytosols were quantified at the specified time points after infection of mouse and human cells and the results were presented in Figure 21B and C. Disruption of ME49 *T. gondii* PVs was nearly completely undetectable in human cells, estimated by the frequency of GRA7 positive cytosols, whereas the numbers of GRA7 positive mouse cells progressively increased over the time of infection.

To examine the rate of *T. gondii* killing in human cells I used an assay based on entry of cytoplasmic EGFP into dead parasites in disrupted vacuoles ((Zhao et al., 2009b) and Figure 18A). From 1000 and 900 intracellular parasites, analysed in IFN γ -

induced and IFN γ -uninduced primary human fibroblasts, infected for 4 h with ME49 *T. gondii*, only 2 and 0 EGFP positive parasites were found in respective samples in stark contrast to IFN γ -stimulated mouse cells presented in Figure 18. In summary, neither vacuolar disruption nor *T. gondii* death, as documented in IFN γ -induced mouse cells, occurs in IFN γ -induced primary human fibroblasts implying the existence of another mechanism of *T. gondii* elimination in human cells.



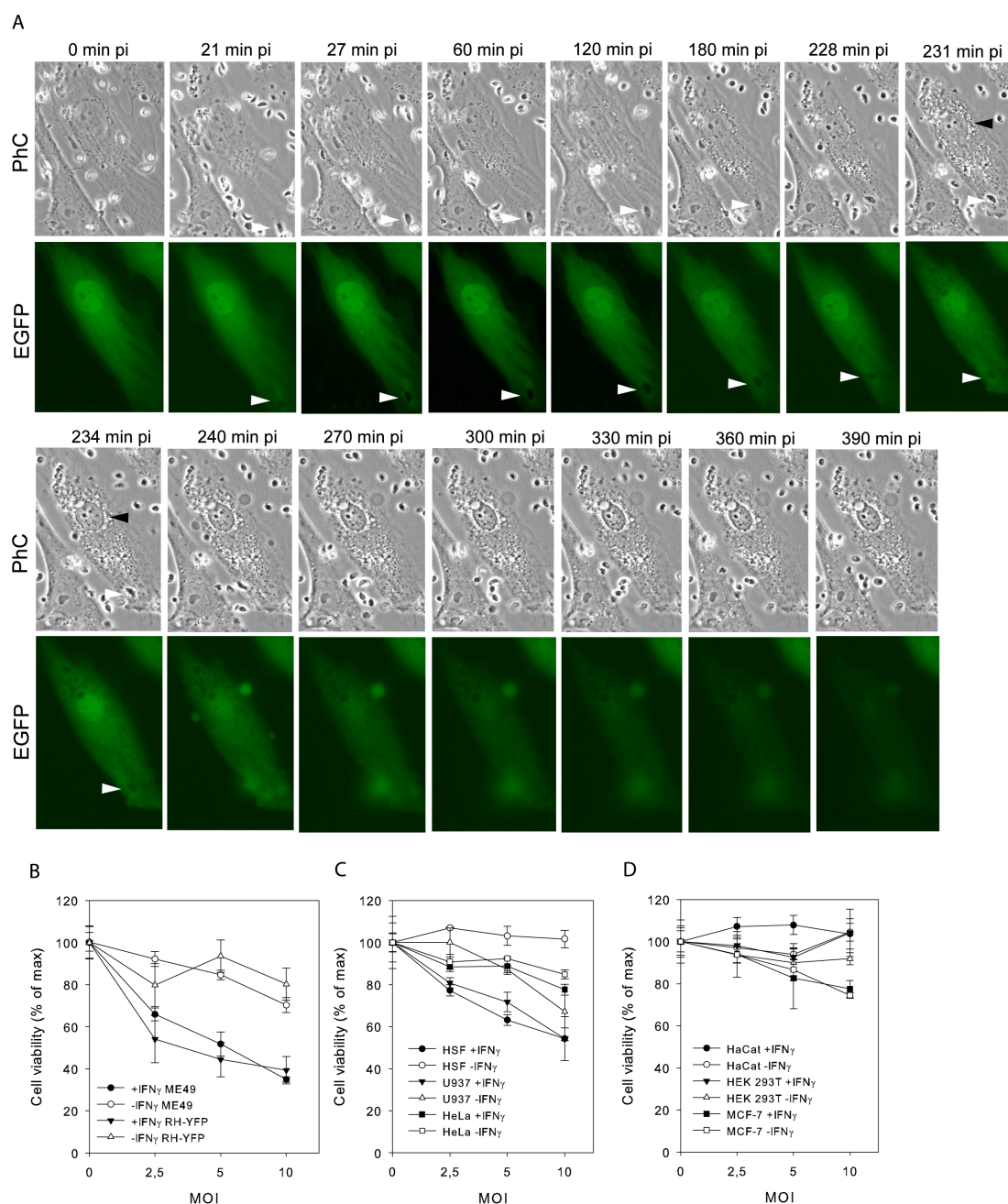
Figures 21 Vacuoles of *T. gondii* do not disrupt in IFN γ -induced primary human fibroblasts. Disruption of the PVM in IFN γ -induced mouse and human fibroblasts was assayed by release of *T. gondii* protein GRA7 from PVs into host cell cytosols. (A) GRA7 is released into cytosol during vacuolar disruption in IFN γ -induced mouse cells. IFN γ -stimulated (upper panels) and untreated (lower panels) MEFs were infected with ME49 *T. gondii* for 6 h and stained for GRA7. IFN γ -induced

disruption of *T. gondii* PVM is accompanied by GRA7 release into host cell cytosol. Arrowheads indicate location of intracellular parasites. PhC is phase contrast. **(B and C)** GRA7 is released into the cytosol of IFN γ -induced mouse but not of IFN γ -induced human fibroblasts. IFN γ -stimulated and untreated MEFs and Hs27 cells were infected with ME49 *T. gondii* for 1, 3 and 6 h and stained for GRA7. GRA7 positive cytosols were counted from 400-500 GRA7 positive cells (containing GRA7 on *T. gondii* PV and in cytoplasm).

4.3 IFN γ stimulates death of distinct types of *T. gondii*-infected human cells

IFN γ -induced mouse fibroblasts undergo necrotic death upon infection with avirulent *T. gondii*, following disruption of PVs (Zhao et al., 2009b). To document the consequences of ME49 *T. gondii* infection in human cells, IFN γ -stimulated Hs27 cells were monitored in live cell microscopy. Hs27 cells were stimulated with IFN γ and in parallel transfected with a construct expressing EGFP to facilitate identification of infected cells, as described in Material and Methods. Figure 22A shows irregular serial movie frames focused on an infected cell (white arrowhead points at *T. gondii* PV). 231-234 min pi (220 min after invasion) the infected cell acquired characteristics of cell death: vacuolarisation of the cytoplasm, partial shrinkage of the nucleus (indicated by black arrowhead) and cell immotility. Strikingly, 234 min pi *T. gondii* appeared to be no longer intra- but extracellular, and, furthermore, cytoplasmic EGFP signal gradually decreased within the observed interval of 234-390 min pi. The frames from another movie (only phase contrast), presented in Appendix 6.3, show death of the infected cell at 278 min pi indicated by partial shrinkage of the nucleus (labelled by the empty arrowhead). These and data from the other movies (not shown) evidenced the signs of cell death (judged by characteristics presented above) at 61 min, 101 min, 155 min, 220 min, 257 and 273 min after invasion which all together define the range of 61-273 min, within which cell death was observed. To summarize, *T. gondii* is able to kill IFN γ -stimulated human cells, and observed cell death is accompanied by loss of plasma membrane integrity.

Decrease of Hs27 cell viability was observed by the colorimetric assay (described in Material and Methods) when cells were stimulated with IFN γ and infected with either virulent type I RH-YFP or avirulent type II ME49 *T. gondii* strains (Figure 22B) at specified MOI. Type I RH-YFP has been reported to fail to induce death of IFN γ -stimulated mouse cells because of the inability to disrupt virulent *T. gondii* vacuoles (Zhao et al., 2009b). On the contrary, human cell death occurs even in absence of vacuolar disruption indicating the differences in initiation step of the cell death in mouse and human systems (Figure 22B).

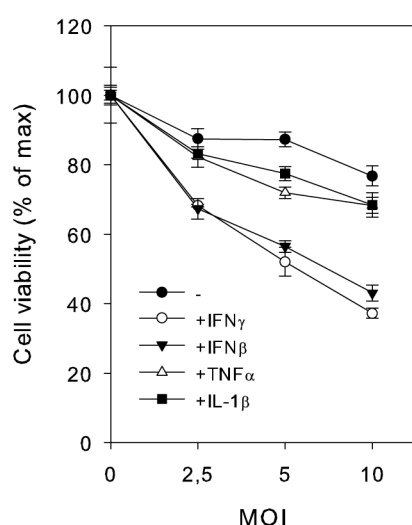


Figures 22 IFN γ induces death of certain types of *T. gondii* infected-human cells.

(A) Hs27 cells were transfected with the expression plasmid pEGFP-N3 and simultaneously induced with IFN γ . After 24 h, the cells were infected with *T. gondii* ME49 strain in microscope slide chambers as described by in Material and Methods and monitored continuously to observe the fate of the parasite and the infected cell. White arrowheads indicate the location of the *T. gondii* PV. After 231 min pi infected cell undergoes dramatic changes: vacuolarisation of the cytoplasm, partial shrinkage of the nucleus (indicated by the black arrowhead), immotility of the cell; cytoplasmic content is released from the cell (instant release of *T. gondii* and gradual release of EGFP). (B) IFN γ decreases viability of ME49 and RH-YFP *T. gondii*-infected Hs27 cells. IFN γ -stimulated Hs27 cells were infected with ME49 and RH-YFP strains of *T. gondii* at indicated MOI for 8 h in triplicates in 96-well plates. Cell viability was measured via colorimetric assay as described in Material and Methods and presented as percentage of cell viability of noninfected (MOI 0) cells. (C and D) IFN γ decreases viability of ME49 *T. gondii*-infected primary human skin fibroblasts (HSF) and human lymphoma cell line (U937) but not of ME49 *T. gondii*-infected cervical carcinoma (HeLa), human keratinocyte (HaCaT), human embryonic kidney cells (HEK 293T) and breast carcinoma (MCF-7) cell lines. IFN γ -stimulated human cells were infected with ME49 *T. gondii* at indicated MOI for 8 h in triplicates in 96-well plates and treated as in (B). Note that *T. gondii* alone induces marked death of IFN γ -unstimulated U937 cells.

It is noteworthy that IFN γ induction alone did not affect viability of analysed human cells (data not shown); infection with *T. gondii* had a slight effect, whereas only combination of IFN γ and infection yielded massive cell mortality.

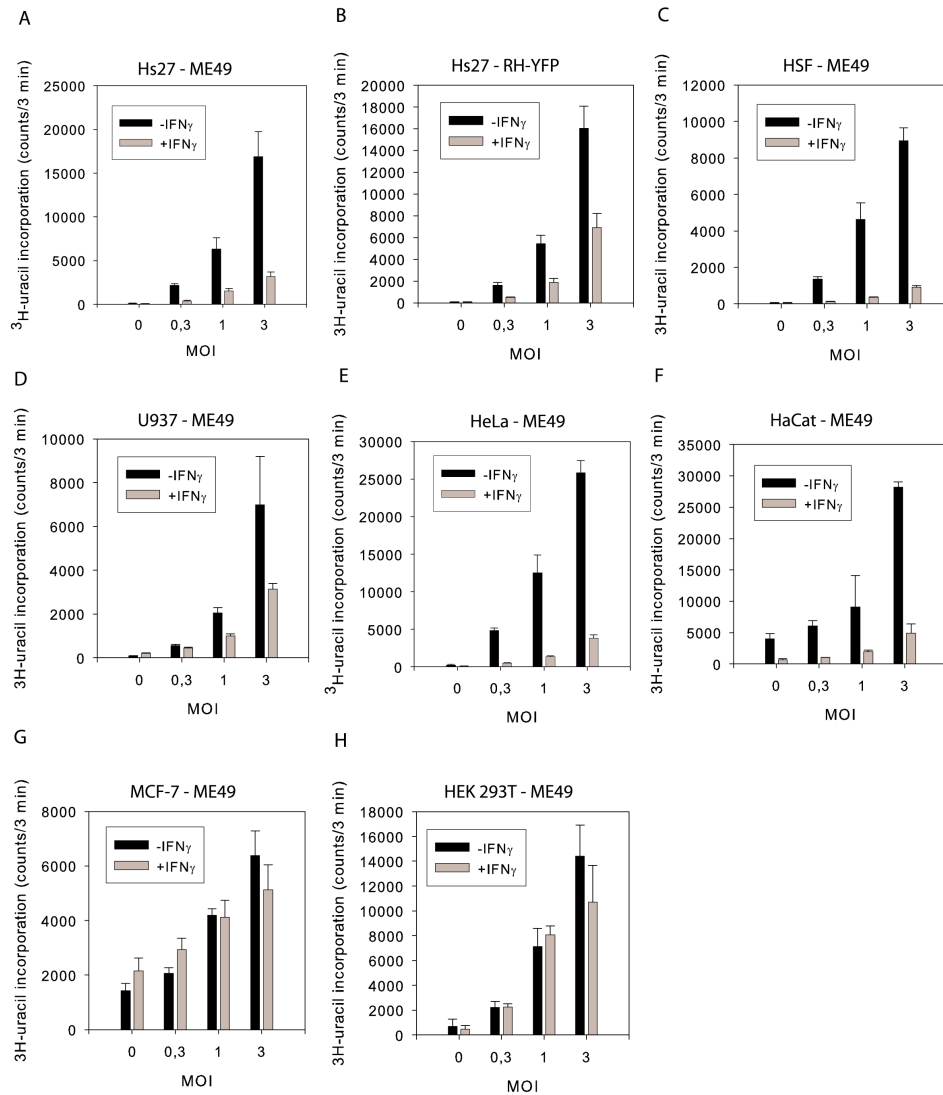
Type I IFN β stimulated death of infected Hs27 cells as efficiently as IFN γ whereas TNF α and IL-1 β , at used concentrations, had only a minor but stable effect (Figure 23 and data not shown). This result demonstrates that, interferons, in one group, and TNF α and IL-1 β , in another group of cytokines, differentially induce death of *T. gondii*-infected primary human cells which could be helpful in identification of the candidate genes, responsible for this effect.



Figures 23 Differential induction of *T. gondii*-dependent Hs27 cell death by distinct cytokines. 7.5×10^3 Hs27 cells were seeded in 96-well plates and induced with IFN γ (200 U/ml), IFN β (1000 U/ml), TNF α (200 U/ml) or IL-1 β (2000 U/ml) for 24 h. The cells were then infected with ME49 *T. gondii* at indicated MOI for 8 h. Cell viability was measured via colorimetric assay as described in Material and Methods and presented as percentage of cell viability of noninfected (MOI 0) cells. TNF α and IL-1 β induce only slight increase of *T. gondii*-infected Hs27 cell death relative to interferons.

Interestingly, IFN γ failed to stimulate the death of cervical carcinoma (HeLa), human keratinocyte (HaCaT), human embryonic kidney cells (HEK 293T) and breast carcinoma (MCF-7) cell lines in contrast to human skin fibroblasts (HSF) and human lymphoma cell line (U937) which displayed striking decrease of viability during ME49 *T. gondii* infection (Figure 22C and D). In case of Hs27, HSF, U937 (cells died and ME49 *T. gondii* growth was inhibited), MCF-7 and HEK 293T (both cell types did not die and ME49 *T. gondii* growth was not controlled by IFN γ) cell death directly correlated with IFN γ -mediated control or lack of control of ME49 *T. gondii* replication, analysed by ^3H -uracil incorporation assay (Figure 22C and D and Figure

24). However, in absence of cell death, IFN γ was still able to restrain ME49 *T. gondii* growth in HeLa and HaCaT cells indicating that in these cell lines cell death was not related to the mechanism of resistance to the parasite (Figure 22C and D and Figure 24). As mentioned above *T. gondii*-infected primary human cells displayed some degree of mortality independently of IFN γ whereas U937 human lymphoma cell line was dying without IFN γ almost as efficient as after stimulation with the cytokine (Figure 22B and C).

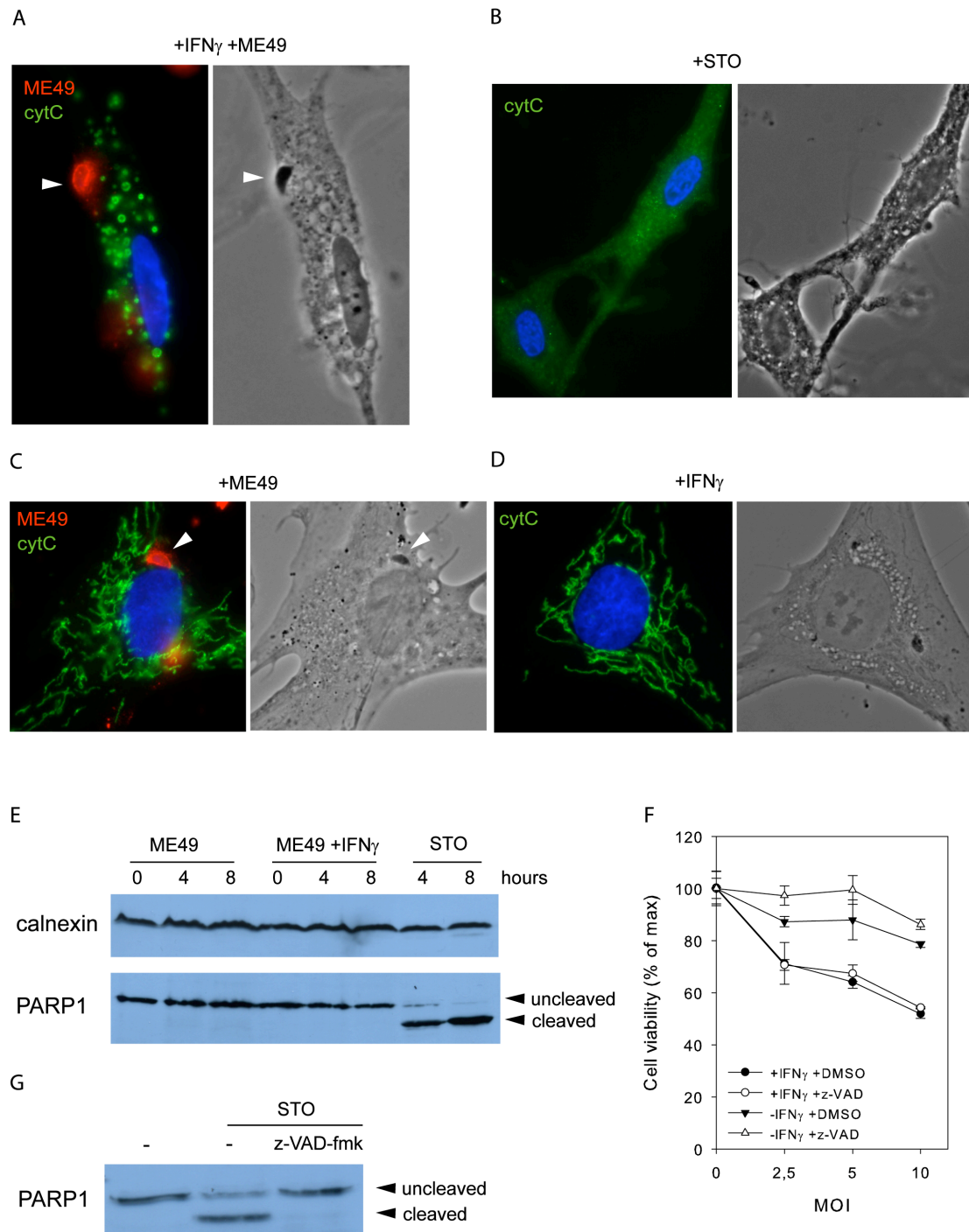


Figures 24 ME49 and RH-YFP *T. gondii* proliferation in IFN γ -stimulated and unstimulated human cells.

Proliferation of *T. gondii* was examined by ³H-uracil incorporation assay as described in Material and Methods. 7.5×10^3 Hs27 (A and B), HSF (C), HeLa (E), HaCaT (F), MCF-7 (G), HEK 293T (H) and 3×10^4 U937 (D), cells were seeded in 96-well plates and induced with IFN γ (200 U/ml) for 24 h. Cells were then infected with RH-YFP (A) and ME49 (B-F) strains of *T. gondii* at indicated MOI for 24 h. The cultures were subsequently labelled with ³H-uracil (0.33 mCi/well) and further incubated for 24 h before freezing. The amount of radioactivity incorporated into proliferating parasites was measured and presented in counts/3 min.

4.4 Human cells, stimulated with IFN γ and infected with *T. gondii*, undergo necrosis but not apoptosis

IFN γ -induced primary human cells infected with ME49 *T. gondii* do not undergo apoptotic cell death based on the following evidence.



Figures 25 IFN γ -stimulated *T. gondii*-infected human cells do not undergo apoptosis.

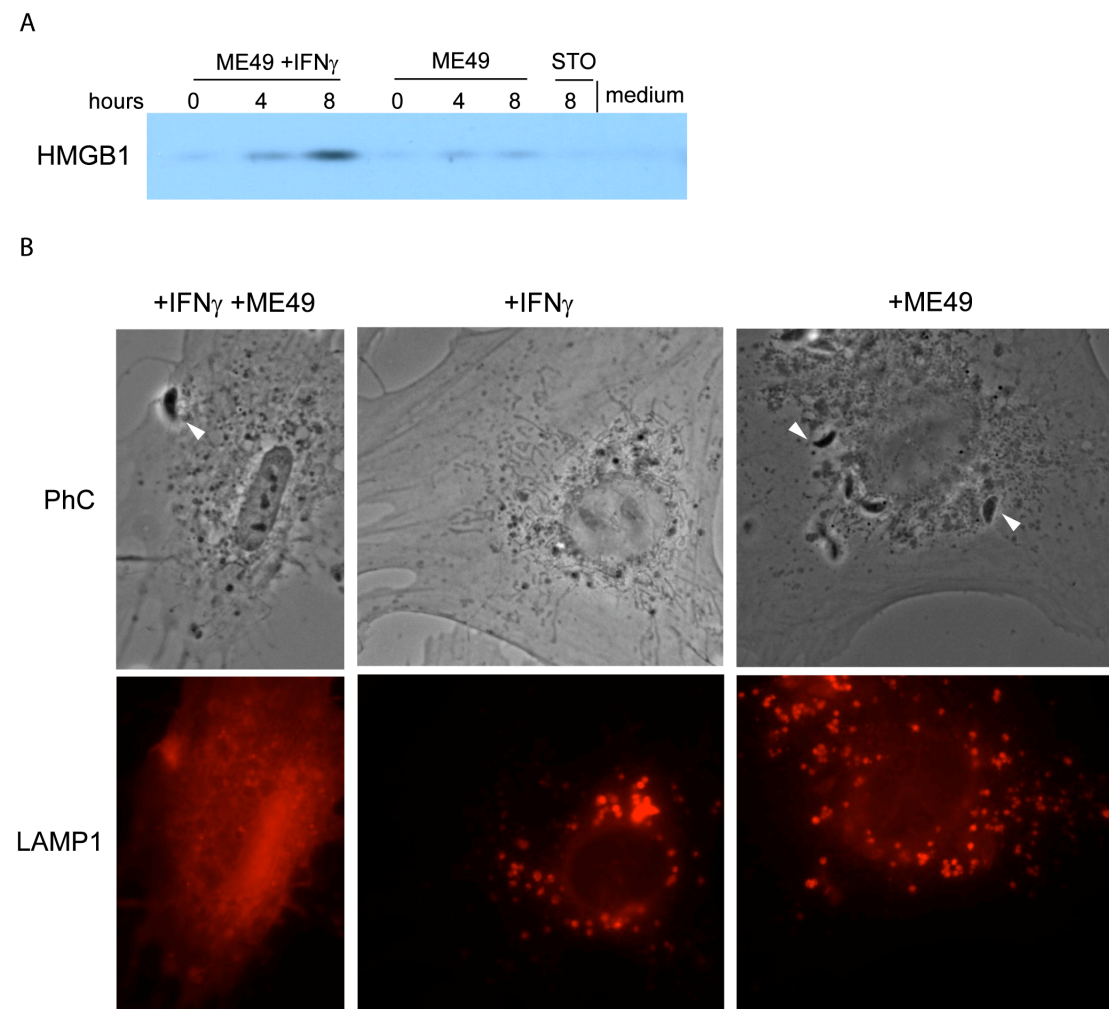
(A-D) Cytochrome C is not released from mitochondria into cytoplasm of IFN γ -stimulated and *T. gondii*-infected Hs27 cells. IFN γ -stimulated (A and D) or unstimulated (C) Hs27 cells were infected with ME49 *T. gondii* for 4 h and stained for *T. gondii* (rabbit serum) and CytC. Cytochrome C is released from mitochondria into cytoplasm of Hs27 cells treated with staurosporine (STO, 1 mM) for 4 h (B). Note that mitochondria of IFN γ -stimulated *T. gondii*-infected Hs27 cell in (A) became

fragmented. (E) PARP1 is not cleaved during IFN γ stimulation and *T. gondii* infection of Hs27 cells. IFN γ -stimulated or unstimulated Hs27 cells were infected with ME49 *T. gondii* for indicated periods of time (uninfected cells are designated as 0 h time point) and analysed by Western Blot using anti-PARP1 antibody and calnexin as a loading control. As a positive control staurosporine (STO, 1 mM) treated cells were used. (F) Pan-caspase inhibitor z-VAD-fmk fails to inhibit IFN γ -stimulated death of *T. gondii*-infected Hs27 cells. IFN γ -stimulated Hs27 cells were pretreated with caspase inhibitor z-VAD-fmk (100 mM) for 2 h and then infected with ME49 and strains of *T. gondii* at indicated MOI for 8 h in 96-well plates. Cell viability was measured via colorimetric assay as described in Material and Methods and presented as percentage of cell viability of noneinfected (MOI 0) cells. (G) z-VAD-fmk efficiently inhibits apoptotic caspases in Hs27 cells. Hs27 cells were pretreated with z-VAD-fmk for 2h followed by stimulation with staurosporine (STO, 1 mM) for 6 h. The amount of PARP1 processing by caspases was analysed by Western blot.

Firstly, one of the hallmarks of apoptosis, release of cytochrome C from mitochondria into the cytosol (Goldstein et al., 2000) did not occur (analysed in fixed cells infected with *T. gondii* for 30 min, 1 h, 3 h and 6 h) during infection and IFN γ stimulation (Figure 25A, C and D and data not shown) whereas cytochrome C release was apparent in cells treated with apoptosis inducer staurosporine (STO) (Figure 25B). Secondly, specific caspase-mediated cleavage of poly(ADP-ribose) polymerase 1, typically occurring during apoptosis (Kaufmann et al., 1993), was not detected in IFN γ -induced infected and uninfected cells in contrast to cells stimulated by STO as a positive control (Figure 25E). Finally, decline of Hs27 cell viability, caused by IFN γ stimulation and ME49 *T. gondii* infection, was not affected by the inhibitor of the apoptotic caspases z-VAD-fmk (Figure 25F; for control experiment see Figure 25G).

As described in the previous section 4.3, plasma membrane integrity was disturbed as a result of IFN γ stimulation and infection of primary human cells with *T. gondii* (Figure 21A). Permeabilisation of cellular plasmalemma is known to be associated with necrotic cell death (Golstein and Kroemer, 2007). To further corroborate occurrence of necrosis of the *T. gondii*-infected IFN γ -stimulated human cells, release of the immune adjuvant HMGB1 from nuclei of dying cells into the medium was analysed (Scaffidi, Misteli, and Bianchi, 2002). Amounts of HMGB1, detected in supernatants of *T. gondii*-infected and IFN γ -induced cells, increased over time indicating plasma and nuclei membrane disruption (0 time point represents uninfected samples, staurosporine treated apoptotic cells and medium were used as negative controls) (Figure 26A). In addition, total rupture of the lysosomes, documented as another feature of necrosis (Guicciardi, Leist, and Gores, 2004), was observed in human cells stimulated with IFN γ and infected with *T. gondii* (Figure 26B).

All together, compelling evidence presented here confirms induction of necrosis in *T. gondii*-infected IFN γ -stimulated human cells. The proinflammatory content of the cell released during the course of necrotic cell death can enhance the immune response to *T. gondii* and subsequent clearance of the parasite *in vivo*.



Figures 26 IFN γ -stimulated *T. gondii*-infected human cells undergo necrosis.

(A) Nuclei protein HMGB1 is released from IFN γ -stimulated *T. gondii*-infected Hs27 cells into culture medium. IFN γ -stimulated or unstimulated Hs27 cells were infected with ME49 *T. gondii* for indicated periods of time (uninfected cells are designated as 0 h time point), culture medium was collected and analysed by Western Blot using anti-HMGB1 antibody. As negative controls, medium and supernatant from staurosporine (STO, 1 mM) treated cells were used. (B) Complete rupture of lysosomes in IFN γ -stimulated *T. gondii*-infected Hs27 cells. IFN γ -stimulated (right and left panels) or unstimulated (middle panels) Hs27 cells were infected with ME49 *T. gondii* (left and middle panels) for 4 h and stained for LAMP1. PhC is phase contrast. Arrowheads indicate the location of intracellular *T. gondii*.

Notably, mitochondria, stained by α -cytochrome C antibody (Figure 25A), appeared fragmented in IFN γ -induced and infected cells suggesting the involvement of this organelle in cell death (Barsoum et al., 2006; Dimmer et al., 2008). Morphology of mitochondria was further assayed by live microscopy of IFN γ -induced human cells preloaded with MitoTracker and infected with ME49 *T. gondii*. Figure 27

contains irregular frames of a video displaying the cell death at 155 min pi. Notably, mitochondria, visualised by MitoTracker Red, became fragmented simultaneously with incomplete shrinkage of the nucleus. Therefore, it is likely that alterations of mitochondrial morphology could solely be a result of a necrotic program but not a trigger of the cell death.

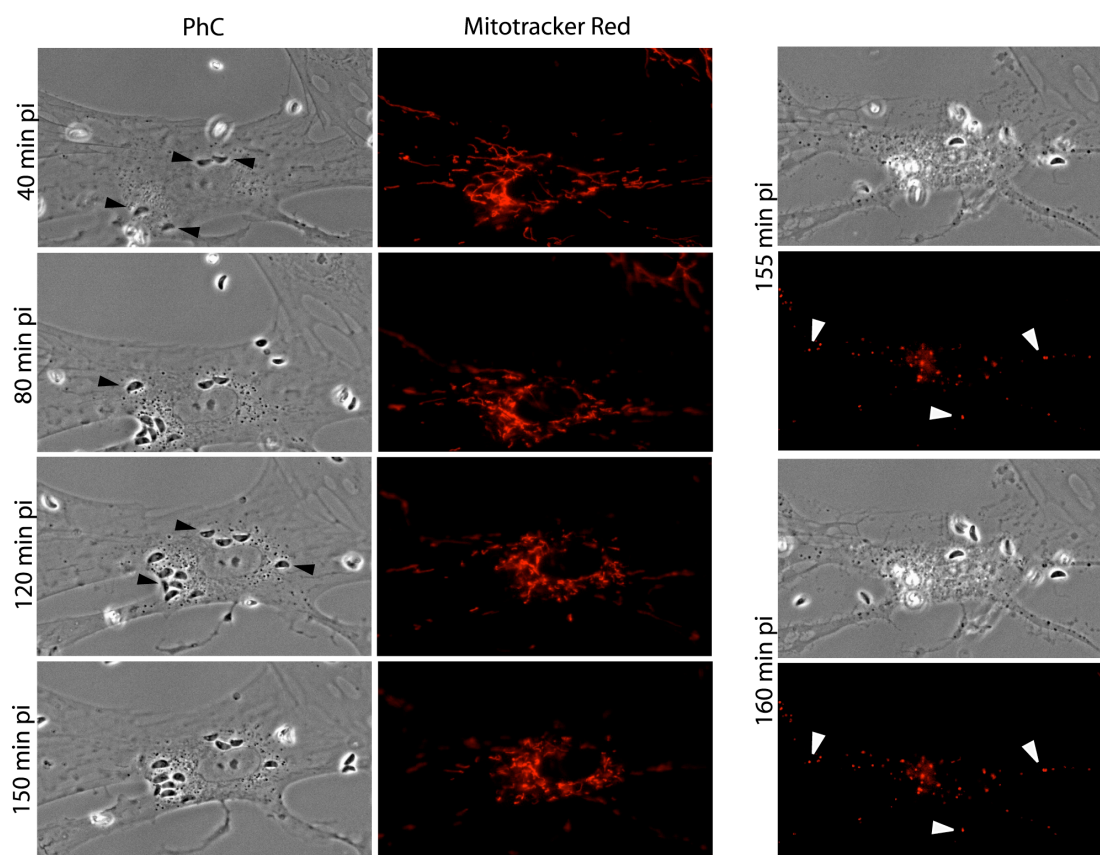


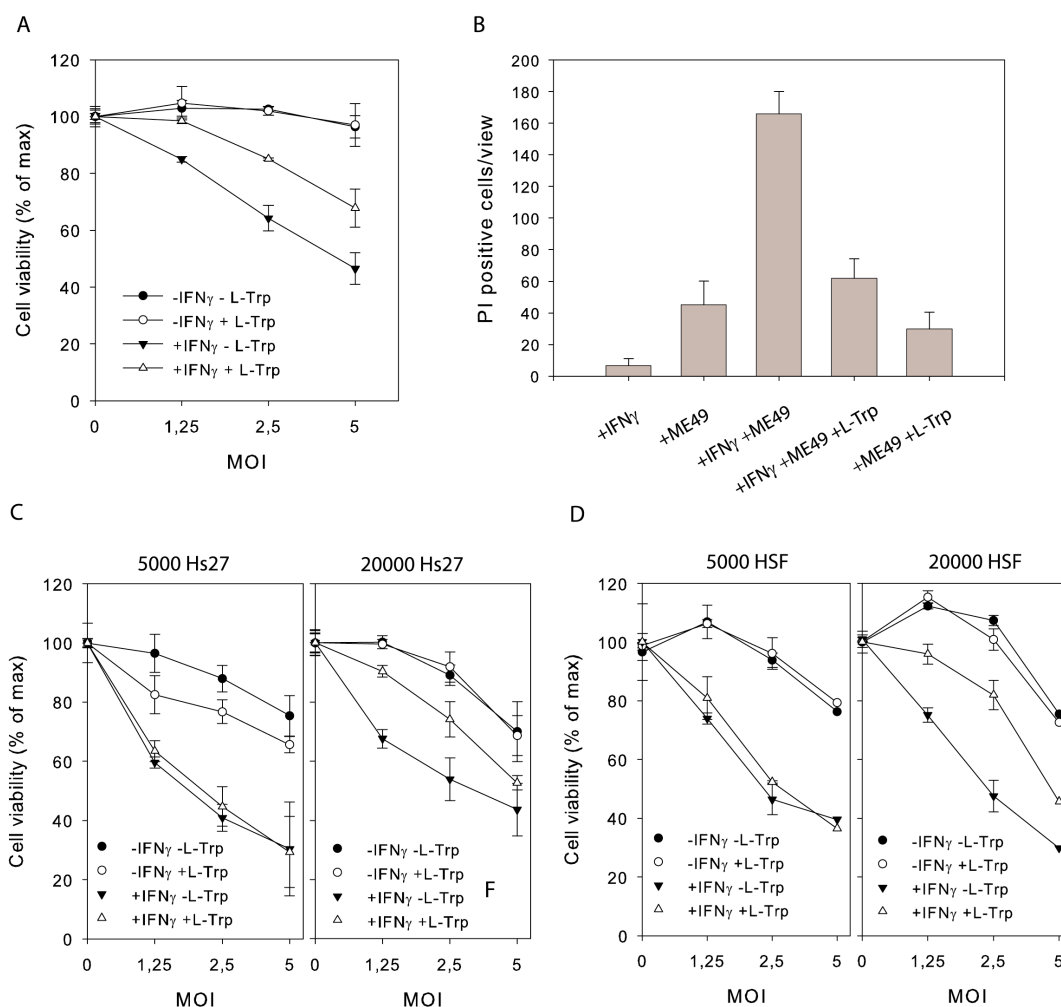
Figure 27 Fragmentation of mitochondria occurs concurrently with late manifestations of necrosis in IFN γ -stimulated *T. gondii*-infected human fibroblasts.

IFN γ -stimulated Hs27 cells were preloaded with MitoTracker Red for 1 h and then infected with *T. gondii* ME49 strain in microscope slide chambers as described in Material and Methods and monitored continuously to observe the infected cell. On 155 min pi frame mitochondria became fragmented (indicated by empty arrowheads) which coincided with partial nucleus shrinkage. Filled arrowheads indicate location of the *T. gondii* PVs.

4.5 Addition of tryptophan inhibits necrosis of human fibroblasts during IDO-dependent but not during IDO-independent course of IFN γ -mediated control of *T. gondii*

Supplementation of the culture medium with tryptophan rescues *T. gondii* growth in IFN γ -stimulated cells during an IDO-dependent course of *T. gondii* control ((Pfefferkorn, 1984; Pfefferkorn and Guyre, 1984; Daubener et al., 2001; Heseler et al., 2008) and Figure 20A and B). Interestingly, the parasite was able to induce death

of IFN γ -induced Hs27 and HSF cells seeded in amounts exerting both IDO-independent and IDO-dependent modes of *T. gondii* growth control (5×10^3 and 2×10^4 cells for IDO-independent and IDO-dependent, respectively) (Figure 28C and D). Therefore, I set out to inspect viability of primary human cells upon stimulation with IFN γ , infection with ME49 *T. gondii* and addition of tryptophan. Strikingly, addition of tryptophan considerably restored viability of dense (seeded at 2×10^4 cells) Hs27 cells after stimulation with IFN γ and 24 h infection with ME49 *T. gondii* (Figure 28A, right panels of C and D). On the contrary, viability of IFN γ -induced Hs27 and HSF cells, seeded in amounts exerting IDO-independent control of *T. gondii* (in amount of 5×10^3 cells), was not affected by tryptophan after infection with the parasite (left panels of Figure 28C and D).



Figures 28 Tryptophan inhibits necrosis of human fibroblasts during IDO-dependent but not during IDO-independent course of IFN γ -mediated *T. gondii* control.

(A) 2×10^4 Hs27 cells were seeded in 96-well plates and induced with IFN γ (200 U/ml) for 72 h. L-Trp was then added to the wells to the final concentration of 0.55 mM and the cells were infected with ME49 *T. gondii* at indicated MOI for 24 h. Cell viability was measured via colorimetric assay as described in Material and Methods and presented as percentage of cell viability of noninfected (MOI 0) cells. (B) L-Tryptophan reduces the frequency of propidium iodide (PI) positive cells in IFN γ -

stimulated *T. gondii*-infected Hs27 cell cultures. 10^5 Hs27 cells were seeded in microscope dishes as described in Material and Methods and induced with IFN γ (200 U/ml) for 72 h. L-Trp was then added to the wells to the final concentration of 0.55 mM and the cells were infected with ME49 *T. gondii* at MOI 5 for 24 h. PI was added to the medium and incubated for 15 min before microscopical analysis. The images of 5 random views from each treatment were taken from which the numbers of PI positive cells were counted. The means and the standard deviations between 5 views are presented. The representative images of all treatments are shown in Appendix 6.4. The experiment was performed twice and the results from one representative are shown. (C and D) indicated amounts of Hs27 (C) and HSF (D) cells were seeded in 96-well plates and induced with IFN γ (200 U/ml) for 24 h. L-Trp was then added to the wells to the final concentration of 0.55 mM and the cells were infected with ME49 *T. gondii* at indicated MOI for 24 h. Cell viability was measured as described in Material and Methods and presented as percentage of cell viability of noninfected (MOI 0) cells.

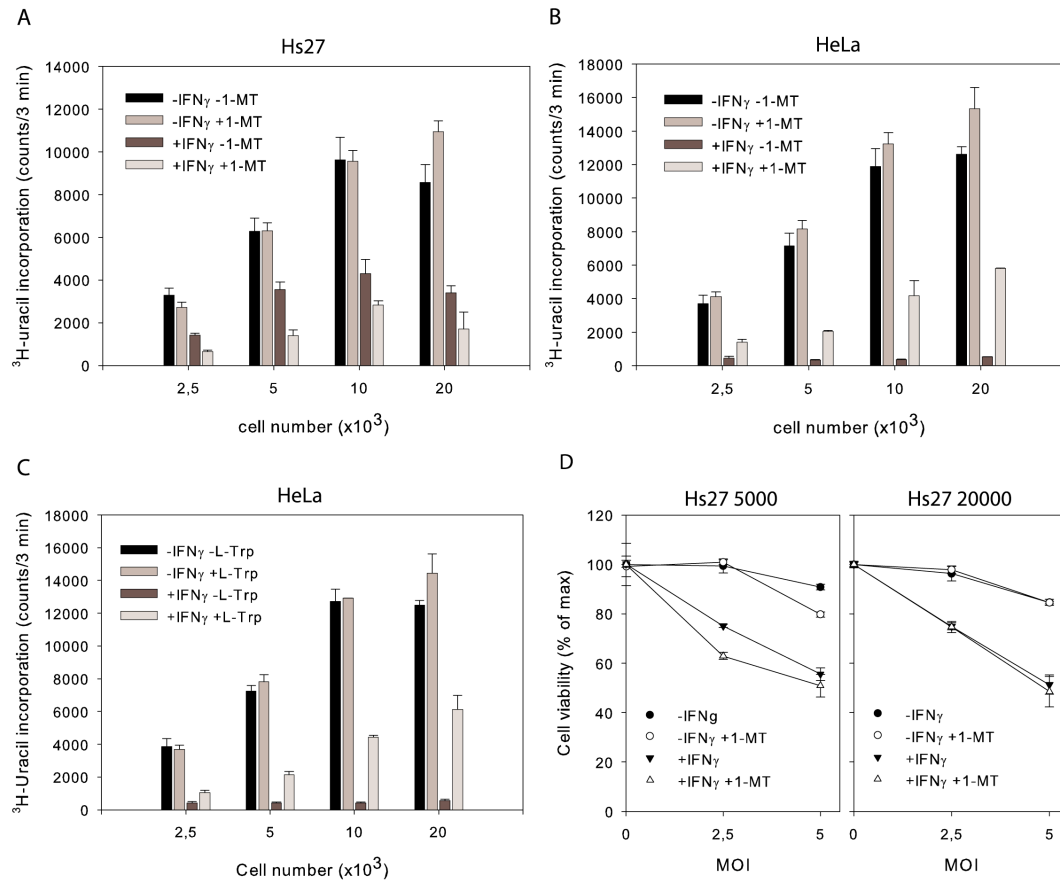
To corroborate in another approach the restoration of dense (and possibly nonproliferating) Hs27 cell viability by tryptophan during induction with IFN γ and infection with avirulent ME49 *T. gondii*, I used DNA intercalator propidium iodide (PI) capable of diffusing into dead cell nuclei and emitting fluorescence if bound to the substrate. PI has been ubiquitously used as a marker for identification of necrotic cells (Dive et al., 1992). Addition of tryptophan to IFN γ -stimulated confluent Hs27 cells (exerting IDO-dependent control of *T. gondii*) before infection with ME49 *T. gondii*, as described in Material and Methods, markedly decreased the frequency of PI positive cells (Figure 28B; representative views are presented in Appendix 6.4). Consistent with this result, IFN γ -induced Hs27 cells, supplemented with tryptophan, appeared less damaged by ME49 *T. gondii* infection compared to the cells without the amino acid, estimated by phase contrast (Appendix 6.4).

To summarise, tryptophan addition restores viability of dense (and probably nonreplicating) but not of subconfluent (and replicating) primary human cells stimulated with IFN γ and infected with *T. gondii*. Tryptophan-mediated rescue of Hs27 cell viability during IFN γ induction and *T. gondii* infection directly correlates with restoration of parasite proliferation in human cells induced with IFN γ (Figure 21). These data strongly emphasize the influence of experimental conditions in determining IFN γ -regulated immunity to *T. gondii*.

4.6 Pharmacological inhibition of IDO rescues *T. gondii* growth in IFN γ -stimulated HeLa cells but not in primary human fibroblasts

IFN γ -stimulated Hs27 and HeLa cells were competent to control *T. gondii* growth at any tested cell concentration (Figure 20 and Figure 29A, B and C). However, cell death was evident only for primary human fibroblasts after IFN γ stimulation and *T.*

gondii infection but not for HeLa cells implying that arrest of the parasite growth could be mediated independently of cell death (Figure 22C and D). To examine whether restriction of *T. gondii* proliferation in HeLa cells was mediated by IDO, I used a potent inhibitor of the enzyme 1-methyl-tryptophan (1-MT) (Heseler et al., 2008).



Figures 29 IDO inhibition by 1-methyl-tryptophan (1-MT) rescues *T. gondii* growth in IFN γ -stimulated HeLa but not in Hs27 primary human fibroblasts.

Proliferation of *T. gondii* was examined by ³H-uracil incorporation assay as described in Material and Methods. Specified amount of Hs27 (A) and HeLa (B) cells were seeded in 96-well plates and induced with IFN γ (200 U/ml) and 1-MT (1.5 mM) for 24 h. The cells were then infected with ME49 *T. gondii* at MOI 1 for 48 h. The cultures were subsequently labelled with ³H-uracil (0.33 mCi /well) and further incubated for 24 h before freezing. The amount of radioactivity incorporated into proliferating parasites was measured and presented in counts/3 min. (C) Indicated amounts of HeLa cells were seeded in 96-well plates and induced with IFN γ (200 U/ml) for 24 h. L-Trp was then added to the wells to the final concentration of 0.55 mM and the cells were infected with ME49 *T. gondii* at MOI 1 for 48 h. The plates were further processed as described in (A and B). (D) Specified amounts of Hs27 cells were seeded in 96-well plates and induced with IFN γ (200 U/ml) for 24 h and 1-MT (1.5 mM). Cell viability was measured as described in Material and Methods and presented as percentage of cell viability of noninfected (MOI 0) cells.

Hs27 and HeLa cells, seeded in specified amounts, were induced with IFN γ and simultaneously treated with 1-MT for 24 h before infection with ME49 *T. gondii*. As anticipated, 1-MT restored *T. gondii* growth in IFN γ -induced HeLa (at any tested cell

concentration) cells but not in Hs27 fibroblasts (Figure 29A, B). 1-MT-mediated rescue of *T. gondii* proliferation in HeLa cells directly correlated with restoration of parasite growth in cells supplemented with exogenous tryptophan (Figure 29B, C). Additionally, IDO inhibition by 1-MT did not affect Hs27 cell mortality, elicited by IFN γ stimulation and *T. gondii* infection (Figure 29D), indicating that cell death was not mediated by the tryptophan-depleting enzymes. It was observed that 1-MT itself slightly decreased viability of the analysed IFN γ -stimulated cells (data not shown).

To summarise, IFN γ -induced HeLa cells efficiently inhibit *T. gondii*-elicited necrosis and use IDO as the major immune factor. The failure of 1-MT to rescue *T. gondii* replication in IFN γ -induced primary human fibroblasts could be attributed to existence of another mechanism, dominant over IDO. All the data described in sections 4.1, and 4.3-4.5 suggest that proinflammatory necrotic cell death could serve as an IDO-independent mechanism of parasite elimination, clearing off infected cells or, alternatively, cell mortality may be a result of events eliminating *T. gondii* in IFN γ -induced primary human cells and culminating in necrosis. Extensive analysis of the molecular mechanism of parasite-induced necrosis is needed to understand the impact of the cell death in cell-autonomous immunity to *T. gondii*.

5 Discussion

Humans and mice possess distinct mechanisms of cell-autonomous immunity to *T. gondii* (Könen-Waisman and Howard, 2007; Coers, Starnbach, and Howard, 2009). The IRG protein system plays a central part in coping with infection in mice (Martens and Howard, 2006; Taylor, 2007). The process of parasite elimination in IFN γ -induced mouse cells begins with accumulation of IRG proteins on the *T. gondii* PV, followed by disruption of the vacuolar membrane, demise of the parasite and necrotic death of the host cell (Zhao et al., 2009b). It has been discussed that this type of cell death could lead to augmentation of the inflammatory response to the parasite *in vivo* by releasing intracellular content (e.g. ATP, HMGB1) (Scaffidi, Misteli, and Bianchi, 2002; Chen et al., 2004). In human cells, tryptophan depletion by IDO has been reported to dominate in resistance to *T. gondii* (Pfefferkorn, 1984; Daubener et al., 2001). However existence of alternative mechanisms has also been previously reported (Woodman, Dimier, and Bout, 1991; MacKenzie et al., 1999).

In this study various aspects of IRG protein loading onto *T. gondii* vacuoles have been analysed. It is shown that parasite elimination entirely depends on the process of IRG protein association with PVs once again emphasizing its crucial role in mouse cell-autonomous resistance to *T. gondii*.

The second part of the study proves existence and provides the basis for IDO-independent mechanism of *T. gondii* containment in IFN γ -stimulated human primary cells. Necrotic death of *T. gondii*-infected and IFN γ -stimulated primary human cells is documented and suggested to execute IDO-independent immunity, reminiscent of the analogous scenario in the mouse system but without participation of IRG proteins (Zhao et al., 2009b).

5.1 Heterogeneity of IRG protein loading onto vacuoles with avirulent *T. gondii*

IRG proteins were detected on vacuoles of avirulent *T. gondii* within minutes of infection (Figure 7A, B and Figure 8A, B). Initiation of loading was followed by rapid increase in frequency of IRG positive vacuoles and amounts of the proteins on individual PVs within 5-30 min after infection (Figure 7). Interestingly, in some cases intracellular parasites remained unloaded for variable periods of time (Figure 8 and (Khaminets et al., 2010)). This lag phase of loading initiation indicates the existence

of the certain conditions (e.g. local concentration of the proteins) which need to be fulfilled for IRG proteins to bind to *T. gondii* PVs. Alternatively, avirulent *T. gondii* could be endowed with the means to delay or disable association of IRG proteins with vacuoles, the phenomenon particularly pronounced in case of virulent strains of the parasite (Figure 8A, Figure 14 and (Khaminets et al., 2010)). The delay in IRG protein association with PVs contributes to heterogeneity of IRG signal on vacuoles. In other words, at any observed time after infection the whole range of vacuoles from nearly completely unloaded to the very intensely loaded with IRG proteins could be found (Figure 7C and D). One obvious explanation for the observed heterogeneity is asynchrony in infection (Figure 8A). However, synchronization of the *T. gondii* infection and thorough washing off free parasites did not affect the range of the IRG signal intensity on the vacuoles indicating of the presence of other factors responsible for the heterogeneity of the IRG protein signal on PVs.

Concentration of the proteins would be another parameter limiting the process of IRG GTPase loading onto *T. gondii* PVs. In particular, prolonged time of IFN γ induction resulted in elevated cellular concentration of IRG proteins and enhanced vacuolar association (Khaminets et al., 2010). Absence of Atg5 or GMS regulators in IFN γ -stimulated cells led to aggregation and degradation of GKS proteins reducing cellular pools of the GKS IRG proteins and thereby diminishing protein accumulation on *T. gondii* PVs during infection (Figure 11 and (Hunn et al., 2008; Henry et al., 2009; Khaminets et al., 2010)). Despite that, it was observed that when a cell containing one IRG positive vacuole was infected by another parasite, the latter accumulated IRG proteins faster than the former implying that cellular concentration of proteins is not the only factor regulating the loading process (Zhao et al., 2009b). Granted that neither delayed infection nor protein concentration had a critical impact on heterogeneity of IRG protein signal on avirulent *T. gondii* PVs, the process of loading appears to be a subject to regulation by numerous host cell and parasite-derived factors. So, the balance between targeting and counter-targeting processes determines the early and crucial step of intracellular pathogen recognition and elimination.

Multiple IRG proteins load sequentially onto avirulent *T. gondii* PVs (Figure 9 and (Khaminets et al., 2010)). Irgb6 and Irgb10 are the pioneer proteins, associating earlier and in higher amounts than the other members of the IRG family studied so far

in C57BL/6 MEFs. The temporal difference in loading of various IRG proteins onto avirulent *T. gondii* PVs analysed at 2 h after avirulent *T. gondii* infection built a spatial hierarchy (Khaminets et al., 2010). IRG proteins occupied various proportions of vacuoles in the order Irgb6>Irgb10>Irga6>Irgd=Irgm2 and in inclusion relationship. In other words, nearly all vacuoles with IRG proteins lower in the hierarchy were also positive for the higher member of the hierarchy. These results indicate a highly correlated occupancy of *T. gondii* PVs by IRG proteins (Khaminets et al., 2010). It is therefore conceivable, that certain IRG proteins provide anchoring sites for and thereby initiate binding of the other proteins. However, removal of Irga6 did not affect loading of Irgd and Irgm2 (lower than Irga6 in the hierarchy) onto avirulent *T. gondii* PVs implying some degree of redundancy (Khaminets et al., 2010) or involvement of additional factors, proteins or lipids, which are to be discovered. Interestingly, amounts of Irgb6 loaded on individual vacuoles appeared to be reduced in cells lacking Irga6 suggesting that binding of IRG proteins to PVs is cooperative. Indeed, in presence of GMS proteins concurrent expression of either Irgb6 or Irgd GKS proteins intensified loading of Irga6 onto *T. gondii* vacuoles (Khaminets et al., 2010). Cooperative loading of IRG GKS proteins onto *T. gondii* vacuoles most certainly results from direct protein-protein interactions, occurring on the PVM, documented elsewhere (Hunn et al., 2008). Accordingly, differential strength of IRG-IRG protein interactions formed at or in close proximity to *T. gondii* vacuoles could underlie hierarchical loading. However this is still to be tested experimentally. Currently it is not clear whether correlated hierarchical loading is essential for resistance to *T. gondii* although it was observed that distorted loading in case of virulent strains (section 5.5) leads to severe defects of resistance to infection (Zhao et al., 2009b; Khaminets et al., 2010).

5.2 Regulation of IRG proteins by Atg5 in IFN γ -stimulated mouse fibroblasts

Mouse cells lacking the autophagic regulator Atg5 are impaired in loading of IRG proteins onto avirulent *T. gondii* vacuoles (Figure 11A and B). Reduced IRG accumulation on *T. gondii* PVs correlate with the virtual loss of IFN γ -mediated inhibition of parasite growth (Könen-Waisman and Howard, 2007). In contrast to Zhao et al, reporting vacuolar deficit only for Irga6 (Zhao et al., 2008), two more GKS IRG proteins, Irgb6 and Irgd, were also found affected in cells lacking Atg5

(Figure 11). Interestingly, in resting as well as in *T. gondii*-infected Atg5-deficient fibroblasts IRG protein aggregates were observed (Figure 13 and (Zhao et al., 2008)), which indicates that the defect in loading results from general protein misbehavior in IFN γ -stimulated cells prior to infection. In line with that idea, mislocalisation of the analysed IRG proteins was accompanied by reduced cellular concentrations of the GTPases (Figure 11C). Pulse-chase analysis revealed diminished half-life of Irgb6 in Atg5-deficient fibroblasts (approximately 3 h) compared to wt cells (approximately 17 h) (Figure 12). Taken all together, it could be inferred that Atg5 has an indirect effect on IRG protein loading onto *T. gondii* PV, since absence of Atg5 causes inappropriate activation of the GKS proteins resulting in their mislocalisation, aggregation and subsequent degradation. Irga6 aggregates in Atg5-deficient cells appeared to be positive for the 10D7 antibody, specific for the GTP-bound state of the protein (Figure 11D and (Papic et al., 2008)). In the parallel scenario GMS IRG proteins have been proposed to regulate nucleotide binding by GKS proteins and thereby prevent the latter from premature activation and aggregation on intracellular membranes (Hunn et al., 2008). In absence of GMS, GKS proteins form aggregates, display dramatically reduced cellular concentrations (Henry et al., 2009) and inefficient loading onto *T. gondii* PVs (Hunn et al., 2008; Henry et al., 2009). It has been also reported that absence of Atg5 led to abnormal cellular accumulation of intracellular proteins forming aggregates and inclusions (Hara et al., 2006). So, Atg5 could be relevant either for normal function of the three GMS proteins (Irgm1, Irgm2 and Irgm3) or directly involved in regulating the nucleotide exchange of the GKS subfamily on the membranes of cytoplasmic compartments ((Hunn et al., 2008) and unpublished data). Alternatively, slight IRG protein aggregates, regularly formed in IFN γ -stimulated cells, may be subjected to autophagic or, possibly, nonautophagic degradation, governed by Atg5. Absence of Atg5, signified by large IRG protein aggregates, may trigger and amplify some recycling systems (e.g. ubiquitin-proteasome system, chaperone-mediated autophagy) to clear the cell from misbehaved proteins (Kaushik et al., 2008). It is still to be examined whether autophagy or some other previously reported or still unidentified role of Atg5 impacts cellular behaviour of IRG proteins (Kuma et al., 2004; Codogno and Meijer, 2006; Yousefi et al., 2006; Hanada et al., 2007; Pua et al., 2007).

5.3 IRG complex formation is required for association with avirulent *T. gondii* PV

A conserved structural module of IRG proteins, G domain, controls their cellular functions. It is established that IRG proteins associate with avirulent *T. gondii* vacuoles in a nucleotide-dependent manner (Martens et al., 2005; Hunn et al., 2008). In the cytosol of IFN γ -stimulated cells, IRG GKS proteins cycle between GTP- and GDP-bound conformations, while their activation on intracellular membranes is inhibited by GMS proteins (Martens and Howard, 2006; Hunn et al., 2008). Premature activation of IRG proteins in the cytoplasm has been reported to take place in absence of GMS proteins and in case of constitutively active dominant negative forms of IRG proteins (Irga6-K82A and Irgb6-K69A) (Martens et al., 2005; Hunn et al., 2008). Irga6-K82A has been shown to form oligomers *in vitro* and to display virtually no GTPase activity (Hunn et al., 2008). Infection with avirulent *T. gondii* triggers rapid binding of GKS proteins to PVs and their stabilization in the GTP-bound state on the vacuolar membranes (Hunn et al., 2008; Papic et al., 2008). The myristoyl group of Irga6 was shown to influence the process of loading since the G2A mutant of the protein exhibited reduced accumulation on avirulent *T. gondii* PVs and also acted as a weak dominant negative diminishing loading of endogenous protein ((Papic, 2007; Papic et al., 2008) and unpublished data). It has been proposed, that GTP binding promotes a conformational change of Irga6 molecule resulting in exposure of N-terminus with attached myristoyl group which is required for efficient targeting to the PVM (Papic, 2007; Papic et al., 2008).

A cluster of Irga6 surface amino acid residues of the G domain, crucial for oligomerisation and GTP hydrolysis but not for nucleotide binding *in vitro*, was termed the “catalytic interface” (Figure 16A and (Pawlowski et al., in preparation)). Here I provide the evidence that the catalytic interface is involved in IRG protein loading onto *T. gondii* vacuoles since all mutated residues (except for K162) markedly reduced frequency of Irga6 positive PVs (Figure 16, Appendix 6.1). This suggests that the interface for GTP-dependent oligomerisation *in vitro* is also required for forming stable IRG-IRG protein interactions on *T. gondii* vacuoles in cells to ensure an efficient loading process. K162 is positioned at the edge of the putative interface and its mutation yielded only a mild defect in association with PVs (Figure 16A and C). As previously reported, GMS-GKS interactions are nucleotide-dependent

and possibly involve the same interface used for GKS-GKS interactions ((Hunn et al., 2008; Pawlowski et al., in preparation)). Hence, some interface mutations could ablate regulatory interactions with GMS proteins resulting in spontaneous GKS protein aggregation in the cytoplasm. Indeed, certain mutants (e.g. E106R, S132R, Appendix 6.1) were clearly aggregated however the other proteins appeared homogeneous and ER-like (e.g. R159E, K161E, Appendix 6.1). To conclude, GKS protein catalytic interface could not only be used for GKS-GKS protein interactions, essential for the loading process, but also for binding to GMS proteins underlying normal behaviour of IRG GTPases in IFN γ -stimulated cells.

5.4 Passive vs. active model of IRG protein association with avirulent *T. gondii* PV

Association of IRG proteins with avirulent *T. gondii* PVs is not actively triggered by signals derived from cellular pathways, induced through PI3 kinase, G protein-coupled receptors, TLR and caspases (Figure 10). Involvement of cytosolic receptors, e.g. NOD-like receptors and CARD helicases, in loading process still remains to be tested. Even though Hook3, a microtubule-associated protein, has been found to interact with Irga6 (Kaiser, Kaufmann, and Zerrahn, 2004), inhibition of microtubule polymerization did not affect IRG protein accumulation on avirulent *T. gondii* PVs (Figure 10).

Alternatively, actin cytoskeleton may actively transport IRG proteins onto parasite-containing vacuoles. It has been recently reported that absence of Irgm1 led to drastically decreased actin remodeling, defects in Rac activation and marked reduction of phalloidin positive signal in the macrophages indicating of disrupted actin polymerization (Henry et al., 2010). However IRG protein signal on avirulent *T. gondii* PVs in Irgm1-deficient fibroblasts is only slightly reduced compared to the wt cells (Zhao, 2008) which could be due to somewhat diminished cellular IRG protein levels (Henry et al., 2009). Thus, indirect evidence suggests that actin cytoskeleton may not play a major role in the process of IRG protein loading onto *T. gondii* PV.

So far, data described here, along with published information (Martens and Howard, 2006; Hunn et al., 2008; Papic et al., 2008) support a “passive” model of IRG protein association with avirulent *T. gondii* PVs. GMS proteins and Atg5 ((Hunn et al., 2008; Zhao et al., 2008; Khaminets et al., 2010) and this study) regulate

dynamic nucleotide exchange of GKS proteins and thereby ensure appropriate localisation of IRG proteins in IFN γ -stimulated resting cells (Figure 30, cases (1) and (2)). Upon infection with *T. gondii*, IRG GTPases may access the vacuolar membrane via diffusion from the cytosolic pools of these proteins since the most abundant IRG proteins on the PVs, Irgb6, Irgb10, Irga6 and Irgd have large cytosolic portions ((Martens et al., 2004; Martens and Howard, 2006) and unpublished data). In contrast to GKS proteins, GMS proteins, Irgm2, Irgm3 and Irgm1 are almost or completely membrane-bound (Martens et al., 2004; Martens and Howard, 2006; Taylor, 2007; Zhao et al., 2010) and load inefficiently or fail to load onto avirulent *T. gondii* PVs (Martens et al., 2005; Khaminets et al., 2010). Therefore the degree of IRG protein association with avirulent *T. gondii* vacuoles correlates with cytosolic amount of a given protein in infected cells. It is not currently clear which mechanism mediates binding of the pioneer IRG protein, Irgb6, to the PVM, however, Irgb10 possesses a myristoylation motif (Bekpen et al., 2005) and this modification may initiate attachment to the vacuolar membrane as shown for Irga6 (Papic, 2007; Papic et al., 2008). Association of IRG proteins lower in the hierarchy with the *T. gondii* vacuoles could be formed and stabilized by homo- and heterotypic interactions within the family documented elsewhere (Hunn et al., 2008) (Figure 30, case (3)). These interactions are apparently built via the G domain of the proteins and require the catalytic interface (Figure 16), documented *in vitro* for Irga6 (Pawlowski et al., in preparation). The myristoyl group of Irga6, a member of the IRG protein family, following Irgb6 and Irgb10 in the loading hierarchy, is required for efficient association with *T. gondii* PVs indicating that solely IRG-IRG interactions are not sufficient for the normal loading process (Papic, 2007; Papic et al., 2008). To conclude, the complexity of the process of IRG protein loading onto *T. gondii* PV is apparently dependent on numerous host cell and microbe factors and is a subject to multiple mechanisms of regulation.

Irgm1 was not detected on the vacuoles of avirulent *T. gondii* (Martens et al., 2005) even though Irgm1-deficient mice succumb to parasite infection with the similar kinetics as mice lacking IFN γ (Collazo et al., 2001). This marked susceptibility of Irgm1-deficient mice to infection could be attributed to immunodeficiency due to malfunction of hematopoietic stem cells and increased mortality of CD4⁺ T lymphocytes (Feng et al., 2004; Feng et al., 2008a; Feng et al.,

2008b). Additionally, Irgm1 and other GMS proteins exert a regulatory role on GKS proteins controlling the normal functioning of the IRG system in IFN γ -induced cells (Hunn et al., 2008; Henry et al., 2009) and, therefore, absence of a single GMS protein could lead to failure of the whole IRG protein system (Hunn and Howard, 2010). Moreover, Irgm1 has been implicated in autophagy and macrophage motility suggesting the involvement of Irgm proteins in regulation of other cellular factors (Gutierrez et al., 2004; Henry et al., 2007; Feng et al., 2008b; Henry et al., 2010). Clearly, GMS proteins stand out from the rest of IRG GTPase family as being one of the major coordinators of cellular response to IFN γ .

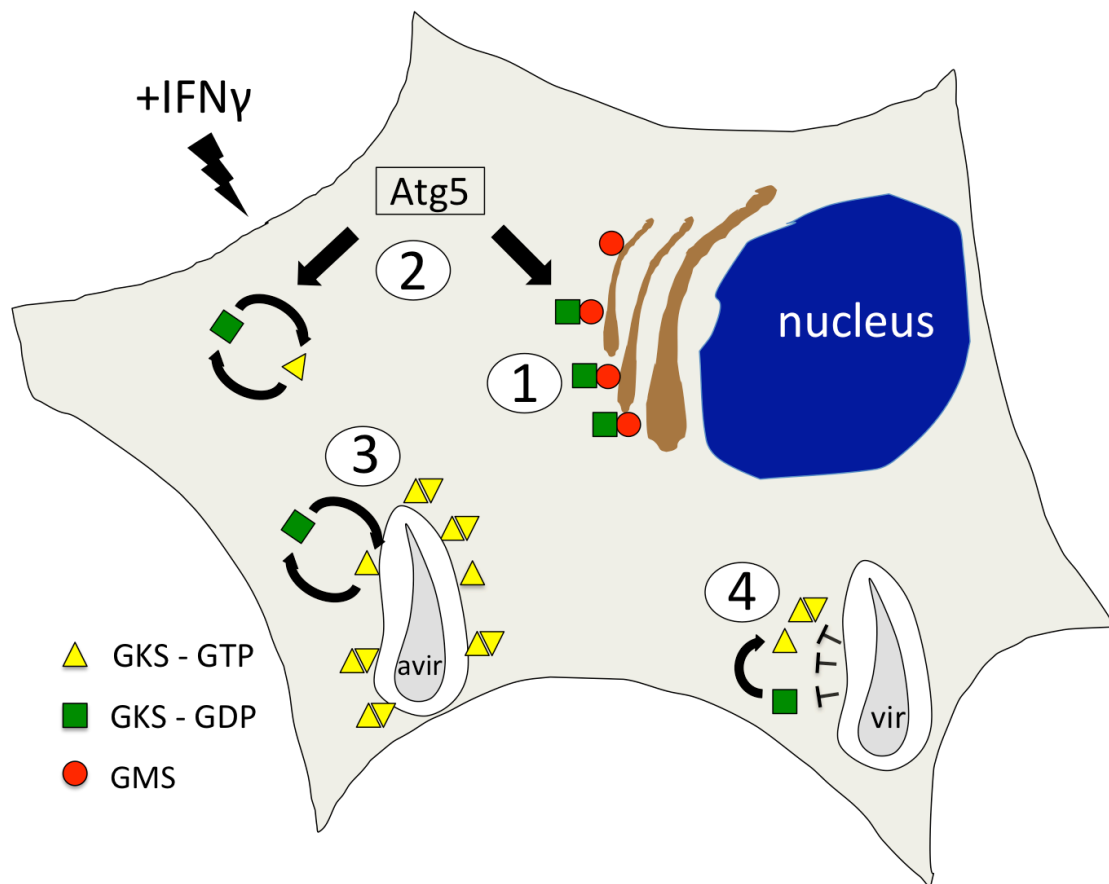


Figure 30 Regulation and function of IRG proteins in IFN γ -stimulated mouse cells.

In resting IFN γ -stimulated mouse cells localisation and nucleotide exchange of GKS proteins (GTP-bound are yellow triangles, GDP-bound are green squares) are tightly regulated by GMS proteins (red circles) of IRG protein family (case 1) and autophagic regulator Atg5 (case 2). Additionally or alternatively, Atg5 may influence behaviour of GKS proteins by acting upstream of GMS proteins. GKS proteins associate with the vacuolar membrane of avirulent (avir) *T. gondii* (case 3) during the process, which stabilises GTP-bound conformation of the proteins at the PVM. Efficient loading of IRG proteins onto the pathogen vacuoles require myristoyl group and GKS protein-protein interactions, formed by the catalytic interface of the protein molecules. Virulent (vir) *T. gondii* inhibits IRG protein association with the vacuole by interfering with any of the steps of the loading process: binding, activation or multimerisation of the proteins at the PVM (case 4). Reduced or ablated loading of IRG proteins onto *T. gondii* PVs results in defective disruption of the vacuolar membrane and, therefore, better survival of the parasite in IFN γ -stimulated mouse cells.

5.5 Reduced accumulation of IRG proteins on virulent *T. gondii* PVs is independent of ROP5, ROP16 and ROP18 virulence determinants of the parasite

IRG proteins are not efficiently loaded onto vacuoles containing virulent *T. gondii* (Figure 14 and Figure 30, case (4)). However, the phenomenon of unloaded vacuoles is not entirely new. It has been documented in this study and elsewhere (Zhao et al., 2009c; Khaminets et al., 2010), that a certain proportion of PVs containing avirulent *T. gondii* strains were not positive for IRG proteins, indicating that some avirulent parasites are able to escape from targeting by IRG proteins. And in case of the virulent parasites, inhibition of IRG protein association with the vacuoles is particularly pronounced for Irgb6 and Irgb10, the pioneer IRG proteins, which are proposed to initiate loading of the following members of the family, such as Irga6 and Irgd (Zhao et al., 2009c; Khaminets et al., 2010). Thus, by targeting the pioneer IRG proteins, virulent strains of *T. gondii* are presumably focused on arresting the primary steps of the loading process and thereby attenuating binding of the majority of IRG proteins to PVs. This model was substantiated by occurrence of a few virulent vacuoles heavily loaded with Irgb6 and Irgb10, which were also strikingly positive for the downstream members of the hierarchy Irga6 and Irgd ((Hunn, 2007; Khaminets et al., 2010) and unpublished data). Therefore, inhibition of IRG protein loading onto virulent PVs is not absolute; certain proportion of vacuoles efficiently initiate binding of IRG proteins and follow the same fate as most of loaded avirulent vacuoles, i.e. undergo disruption and death of the enclosed parasite ((Zhao et al., 2009b) and unpublished data). This once again emphasizes the initiation step of the loading process to be the target for inhibition by virulent and to some extent avirulent *T. gondii* strains, and proves to be decisive in elimination of the parasite.

In cells coinfecting with both virulent and avirulent parasites the loading phenotype remains unchanged, i.e. virulent vacuoles are virtually unloaded by IRG proteins while the amount of proteins loaded onto avirulent *T. gondii* PVs is comparable to the signal on PVs in cells infected only with avirulent parasites (Figure 15A and B). This result suggests that the processes of IRG protein accumulation on avirulent *T. gondii* PVs and evasion of the IRG vacuolar targeting mechanism by virulent vacuoles are presumably not mediated by secreted factors released by the parasite into the cytosol of infected cells. On the contrary, it is likely that activation of loading initiation and

interference with the IRG protein association occur locally, at the vacuolar membrane. Major virulence determinants secreted from the rhoptries of the invading parasite into the cytoplasm of infected cells, ROP5, ROP16 and ROP18 (Taylor et al., 2006; Saeij et al., 2006; El Hajj et al., 2007; Saeij et al., 2007) did not affect vacuolar loading with IRG proteins under employed experimental conditions (Figure 15C, D and (Zhao et al., 2009a)). Moreover, virulent alleles of the ROP proteins did not influence cell-autonomous control of parasite growth in IFN γ -stimulated mouse cells, analysed using gain- or loss-of-function *T. gondii* mutants (Zhao et al., 2009a; Khaminets et al., 2010).

ROP18 has been recently shown to mediate phosphorylation of Irga6 and Irgb6 proteins in mouse fibroblasts and macrophages, respectively (Fentress et al., submitted; Steinfeldt et al., submitted). Additionally, expression of the virulent allele of ROP18 in *T. gondii* was associated with reduction of IRG signal on PVs in infected cells (Fentress et al., submitted; Steinfeldt et al., submitted). Switch I region threonines T102 and T108 of Irga6 (proposed to be a part of catalytic interface) have been identified as the targets of ROP18, and phosphorylation of these residues led to near complete inability to oligomerize and hydrolyze GTP *in vitro* and striking defect in association with PVs in avirulent ME49 *T. gondii*-infected cells (Steinfeldt et al., submitted). This result is consistent with the analysis of Irga6 interface mutants documented in this study (sections 3.8 and 5.3). Interestingly, a clear reduction of Irga6 association with PVs of type III CTG parasite, expressing type I GT-1 ROP18, relative to the parental type III CTG strain was only observed in infected MEFs stimulated with low doses of IFN γ (0.3 U/ml) (Steinfeldt et al., submitted). It is therefore not surprising that the approach to test the effect of ROP18 on IRG protein loading onto *T. gondii* PVs, employed here, failed due to the use of 200 U/ml of IFN γ . These and other data indicate the direct competition between ROP18 as a virulence determinant and IRG proteins as antimicrobial factors (Fentress et al., submitted; Steinfeldt et al., submitted). The signal of phospho-Irga6 in IFN γ -induced MEFs infected with type III CTG parasite, expressing type I GT-1 ROP18, appeared to be somewhat weaker than in cells infected with type I strains of *T. gondii*. And, as mentioned above, the defect in Irga6 loading onto type III CTG parasite, expressing type I GT-1 ROP18, was only apparent in cells stimulated with low doses of IFN γ . These data strongly suggest that even though ROP18 is able to phosphorylate and

thereby interfere with Irga6 and Irgb6 loading onto *T. gondii* PVs, only a certain combination of virulence factors in the right genetic environment would be capable of fully subverting IRG-mediated immunity at the cell-autonomous level (Saeij et al., 2006; Fentress et al., submitted; Steinfeldt et al., submitted).

It has been reported that Irgb10 mediates IFN γ -endowed resistance to human pathogen *Chlamydia trachomatis* in the mouse system *in vivo* and in cell culture (Bernstein-Hanley et al., 2006; Coers et al., 2008). Moreover, inclusions with *C. trachomatis* accumulate Irgb10 suggesting direct interference of the protein with the intracellular life style of the pathogen (Coers et al., 2008). Natural pathogen of *Muridae*, *Chlamydia muridarum* (MoPn), is resistant to IFN γ -mediated murine cell-autonomous immunity and, importantly, inclusions of the parasite are negative for Irgb10 in infected mouse cells (Nelson et al., 2005; Roshick et al., 2006; Coers et al., 2008). In humans *C. muridarum* is efficiently contained by IDO-mediated tryptophan depletion in contrast to the several *C. trachomatis* strains, isolated from the human urogenital tract, which express tryptophan synthase to overcome the inhibitory action of IDO (Read et al., 2000; Roshick et al., 2006; McClarty, Caldwell, and Nelson, 2007). Thus, in case of *Chlamydia* host tropism determines the adaptations of the pathogen and therefore the ability to subvert the host-specific cellular immune response.

5.6 Loading of IRG proteins onto *T. gondii* vacuoles is crucial for parasite elimination in IFN γ -induced mouse fibroblasts

It was previously observed that virtually every avirulent *T. gondii* vacuole loaded with IRG proteins undergoes disruption followed by killing of the parasite (Zhao et al., 2009b). Furthermore, overexpression of Irga6-cTag1 in IFN γ -stimulated astrocytes was associated with marked reduction of intracellular *T. gondii* compared to cells expressing dominant negative Irga6 version Irga6-K82A-cTag1, deficient in vacuolar IRG protein loading (Martens et al., 2005). In this study the role of vacuolar loading with IRG proteins in direct *T. gondii* elimination was further addressed using several strategies. Firstly, dominant negative IRG protein Irgb6-K69A has been employed to inhibit PV association of not only ectopically expressed protein in cells but also of endogenous IRG proteins ((Hunn et al., 2008) and Figure 17). Secondly, killing of virulent *T. gondii* in IFN γ -induced mouse fibroblasts was examined since

vacuoles containing virulent parasites were deficient in loading with IRG proteins ((Zhao et al., 2009a; Zhao et al., 2009c; Khaminets et al., 2010) and Figure 14). And finally, misbehavior of IRG proteins in Atg5-deficient mouse fibroblasts led to severely impaired binding to parasite PVs ((Zhao et al., 2008) and Figure 11) providing another model to study the role of the loading process in *T. gondii* elimination. Parasite viability in mouse cells was evaluated by “EGFP/Cherry entry assay” based on influx of ectopically expressed cytoplasmic marker into permeabilised intracellular parasites in disrupted vacuoles indicative of *T. gondii* death (Zhao et al., 2009b). To summarize, in all examined cases defects in association of IRG proteins with *T. gondii* vacuoles resulted in substantial or almost complete suppression of parasite elimination in IFN γ -stimulated mouse cells (Figure 18). Additionally, in cells, coinfecting with *T. gondii* of differential virulence, killing mechanisms function in a manner resembling elimination of the parasite in separate infection experiments, in a vacuole-autonomous fashion (Figure 18D and Figure 19). In other words, certain proportion of avirulent parasites became permeable to cytoplasmic Cherry in contrast to the virulent *T. gondii* which remained negative for Cherry and, presumably, viable. This indicates, that the mechanism of killing of individual intracellular tachyzoites is localised to the individual parasite-containing vacuoles and therefore entirely reliant on loading with IRG proteins. It is, however, plausible that expression of the dominant negative IRG proteins, infection with virulent *T. gondii* and absence of Atg5 could influence other IRG-independent cellular processes essential for resistance to the parasite, which are subject for future investigation. Nevertheless, the cumulative evidence presented here together with published data (Martens et al., 2005; Ling et al., 2006; Melzer et al., 2008; Zhao et al., 2008; Zhao et al., 2009b) provides a strong link between loading of *T. gondii* vacuoles by IRG proteins and elimination of the parasite.

5.7 Amount of cultured cells determines the mechanism of *T. gondii* growth inhibition in IFN γ -stimulated primary human fibroblasts

To date, depletion of cellular tryptophan by IDO in IFN γ -induced human cells has been reported to be the principal cell-autonomous mechanism of resistance to *T. gondii* and other pathogens such as *C. trachomatis*, *Neospora caninum*, measles virus, herpes virus (Pfefferkorn, 1984; Thomas et al., 1993; Daubener et al., 2001; Adams et

al., 2004; Obojes et al., 2005; Spekker et al., 2009). In human endothelial cells and macrophages, *T. gondii* growth restriction has been shown to be mediated in an IDO-independent and so far undefined fashion (Woodman, Dimier, and Bout, 1991; MacKenzie et al., 1999). In this study addition of tryptophan excess to primary human fibroblasts restored IFN γ -inhibited *T. gondii* growth provided high amounts of cells (e.g. 2×10^4) were seeded (Figure 20). Strikingly, $2,5 \times 10^3$ - 5×10^3 IFN γ -induced human foreskin (Hs27) and human skin (HSF) fibroblasts, seeded 2 days before infection and probably still proliferating at the time of infection, restricted *T. gondii* replication in an IDO-independent way. It is currently unclear which factors underlie the antimicrobial activities in proliferating cells and control switching between IDO-dependent and IDO-independent mechanisms of the parasite growth inhibition in IFN γ -induced human cells. However, programmed death of *T. gondii*-infected IFN γ -stimulated human cells, discussed in sections 5.8 and 5.9, could provide clues for understanding the cell-autonomous antiparasitic programs induced by the cytokine in humans.

5.8 *T. gondii* infection stimulates necrosis of IFN γ -induced primary human cells

Evidence of an IDO-independent mechanism of *T. gondii* control in IFN γ -induced human cells prompted further investigation of various aspects of the pathogen-host cell interaction. In mouse cells, IRG proteins participate in the process of vacuolar disruption, which leads to killing of the parasite and subsequent death of the infected cell ((Martens et al., 2005; Ling et al., 2006; Zhao et al., 2009b; Khaminets et al., 2010) and this study). Therefore the question was asked: do any of these events take place in human cells? Neither disruption nor parasite killing was detected in IFN γ -stimulated human fibroblasts evaluated by GRA7 diffusion and EGFP entry assays, respectively, in contrast to mouse cells (Figure 21). It is not surprising that the vacuolar membrane of *T. gondii* remains intact during the course of infection due to the lack of the entire IFN γ -inducible IRG system in man (Bekpen et al., 2005). Moreover, IRGM, previously implicated in cell-autonomous resistance to bacterial parasites (Gutierrez et al., 2004; Lapaquette et al., 2010), has not been reported in the context of *T. gondii* infection.

In spite of lack of detectable loss of vacuolar integrity, a striking decrease of cell viability was evident in Hs27 cell cultures stimulated by IFN γ and infected with avirulent *T. gondii* (Figure 21 and Figure 22). Additionally, virulent RH-YFP strain of *T. gondii* elicited death of human cells as efficiently as avirulent ME49 parasites (Figure 22B) indicating distinct mechanisms of programmed death initiation in human and mouse cells (Zhao et al., 2009b). Cell death occurs during IDO-dependent and IDO-independent modes of resistance to *T. gondii*, analysed in cultures containing disparate amounts of cells (Figure 28C). Interestingly, HeLa, HaCaT and HEK 293T cell lines were resistant to IFN γ -dependent *T. gondii*-induced cell death while U937 exhibited relatively high mortality after infection with the parasite even without IFN γ stimulation (Figure 22). The latter was likely due to basal secretion of type I IFN by the differentiated U937 macrophages.

T. gondii induced necrosis but not apoptosis in IFN γ -stimulated human cells based on the following observations: no diffusion of cytochrome C into the cytoplasm from mitochondria, no apoptotic caspase-dependent cleavage of PARP1, inability of the pan-caspase inhibitor z-VAD-fmk to inhibit cell death, loss of plasma membrane integrity, subsequent release of cytosolic content and nuclei protein HMGB1 into the medium and total disruption of lysosomes (Figures 22, 25 and 26). It is still a future task to analyse the involvement of caspase-1, a marker of necrotic-like type of cell death termed “pyroptosis”, which activation is associated with cleavage and secretion of IL-1 β from infected or drug-stimulated cells (Fernandes-Alnemri et al., 2007; Petrilli et al., 2007a; Petrilli et al., 2007b; Willingham et al., 2007; Labbe and Saleh, 2008; Yeretssian, Labbe, and Saleh, 2008).

Programmed cell death is a common mechanism of containing infections although it could be frequently employed by pathogens for their own survival and multiplication (Labbe and Saleh, 2008). Apoptosis is the type of cell death, executed by caspases, which results in “silent” removal of unwanted or harmful cells during embryonic development, tissue homeostasis and immune regulation. Cellular necrosis, which could be triggered by ROS, RARP1 or apoptosis-inducing factor (AIF) is associated with release of nuclear and cytoplasmic content into medium, thus stimulating inflammation at the loci of damage or infection (Festjens, Vanden Berghe, and Vandenabeele, 2006; Boujrad et al., 2007; Galluzzi et al., 2007). HMGB1, ATP, heat shock proteins and other danger-associated molecular patterns (DAMPs), derived

from dying cells, have been identified as potent proinflammatory stimuli *in vivo* and in cell culture (Matzinger, 1994; Basu et al., 2000; Andersson et al., 2002; Scaffidi, Misteli, and Bianchi, 2002; Iwasaki and Medzhitov, 2004; Mariathasan et al., 2006; Ogura, Sutterwala, and Flavell, 2006). In this way, necrosis can significantly amplify inflammation, on one hand, to localise the parasites, promote migration and proliferation of immune cells to contain the infection and, on the other hand, to aid tissue damage occurred during uncontrolled replication of the parasites resulting in the septic shock and death of the organism (Basu et al., 2000; Mordue et al., 2001; Shi and Rock, 2002; Sunden-Cullberg et al., 2005; Festjens, Vanden Berghe, and Vandenabeele, 2006; Iyer et al., 2009).

Supplementation of culture medium with tryptophan reduced *T. gondii*-induced death of IFN γ -stimulated primary human fibroblasts (Figure 28). This restoration of cell viability was only evident in dense cells exerting IDO-dependent immunity, but not in replicating fibroblasts (Figure 28C and D). Direct correlation between tryptophan-mediated increase of cell viability and rescue of *T. gondii* growth in IFN γ -stimulated human fibroblasts indicates that tryptophan does not only fulfill the parasite need for an essential amino acid but also promotes host cell survival in the context of infection. Inhibition of IDO by 1-MT failed to override *T. gondii*-induced necrosis of IFN γ -stimulated infected primary human fibroblasts (at any tested cell density) and consequently was not able to restore growth of the parasite in IFN γ -activated Hs27 cells (Figure 29). Based on the latter observations, it is unlikely that IDO activity is involved in infection-elicited programmed necrosis although this is still to be confirmed. The molecular basis of the tryptophan-mediated inhibition of necrosis in IFN γ -stimulated and *T. gondii*-infected human fibroblasts is not understood and poses a subject for future studies (de la Maza and Peterson, 1988; Moosmann and Behl, 2000; Cannon and Pate, 2006; Hsu et al., 2009).

5.9 IDO-dependent and IDO-independent mechanisms of IFN γ -induced *T. gondii* growth restriction in human cells

A model of IFN γ -mediated mechanisms of *T. gondii* control in human cells is summarized in Figure 31. The core of the model is based on the fact that conditions of cultured cells determine the program of the parasite growth inhibition: IDO-independent in proliferating and IDO-dependent in nonproliferating cells. It is highly

suggestive that necrotic death of IFN γ -induced and *T. gondii*-infected human cells, discovered in the course of this study, contributes to cell-autonomous immunity to the pathogen. Moreover, necrosis is associated with release of the proinflammatory content of the cell and thereby can amplify the immune response to *T. gondii* *in vivo*.

One might speculate that necrosis represents the IDO-independent mechanism since cell death directly correlates with IFN γ -mediated inhibition of *T. gondii* replication in primary human cells (Figure 29 and 31A). It is also plausible that a series of events, taking place before necrosis and leading to cell death, are responsible for parasite elimination but this is still to be examined. IDO-dependent mechanism or depletion of cellular tryptophan is only apparent in nonreplicating cells when necrosis is suppressed by supplementing the culture medium with tryptophan (Figure 30B). Thus, addition of tryptophan to the cells has a dual effect: on one hand it restores cell viability by a yet unknown mechanism and on the other hand provides a source of essential amino acid for *T. gondii* replication overcoming IDO activity.

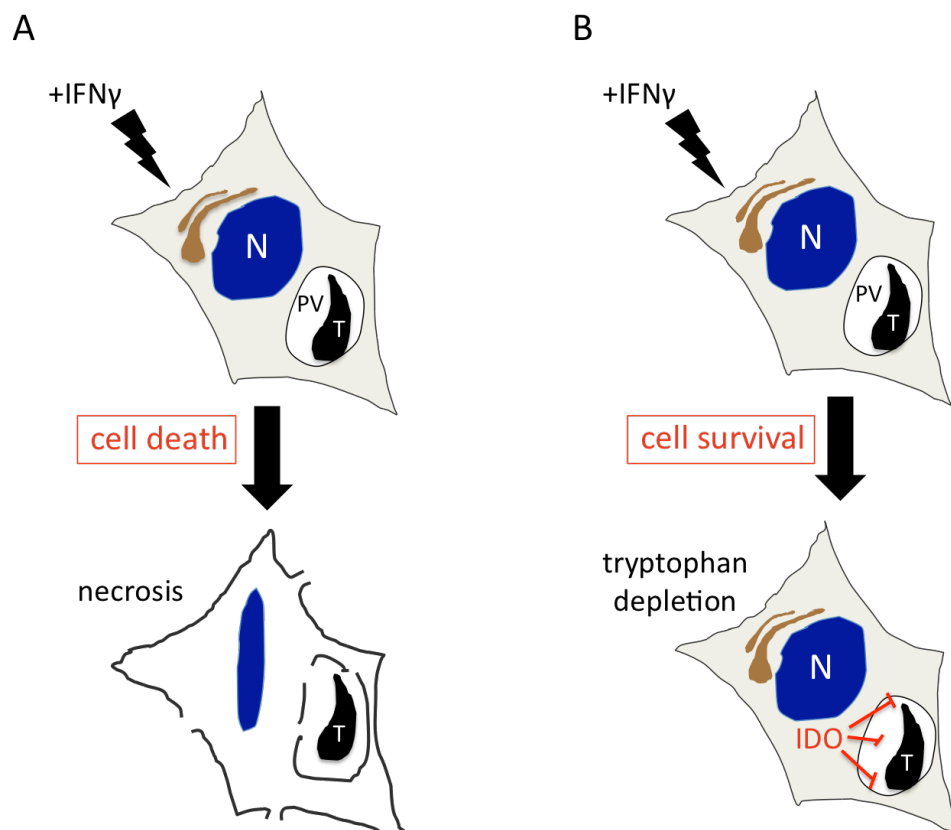


Figure 31 Model of the mechanisms of IFN γ -mediated resistance to *T. gondii* in human cells.

(A) Infection with *T. gondii* leads to necrosis of IFN γ -induced primary human fibroblasts accompanied by release of cellular proinflammatory content into the medium. Cell death inhibition could be achieved by addition of tryptophan into cell cultures or by using necrosis-resistant HeLa cells. (B) In survived cells IDO depletes cellular tryptophan and thereby suppresses proliferation of *T. gondii* in IFN γ -stimulated human cells. Thus, IFN γ arms human cells with at least 2-step defence system:

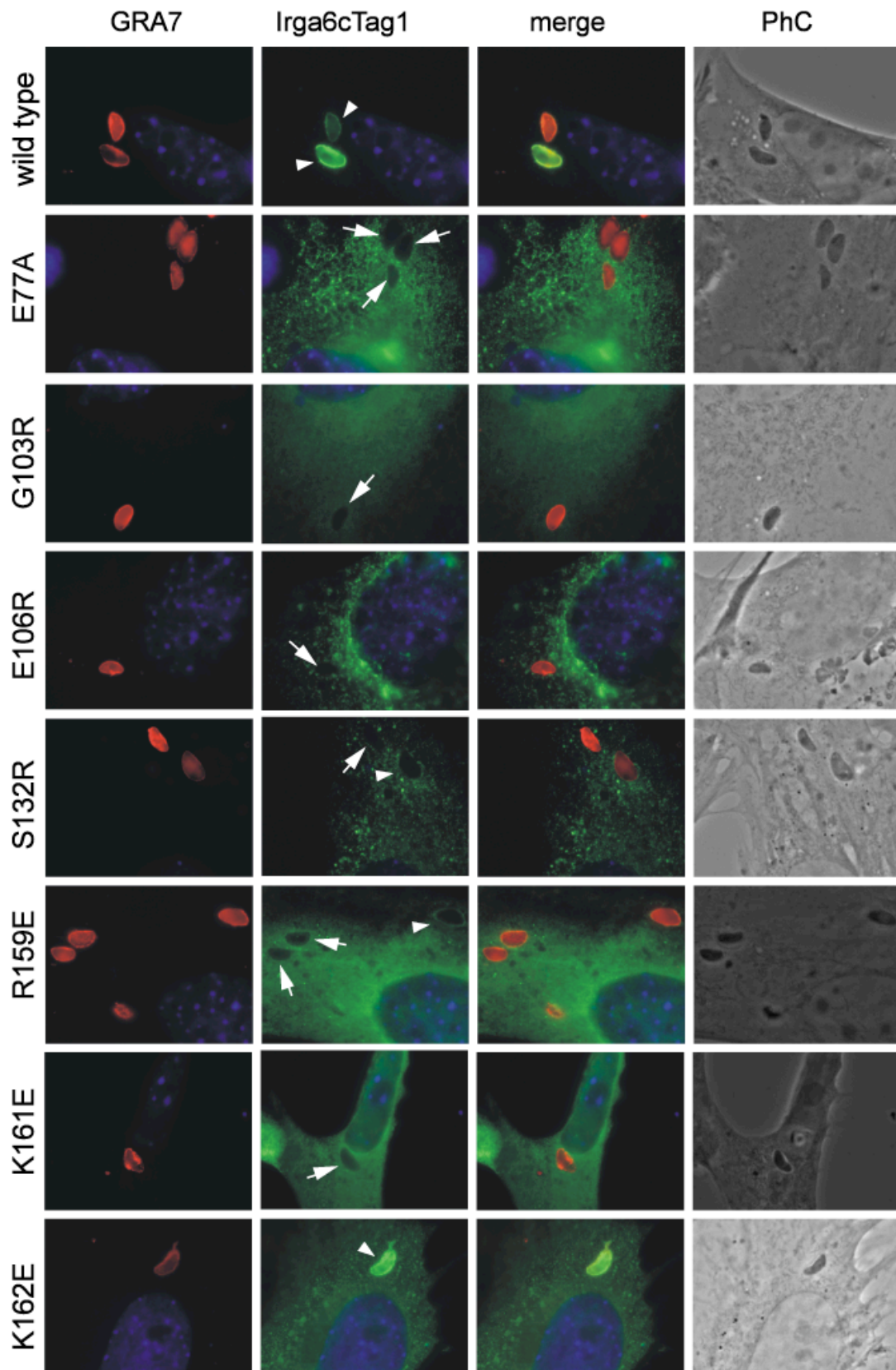
programmed necrosis and tryptophan depletion.

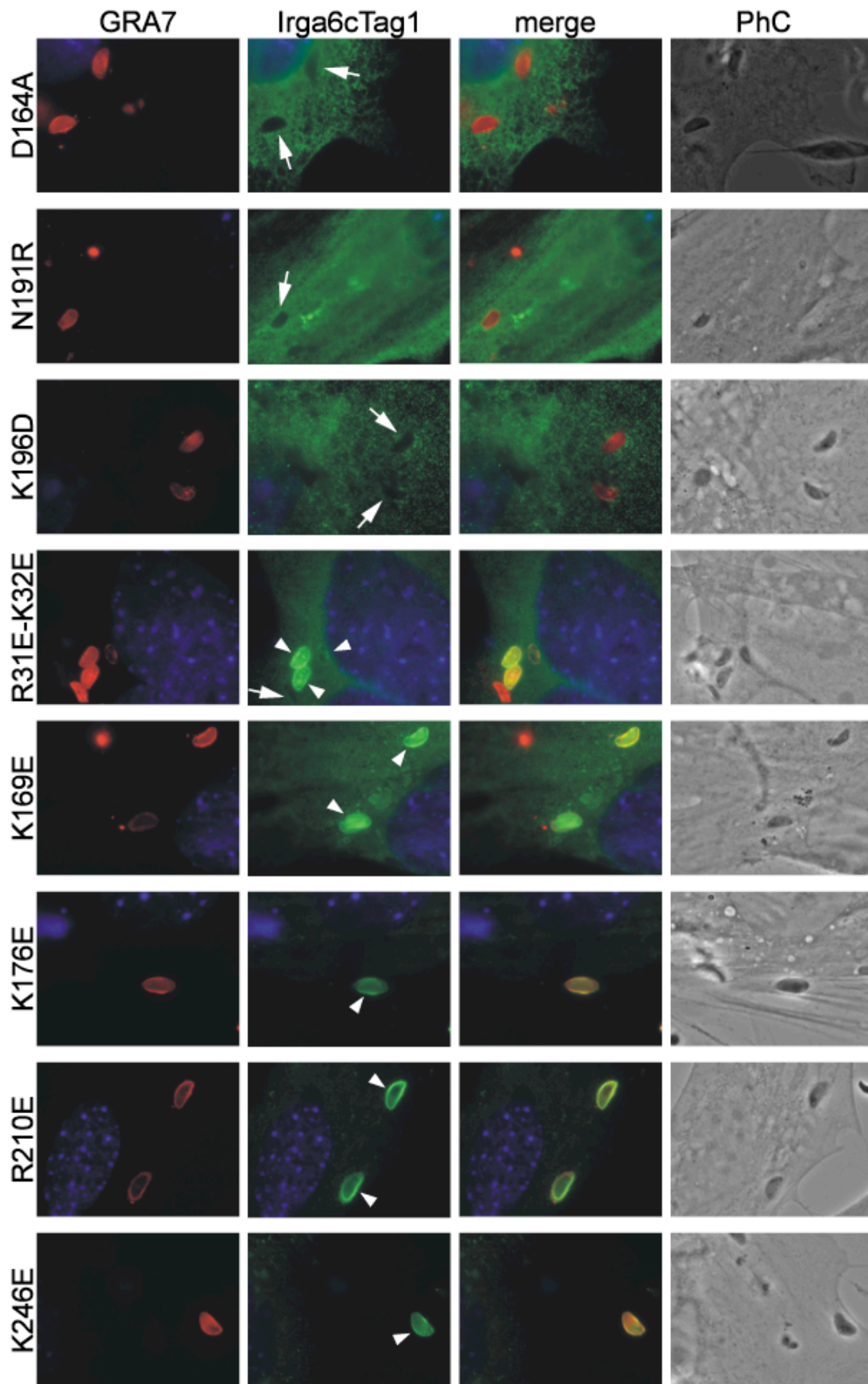
HeLa cells could serve as a model for studying IDO-dependent *T. gondii* growth restriction given their ability to resist necrosis induced by the parasite. Pharmacological inhibition of IDO rescues *T. gondii* growth in IFN γ -stimulated HeLa cells but not in primary human fibroblasts (Figure 29) indicating that an IDO-independent mechanism is dominant over IDO-dependent parasite growth restriction in primary human cells. This result also suggests that the relative contribution of IDO-dependent and IDO-independent programs to *T. gondii* control in IFN γ -induced human cells may vary among the different cell types. The inability to restore *T. gondii* growth by 1-MT-mediated inhibition of IDO in IFN γ -stimulated human cells shown here confronts previously published reports (Heseler et al., 2008). It is therefore essential to proceed with further investigation using other approaches such as siRNA or a panel of various IDO inhibitors.

There are still a number of unanswered questions related to the model presented here (Figure 31) which are to be studied in detail in the future. What is the molecular basis of *T. gondii*-induced necrosis in IFN γ -stimulated human fibroblasts? What are the additional factors involved in cell death and what is their impact on cell-autonomous immunity to the parasite? How does tryptophan restore viability of dense human fibroblast cultures after IFN γ stimulation and *T. gondii* infection? And finally, what are the mechanisms of the parasite recognition in human cells?

6 Appendix

6.1 Figure 32. Association of wt, catalytic interface and secondary patch mutants of Irga6-cTag1 with ME49 *T. gondii* PV





Figures 32 Association of wt, catalytic interface and secondary patch mutants of Irga6-cTag1 with ME49 *T. gondii* PV.

Irga6^{-/-} MEFs were induced with IFN γ and simultaneously transfected with pGW1H constructs expressing wt, catalytic interface (E77A, G103R, S132R, R159E, K161E, K162E, D164A, N191R, E106R, K196D) or secondary patch (R31E-K32E, K169E, K176E, R210E, K246E) mutants of Irga6-cTag1 for 24 h. The cells were subsequently infected with ME49 *T. gondii* for 2 h and stained for cTag1 (green) to identify transfected proteins and for GRA7 (red) to identify intracellular parasites. PhC is phase contrast. Arrowheads and arrows indicate cTag1-positive and cTag1-negative PVs, respectively. Note, that the intensity of PV loading for all catalytic interface Irga6-cTag1 mutants (except for K162E) is much weaker (e.g. R159E) even though the vacuoles were counted as cTag1 positive.

6.2 Permeabilisation of avirulent *T. gondii* to cytoplasmic Cherry in IFN γ -stimulated infected MEFs

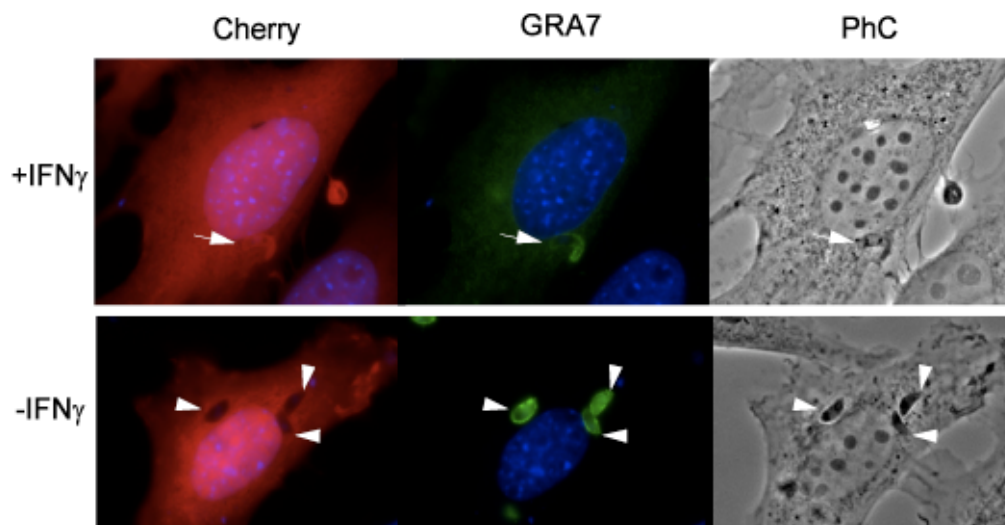


Figure 33. Permeabilisation of avirulent *T. gondii* to cytoplasmic Cherry in IFN γ -stimulated MEFs.

MEFs were stimulated with IFN γ and simultaneously transfected with pmCherry-N3, expressing Cherry, for 24 h and then infected with ME49 *T. gondii* for 4 h. Intracellular parasites were identified by staining for GRA7 and by phase contrast (PhC). Arrow indicates Cherry-positive dead parasite in IFN γ -stimulated MEFs and the arrowheads indicate live *T. gondii* in untreated cells. Note that the vacuolar membrane (identified by GRA7) of the permeabilized parasite is disrupted and the PV protein GRA7 diffused into the cytoplasm of infected cell.

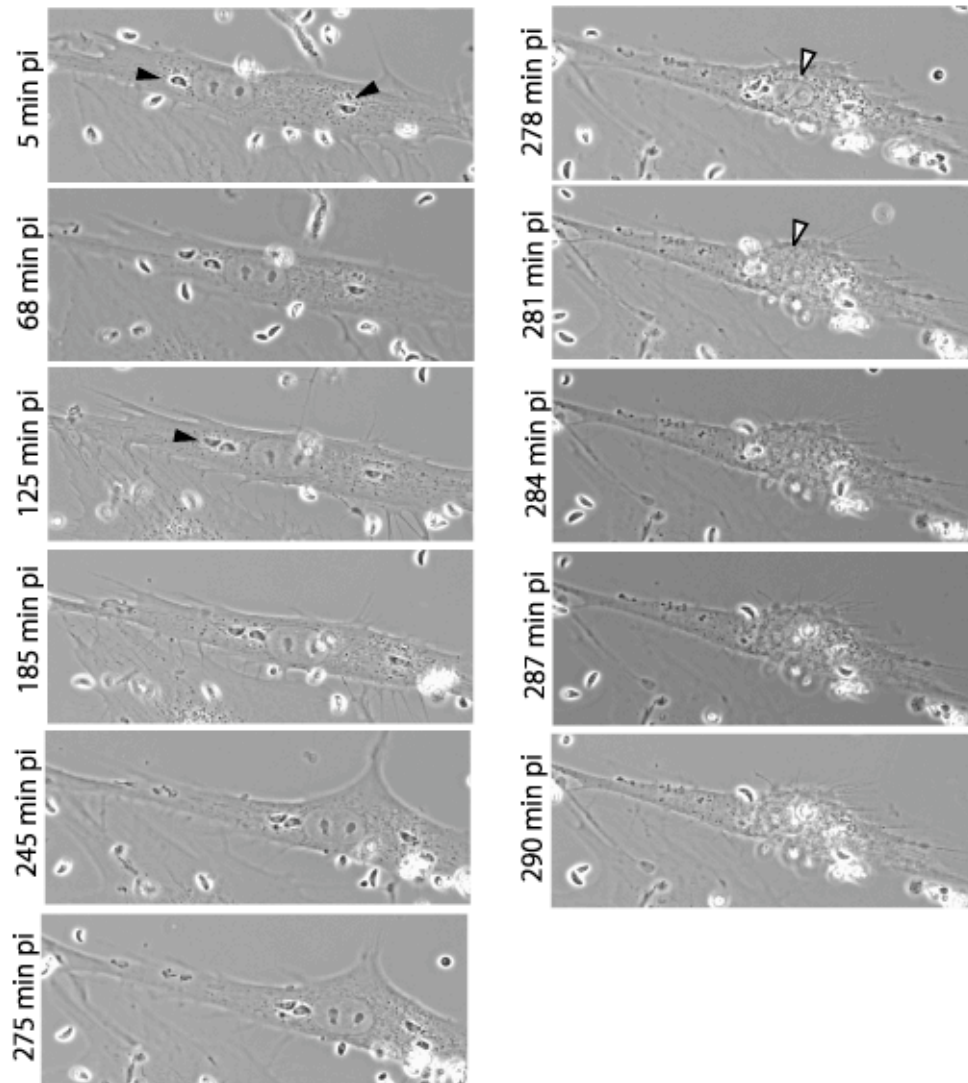
6.3 IFN γ induces death of *T. gondii*-infected human cells

Figure 34 IFN γ induces death of *T. gondii*-infected human cells.

IFN γ -stimulated Hs27 cells were infected with *T. gondii* ME49 strain in microscope slide chambers as described by in Material and Methods and monitored continuously to observe the infected cell. Filled arrowheads indicate the location of the *T. gondii* PVs. Partial shrinkage of the nucleus (indicated by the empty arrowhead) and release of cytoplasmic content evidenced the death of the cell after 278 min pi.

6.4 Analysis of Hs27 cell viability by PI staining

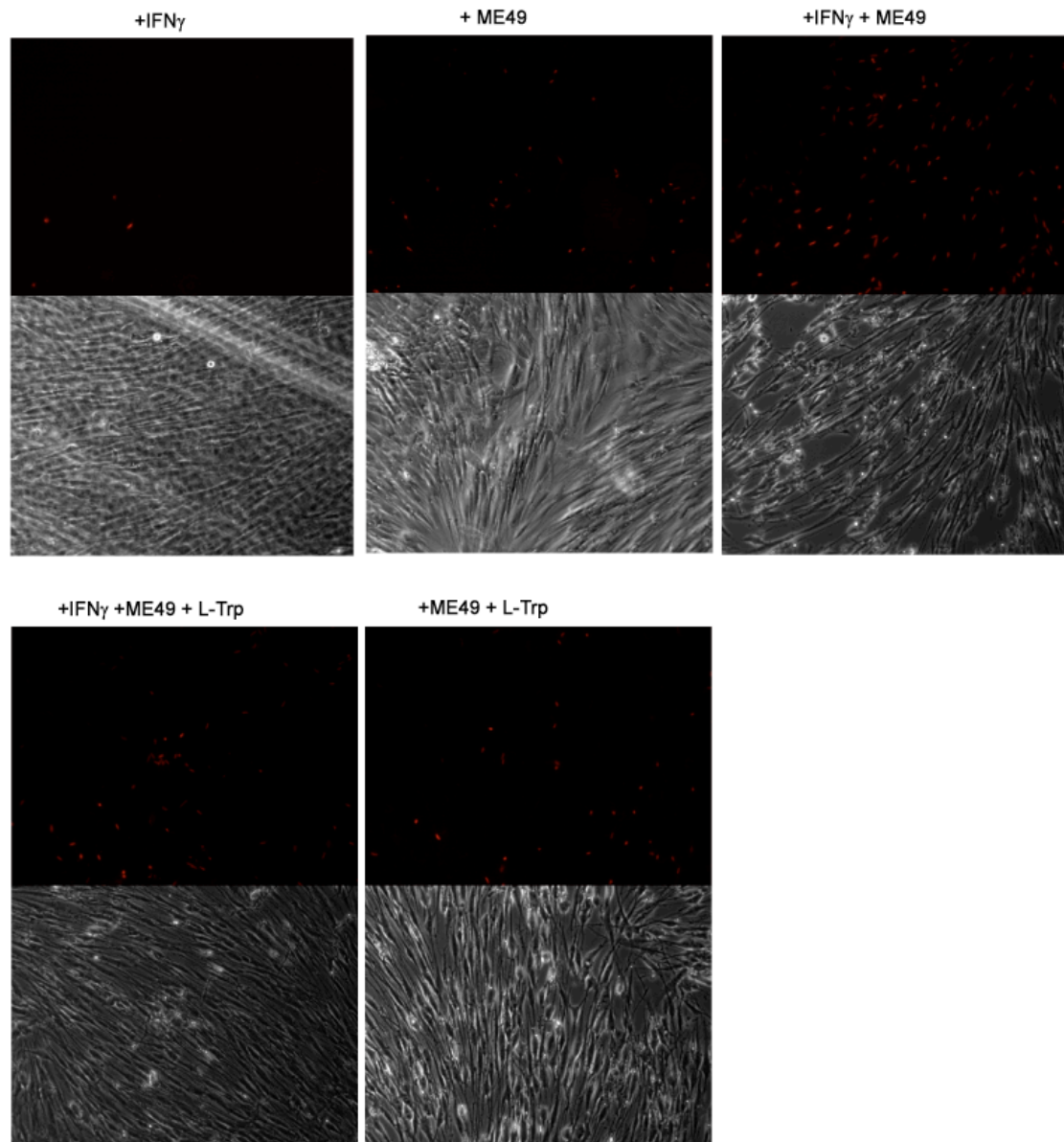


Figure 35 Analysis of Hs27 cell viability by PI staining.

10^5 Hs27 cells were seeded in microscope dishes as described in Material and Methods and induced with IFN γ (200 U/ml) for 72 h. L-Trp was then added to the wells to the final concentration of 0.55 mM and the cells were infected with ME49 *T. gondii* at MOI 5 for 24 h. PI was added to the medium and incubated for 15 min before microscopical analysis. The images of 5 random views from each treatment were taken and the representative views are shown.

7 References

- Adachi, O., Kawai, T., Takeda, K., Matsumoto, M., Tsutsui, H., Sakagami, M., Nakanishi, K., and Akira, S. (1998). Targeted disruption of the MyD88 gene results in loss of IL-1- and IL-18-mediated function. *Immunity* **9**(1), 143-50.
- Adams, L. B., Hibbs, J. B., Jr., Taintor, R. R., and Krahenbuhl, J. L. (1990). Microbiostatic effect of murine-activated macrophages for *Toxoplasma gondii*. Role for synthesis of inorganic nitrogen oxides from L-arginine. *J Immunol* **144**(7), 2725-9.
- Adams, O., Besken, K., Oberdorfer, C., MacKenzie, C. R., Russing, D., and Daubener, W. (2004). Inhibition of human herpes simplex virus type 2 by interferon gamma and tumor necrosis factor alpha is mediated by indoleamine 2,3-dioxygenase. *Microbes Infect* **6**(9), 806-12.
- Akira, S., Uematsu, S., and Takeuchi, O. (2006). Pathogen recognition and innate immunity. *Cell* **124**(4), 783-801.
- Alexander, D. L., Mital, J., Ward, G. E., Bradley, P., and Boothroyd, J. C. (2005). Identification of the moving junction complex of *Toxoplasma gondii*: a collaboration between distinct secretory organelles. *PLoS Pathog* **1**(2), e17.
- Aliberti, J., Viola, J. P., Vieira-de-Abreu, A., Bozza, P. T., Sher, A., and Scharfstein, J. (2003). Cutting edge: bradykinin induces IL-12 production by dendritic cells: a danger signal that drives Th1 polarization. *J Immunol* **170**(11), 5349-53.
- Aline, F., Bout, D., and Dimier-Poisson, I. (2002). Dendritic cells as effector cells: gamma interferon activation of murine dendritic cells triggers oxygen-dependent inhibition of *Toxoplasma gondii* replication. *Infect Immun* **70**(5), 2368-74.
- Anderson, S. L., Carton, J. M., Lou, J., Xing, L., and Rubin, B. Y. (1999). Interferon-induced guanylate binding protein-1 (GBP-1) mediates an antiviral effect against vesicular stomatitis virus and encephalomyocarditis virus. *Virology* **256**(1), 8-14.
- Andersson, U., Erlandsson-Harris, H., Yang, H., and Tracey, K. J. (2002). HMGB1 as a DNA-binding cytokine. *J Leukoc Biol* **72**(6), 1084-91.
- Andrade, R. M., Wessendarp, M., Gubbels, M. J., Striepen, B., and Subauste, C. S. (2006). CD40 induces macrophage anti-*Toxoplasma gondii* activity by

- triggering autophagy-dependent fusion of pathogen-containing vacuoles and lysosomes. *J Clin Invest* **116**(9), 2366-77.
- Bach, E. A., Aguet, M., and Schreiber, R. D. (1997). The IFN gamma receptor: a paradigm for cytokine receptor signaling. *Annu Rev Immunol* **15**, 563-91.
- Bancroft, G. J. (1993). The role of natural killer cells in innate resistance to infection. *Curr Opin Immunol* **5**(4), 503-10.
- Barsoum, M. J., Yuan, H., Gerencser, A. A., Liot, G., Kushnareva, Y., Graber, S., Kovacs, I., Lee, W. D., Waggoner, J., Cui, J., White, A. D., Bossy, B., Martinou, J. C., Youle, R. J., Lipton, S. A., Ellisman, M. H., Perkins, G. A., and Bossy-Wetzel, E. (2006). Nitric oxide-induced mitochondrial fission is regulated by dynamin-related GTPases in neurons. *EMBO J* **25**(16), 3900-11.
- Bastin, P., Bagherzadeh, Z., Matthews, K. R., and Gull, K. (1996). A novel epitope tag system to study protein targeting and organelle biogenesis in *Trypanosoma brucei*. *Mol Biochem Parasitol* **77**(2), 235-9.
- Basu, S., Binder, R. J., Suto, R., Anderson, K. M., and Srivastava, P. K. (2000). Necrotic but not apoptotic cell death releases heat shock proteins, which deliver a partial maturation signal to dendritic cells and activate the NF-kappa B pathway. *Int Immunol* **12**(11), 1539-46.
- Bazer, F. W., Spencer, T. E., and Ott, T. L. (1997). Interferon tau: a novel pregnancy recognition signal. *Am J Reprod Immunol* **37**(6), 412-20.
- Bekpen, C., Hunn, J. P., Rohde, C., Parvanova, I., Guethlein, L., Dunn, D. M., Glowalla, E., Leptin, M., and Howard, J. C. (2005). The interferon-inducible p47 (IRG) GTPases in vertebrates: loss of the cell autonomous resistance mechanism in the human lineage. *Genome Biol* **6**(11), R92.
- Bermudez, L. E., Covaro, G., and Remington, J. (1993). Infection of murine macrophages with *Toxoplasma gondii* is associated with release of transforming growth factor beta and downregulation of expression of tumor necrosis factor receptors. *Infect Immun* **61**(10), 4126-30.
- Bernabei, P., Allione, A., Rigamonti, L., Bosticardo, M., Losana, G., Borghi, I., Forni, G., and Novelli, F. (2001). Regulation of interferon-gamma receptor (INF-gammaR) chains: a peculiar way to rule the life and death of human lymphocytes. *Eur Cytokine Netw* **12**(1), 6-14.
- Bernstein-Hanley, I., Coers, J., Balsara, Z. R., Taylor, G. A., Starnbach, M. N., and

- Dietrich, W. F. (2006). The p47 GTPases Igtp and Irgb10 map to the Chlamydia trachomatis susceptibility locus Ctrq-3 and mediate cellular resistance in mice. *Proc Natl Acad Sci U S A* **103**(38), 14092-7.
- Boehm, U., Guethlein, L., Klamp, T., Ozbek, K., Schaub, A., Fütterer, A., Pfeffer, K., and Howard, J. C. (1998). Two families of GTPases dominate the complex cellular response to interferon- γ . *J. Immunol.* **161**, 6715-6723.
- Boehm, U., Klamp, T., Groot, M., and Howard, J. C. (1997). Cellular responses to interferon- γ . *Annu. Rev. Immunol.* **15**, 749-795.
- Bonhomme, A., Maine, G. T., Beorchia, A., Bulet, H., Aubert, D., Villena, I., Hunt, J., Chovan, L., Howard, L., Brojanac, S., Sheu, M., Tyner, J., Pluot, M., and Pinon, J. M. (1998). Quantitative immunolocalization of a P29 protein (GRA7), a new antigen of toxoplasma gondii. *J Histochem Cytochem* **46**(12), 1411-22.
- Borden, E. C., Sen, G. C., Uze, G., Silverman, R. H., Ransohoff, R. M., Foster, G. R., and Stark, G. R. (2007). Interferons at age 50: past, current and future impact on biomedicine. *Nat Rev Drug Discov* **6**(12), 975-90.
- Bougnères, L., Helft, J., Tiwari, S., Vargas, P., Chang, B. H., Chan, L., Campisi, L., Lauvau, G., Hugues, S., Kumar, P., Kamphorst, A. O., Dumenil, A. M., Nussenzweig, M., MacMicking, J. D., Amigorena, S., and Guermonprez, P. (2009). A role for lipid bodies in the cross-presentation of phagocytosed antigens by MHC class I in dendritic cells. *Immunity* **31**(2), 232-44.
- Boujrad, H., Gubkina, O., Robert, N., Krantic, S., and Susin, S. A. (2007). AIF-mediated programmed necrosis: a highly regulated way to die. *Cell Cycle* **6**(21), 2612-9.
- Boukamp, P., Petrussewa, R. T., Breitkreutz, D., Hornung, J., Markham, A., and Fusenig, N. E. (1988). Normal keratinization in a spontaneously immortalized aneuploid human keratinocyte cell line. *J. Cell Biol.* **106**, 761-771.
- Brookman, J. L., Stott, A. J., Cheeseman, P. J., Burns, N. R., Adams, S. E., Kingsman, A. J., and Gull, K. (1995). An immunological analysis of Ty1 virus-like particle structure. *Virology* **207**(1), 59-67.
- Butcher, B. A., and Denkers, E. Y. (2002). Mechanism of entry determines the ability of Toxoplasma gondii to inhibit macrophage proinflammatory cytokine production. *Infect Immun* **70**(9), 5216-24.

- Butcher, B. A., Greene, R. I., Henry, S. C., Annecharico, K. L., Weinberg, J. B., Denkers, E. Y., Sher, A., and Taylor, G. A. (2005a). p47 GTPases Regulate *Toxoplasma gondii* Survival in Activated Macrophages. *Infect Immun* **73**(6), 3278-86.
- Butcher, B. A., Kim, L., Johnson, P. F., and Denkers, E. Y. (2001). *Toxoplasma gondii* tachyzoites inhibit proinflammatory cytokine induction in infected macrophages by preventing nuclear translocation of the transcription factor NF-kappa B. *J Immunol* **167**(4), 2193-201.
- Butcher, B. A., Kim, L., Panopoulos, A. D., Watowich, S. S., Murray, P. J., and Denkers, E. Y. (2005b). IL-10-independent STAT3 activation by *Toxoplasma gondii* mediates suppression of IL-12 and TNF-alpha in host macrophages. *J Immunol* **174**(6), 3148-52.
- Cannon, M. J., and Pate, J. L. (2006). Indoleamine 2,3-dioxygenase participates in the interferon-gamma-induced cell death process in cultured bovine luteal cells. *Biol Reprod* **74**(3), 552-9.
- Carlow, D. A., Teh, S.-J., and Teh, H.-S. (1998). Specific antiviral activity demonstrated by TGTP, a member of a new family of interferon-induced GTPases. *J. Immunol.* **161**, 2348-2355.
- Carmen, J. C., and Sinai, A. P. (2007). Suicide prevention: disruption of apoptotic pathways by protozoan parasites. *Mol Microbiol* **64**(4), 904-16.
- Carruthers, V. B., and Sibley, L. D. (1997). Sequential protein secretion from three distinct organelles of *Toxoplasma gondii* accompanies invasion of human fibroblasts. *Eur J Cell Biol* **73**(2), 114-23.
- Carter, C. C., Gorbacheva, V. Y., and Vestal, D. J. (2005). Inhibition of VSV and EMCV replication by the interferon-induced GTPase, mGBP-2: differential requirement for wild-type GTP binding domain. *Arch Virol* **150**(6), 1213-20.
- Chawla-Sarkar, M., Lindner, D. J., Liu, Y. F., Williams, B. R., Sen, G. C., Silverman, R. H., and Borden, E. C. (2003). Apoptosis and interferons: role of interferon-stimulated genes as mediators of apoptosis. *Apoptosis* **8**(3), 237-49.
- Checroun, C., Wehrly, T. D., Fischer, E. R., Hayes, S. F., and Celli, J. (2006). Autophagy-mediated reentry of *Francisella tularensis* into the endocytic compartment after cytoplasmic replication. *Proc Natl Acad Sci U S A* **103**(39), 14578-83.

- Chen, G., Ward, M. F., Sama, A. E., and Wang, H. (2004). Extracellular HMGB1 as a proinflammatory cytokine. *J Interferon Cytokine Res* **24**(6), 329-33.
- Chin, Y. E., Kitagawa, M., Kuida, K., Flavell, R. A., and Fu, X. Y. (1997). Activation of the STAT signaling pathway can cause expression of caspase 1 and apoptosis. *Mol Cell Biol* **17**(9), 5328-37.
- Codogno, P., and Meijer, A. J. (2006). Atg5: more than an autophagy factor. *Nat Cell Biol* **8**(10), 1045-7.
- Coers, J., Bernstein-Hanley, I., Grotzky, D., Parvanova, I., Howard, J. C., Taylor, G. A., Dietrich, W. F., and Starnbach, M. N. (2008). Chlamydia muridarum evades growth restriction by the IFN-gamma-inducible host resistance factor Irgb10. *J Immunol* **180**(9), 6237-45.
- Coers, J., Starnbach, M. N., and Howard, J. C. (2009). Modeling infectious disease in mice: co-adaptation and the role of host-specific IFNgamma responses. *PLoS Pathog* **5**(5), e1000333.
- Collazo, C. M., Yap, G. S., Hieny, S., Caspar, P., Feng, C. G., Taylor, G. A., and Sher, A. (2002). The function of gamma interferon-inducible GTP-binding protein IGTP in host resistance to *Toxoplasma gondii* is Stat1 dependent and requires expression in both hematopoietic and nonhematopoietic cellular compartments. *Infect Immun.* **70**, 6933-9.
- Collazo, C. M., Yap, G. S., Sempowski, G. D., Lusby, K. C., Tessarollo, L., Woude, G. F. V., Sher, A., and Taylor, G. A. (2001). Inactivation of LRG-47 and IRG-47 Reveals a Family of Interferon {gamma}-inducible Genes with Essential, Pathogen-specific Roles in Resistance to Infection. *J. Exp. Med.* **194**(2), 181-188.
- Daubener, W., Spors, B., Hucke, C., Adam, R., Stins, M., Kim, K. S., and Schroten, H. (2001). Restriction of *Toxoplasma gondii* growth in human brain microvascular endothelial cells by activation of indoleamine 2,3-dioxygenase. *Infect Immun* **69**(10), 6527-31.
- de la Maza, L. M., and Peterson, E. M. (1988). Dependence of the in vitro antiproliferative activity of recombinant human gamma-interferon on the concentration of tryptophan in culture media. *Cancer Res* **48**(2), 346-50.
- Degrandi, D., Konermann, C., Beuter-Gunia, C., Kresse, A., Wurthner, J., Kurig, S., Beer, S., and Pfeffer, K. (2007). Extensive characterization of IFN-induced

- GTPases mGBP1 to mGBP10 involved in host defense. *J Immunol* **179**(11), 7729-40.
- Denkers, E. Y. (2003). From cells to signaling cascades: manipulation of innate immunity by *Toxoplasma gondii*. *FEMS Immunol Med Microbiol* **39**(3), 193-203.
- Denkers, E. Y., and Butcher, B. A. (2005). Sabotage and exploitation in macrophages parasitized by intracellular protozoans. *Trends Parasitol* **21**(1), 35-41.
- Deretic, V. (2005). Autophagy in innate and adaptive immunity. *Trends Immunol* **26**(10), 523-8.
- Deretic, V. (2006). Autophagy as an immune defense mechanism. *Curr Opin Immunol* **18**(4), 375-82.
- Dimier, I. H., and Bout, D. T. (1998). Interferon-gamma-activated primary enterocytes inhibit *Toxoplasma gondii* replication: a role for intracellular iron. *Immunology* **94**(4), 488-95.
- Dimmer, K. S., Navoni, F., Casarin, A., Trevisson, E., Endeles, S., Winterpacht, A., Salviati, L., and Scorrano, L. (2008). LETM1, deleted in Wolf-Hirschhorn syndrome is required for normal mitochondrial morphology and cellular viability. *Hum Mol Genet* **17**(2), 201-14.
- Ding, M., Kwok, L. Y., Schluter, D., Clayton, C., and Soldati, D. (2004). The antioxidant systems in *Toxoplasma gondii* and the role of cytosolic catalase in defence against oxidative injury. *Mol Microbiol* **51**(1), 47-61.
- Dive, C., Gregory, C. D., Phipps, D. J., Evans, D. L., Milner, A. E., and Wyllie, A. H. (1992). Analysis and discrimination of necrosis and apoptosis (programmed cell death) by multiparameter flow cytometry. *Biochim Biophys Acta* **1133**(3), 275-85.
- Dobrowolski, J., and Sibley, L. D. (1997). The role of the cytoskeleton in host cell invasion by *Toxoplasma gondii*. *Behring Inst Mitt*(99), 90-6.
- Donald, R. G., and Roos, D. S. (1998). Gene knock-outs and allelic replacements in *Toxoplasma gondii*: HXGPRT as a selectable marker for hit-and-run mutagenesis. *Mol Biochem Parasitol* **91**(2), 295-305.
- Dubey, J. P. (1977). Taxonomy of *Sarcocystis* and other *Coccidia* of cats and dogs. *J Am Vet Med Assoc* **170**(8), 778, 782.
- Dubremetz, J. F., Achbarou, A., Bermudes, D., and Joiner, K. A. (1993). Kinetics and

- pattern of organelle exocytosis during *Toxoplasma gondii*/host-cell interaction. *Parasitol Res* **79**(5), 402-8.
- Dubremetz, J. F., and Schwartzman, J. D. (1993). Subcellular organelles of *Toxoplasma gondii* and host cell invasion. *Res Immunol* **144**(1), 31-3.
- Egan, C. E., Sukhumavasi, W., Butcher, B. A., and Denkers, E. Y. (2009). Functional aspects of Toll-like receptor/MyD88 signalling during protozoan infection: focus on *Toxoplasma gondii*. *Clin Exp Immunol* **156**(1), 17-24.
- El Hajj, H., Demey, E., Poncet, J., Lebrun, M., Wu, B., Galeotti, N., Fourmaux, M. N., Mercereau-Puijalon, O., Vial, H., Labesse, G., and Dubremetz, J. F. (2006). The ROP2 family of *Toxoplasma gondii* rhoptry proteins: proteomic and genomic characterization and molecular modeling. *Proteomics* **6**(21), 5773-84.
- El Hajj, H., Lebrun, M., Arold, S. T., Vial, H., Labesse, G., and Dubremetz, J. F. (2007). ROP18 is a rhoptry kinase controlling the intracellular proliferation of *Toxoplasma gondii*. *PLoS Pathog* **3**(2), e14.
- Feng, C. G., Collazo-Custodio, C. M., Eckhaus, M., Hieny, S., Belkaid, Y., Elkins, K., Jankovic, D., Taylor, G. A., and Sher, A. (2004). Mice deficient in LRG-47 display increased susceptibility to mycobacterial infection associated with the induction of lymphopenia. *J. Immunol.* **172**, 1163-8.
- Feng, C. G., Weksberg, D. C., Taylor, G. A., Sher, A., and Goodell, M. A. (2008a). The p47 GTPase Lrg-47 (Irgm1) links host defense and hematopoietic stem cell proliferation. *Cell Stem Cell* **2**(1), 83-9.
- Feng, C. G., Zheng, L., Jankovic, D., Bafica, A., Cannons, J. L., Watford, W. T., Chaussabel, D., Hieny, S., Caspar, P., Schwartzberg, P. L., Lenardo, M. J., and Sher, A. (2008b). The immunity-related GTPase Irgm1 promotes the expansion of activated CD4+ T cell populations by preventing interferon-gamma-induced cell death. *Nat Immunol* **9**(11), 1279-87.
- Fentress, S. J., Dunay, I. R., Behnke, M. S., Rommereim, L. M., Fox, B. A., Bzik, D. J., Beatty, W. L., Taylor, G. A., Turk, B. E., and Sibley, L. D. (submitted). *Toxoplasma* ROP18 kinase subverts host defenses by phosphorylating immunity-related GTPases.
- Fernandes-Alnemri, T., Wu, J., Yu, J. W., Datta, P., Miller, B., Jankowski, W., Rosenberg, S., Zhang, J., and Alnemri, E. S. (2007). The pyroptosome: a

- supramolecular assembly of ASC dimers mediating inflammatory cell death via caspase-1 activation. *Cell Death Differ* **14**(9), 1590-604.
- Festjens, N., Vanden Berghe, T., and Vandenabeele, P. (2006). Necrosis, a well-orchestrated form of cell demise: signalling cascades, important mediators and concomitant immune response. *Biochim Biophys Acta* **1757**(9-10), 1371-87.
- Fischer, H. G., Stachelhaus, S., Sahm, M., Meyer, H. E., and Reichmann, G. (1998). GRA7, an excretory 29 kDa *Toxoplasma gondii* dense granule antigen released by infected host cells. *Mol Biochem Parasitol* **91**(2), 251-62.
- Fisher, S. A., Tremelling, M., Anderson, C. A., Gwilliam, R., Bumpstead, S., Prescott, N. J., Nimmo, E. R., Massey, D., Berzuini, C., Johnson, C., Barrett, J. C., Cummings, F. R., Drummond, H., Lees, C. W., Onnie, C. M., Hanson, C. E., Blaszczyk, K., Inouye, M., Ewels, P., Ravindrarajah, R., Keniry, A., Hunt, S., Carter, M., Watkins, N., Ouwehand, W., Lewis, C. M., Cardon, L., Lobo, A., Forbes, A., Sanderson, J., Jewell, D. P., Mansfield, J. C., Deloukas, P., Mathew, C. G., Parkes, M., and Satsangi, J. (2008). Genetic determinants of ulcerative colitis include the ECM1 locus and five loci implicated in Crohn's disease. *Nat Genet* **40**(6), 710-2.
- Frenkel, J. K. (1988). Pathophysiology of toxoplasmosis. *Parasitol Today* **4**(10), 273-8.
- Fritz, J. H., Ferrero, R. L., Philpott, D. J., and Girardin, S. E. (2006). Nod-like proteins in immunity, inflammation and disease. *Nat Immunol* **7**(12), 1250-7.
- Galluzzi, L., Maiuri, M. C., Vitale, I., Zischka, H., Castedo, M., Zitvogel, L., and Kroemer, G. (2007). Cell death modalities: classification and pathophysiological implications. *Cell Death Differ* **14**(7), 1237-43.
- Gazzinelli, R. T., Amichay, D., Sharton-Kersten, T., Grunwald, E., Farber, J. M., and Sher, A. (1996). Role of macrophage-derived cytokines in the induction and regulation of cell-mediated immunity to *Toxoplasma gondii*. *Curr Top Microbiol Immunol* **219**, 127-39.
- Gazzinelli, R. T., Hayashi, S., Wysocka, M., Carrera, L., Kuhn, R., Muller, W., Roberge, F., Trinchieri, G., and Sher, A. (1994a). Role of IL-12 in the initiation of cell mediated immunity by *Toxoplasma gondii* and its regulation by IL-10 and nitric oxide. *J Eukaryot Microbiol* **41**(5), 9S.
- Gazzinelli, R. T., Wysocka, M., Hayashi, S., Denkers, E. Y., Hieny, S., Caspar, P.,

- Trinchieri, G., and Sher, A. (1994b). Parasite-induced IL-12 stimulates early IFN-gamma synthesis and resistance during acute infection with *Toxoplasma gondii*. *J Immunol* **153**(6), 2533-43.
- Ghosh, A., Uthaiyah, R., Howard, J., Herrmann, C., and Wolf, E. (2004). Crystal structure of IIGP1: a paradigm for interferon-inducible p47 resistance GTPases. *Mol Cell* **15**(5), 727-39.
- Goebel, S., Gross, U., and Luder, C. G. (2001). Inhibition of host cell apoptosis by *Toxoplasma gondii* is accompanied by reduced activation of the caspase cascade and alterations of poly(ADP-ribose) polymerase expression. *J Cell Sci* **114**(Pt 19), 3495-505.
- Goldstein, J. C., Waterhouse, N. J., Juin, P., Evan, G. I., and Green, D. R. (2000). The coordinate release of cytochrome c during apoptosis is rapid, complete and kinetically invariant. *Nat Cell Biol* **2**(3), 156-62.
- Golstein, P., and Kroemer, G. (2007). Cell death by necrosis: towards a molecular definition. *Trends Biochem Sci* **32**(1), 37-43.
- Gorbacheva, V. Y., Lindner, D., Sen, G. C., and Vestal, D. J. (2002). The interferon (IFN)-induced GTPase, mGBP-2. Role in IFN-gamma-induced murine fibroblast proliferation. *J Biol Chem*. **277**, 6080-7.
- Gross, U., Muller, W. A., Knapp, S., and Heesemann, J. (1991). Identification of a virulence-associated antigen of *Toxoplasma gondii* by use of a mouse monoclonal antibody. *Infect Immun* **59**(12), 4511-6.
- Gubbels, M. J., Li, C., and Striepen, B. (2003). High-throughput growth assay for *Toxoplasma gondii* using yellow fluorescent protein. *Antimicrob Agents Chemother* **47**(1), 309-16.
- Guenzi, E., Topolt, K., Cornali, E., Lubeseder-Martellato, C., Jorg, A., Matzen, K., Zietz, C., Kremmer, E., Nappi, F., Schwemmle, M., Hohenadl, C., Barillari, G., Tschachler, E., Monini, P., Ensoli, B., and Sturzl, M. (2001). The helical domain of GBP-1 mediates the inhibition of endothelial cell proliferation by inflammatory cytokines. *EMBO J*. **20**, 5568-77.
- Guenzi, E., Topolt, K., Lubeseder-Martellato, C., Jorg, A., Naschberger, E., Benelli, R., Albini, A., and Sturzl, M. (2003). The guanylate binding protein-1 GTPase controls the invasive and angiogenic capability of endothelial cells through inhibition of MMP-1 expression. *EMBO J* **22**(15), 3772-82.

- Guicciardi, M. E., Leist, M., and Gores, G. J. (2004). Lysosomes in cell death. *Oncogene* **23**(16), 2881-90.
- Guo, Z. G., Gross, U., and Johnson, A. M. (1997). Toxoplasma gondii virulence markers identified by random amplified polymorphic DNA polymerase chain reaction. *Parasitol Res* **83**(5), 458-63.
- Gutierrez, M. G., Master, S. S., Singh, S. B., Taylor, G. A., Colombo, M. I., and Deretic, V. (2004). Autophagy is a defense mechanism inhibiting BCG and Mycobacterium tuberculosis survival in infected macrophages. *Cell* **119**(6), 753-66.
- Habara-Ohkubo, A., Shirahata, T., Takikawa, O., and Yoshida, R. (1993). Establishment of an antitoxoplasma state by stable expression of mouse indoleamine 2,3-dioxygenase. *Infect Immun* **61**(5), 1810-3.
- Haller, O., and Kochs, G. (2002). Interferon-induced MX proteins: dynamin-like GTPases with antiviral activity. *Traffic* **3**(10), 710-7.
- Hanada, T., Noda, N. N., Satomi, Y., Ichimura, Y., Fujioka, Y., Takao, T., Inagaki, F., and Ohsumi, Y. (2007). The Atg12-Atg5 conjugate has a novel E3-like activity for protein lipidation in autophagy. *J Biol Chem* **282**(52), 37298-302.
- Hara, T., Nakamura, K., Matsui, M., Yamamoto, A., Nakahara, Y., Suzuki-Migishima, R., Yokoyama, M., Mishima, K., Saito, I., Okano, H., and Mizushima, N. (2006). Suppression of basal autophagy in neural cells causes neurodegenerative disease in mice. *Nature* **441**(7095), 885-9.
- Hauptmann, R., and Swetly, P. (1985). A novel class of human type I interferons. *Nucleic Acids Res* **13**(13), 4739-49.
- Henry, S. C., Daniell, X., Indaram, M., Whitesides, J. F., Sempowski, G. D., Howell, D., Oliver, T., and Taylor, G. A. (2007). Impaired macrophage function underscores susceptibility to Salmonella in mice lacking Irgm1 (LRG-47). *J Immunol* **179**(10), 6963-72.
- Henry, S. C., Daniell, X. G., Burroughs, A. R., Indaram, M., Howell, D. N., Coers, J., Starnbach, M. N., Hunn, J. P., Howard, J. C., Feng, C. G., Sher, A., and Taylor, G. A. (2009). Balance of Irgm protein activities determines IFN-gamma-induced host defense. *J Leukoc Biol* **85**(5), 877-85.
- Henry, S. C., Traver, M., Daniell, X., Indaram, M., Oliver, T., and Taylor, G. A. (2010). Regulation of macrophage motility by Irgm1. *J Leukoc Biol* **87**(2),

333-43.

- Heseler, K., Spekker, K., Schmidt, S. K., MacKenzie, C. R., and Daubener, W. (2008). Antimicrobial and immunoregulatory effects mediated by human lung cells: role of IFN-gamma-induced tryptophan degradation. *FEMS Immunol Med Microbiol* **52**(2), 273-81.
- Hinshaw, J. E. (2000). Dynamin and its role in membrane fission. *Annu Rev Cell Dev Biol* **16**, 483-519.
- Howe, D. K., and Sibley, L. D. (1995). *Toxoplasma gondii* comprises three clonal lineages: correlation of parasite genotype with human disease. *J Infect Dis* **172**(6), 1561-6.
- Hsu, C. P., Hariharan, N., Alcendor, R. R., Oka, S., and Sadoshima, J. (2009). Nicotinamide phosphoribosyltransferase regulates cell survival through autophagy in cardiomyocytes. *Autophagy* **5**(8), 1229-31.
- Hunn, J. P. (2007). Ph. D. thesis. University of Cologne, Cologne.
- Hunn, J. P., and Howard, J. C. (2010). The mouse resistance protein, Irgm1 (LRG-47): a regulator or an effector of pathogen defense? *PLoS Pathog* **Accepted article**.
- Hunn, J. P., Koenen-Waisman, S., Papic, N., Schroeder, N., Pawlowski, N., Lange, R., Kaiser, F., Zerrahn, J., Martens, S., and Howard, J. C. (2008). Regulatory interactions between IRG resistance GTPases in the cellular response to *Toxoplasma gondii*. *EMBO J* **27**(19), 2495-509.
- Hunter, C. A., Candolfi, E., Subauste, C., Van Cleave, V., and Remington, J. S. (1995). Studies on the role of interleukin-12 in acute murine toxoplasmosis. *Immunology* **84**(1), 16-20.
- Inagaki, Y., Yamagishi, S., Amano, S., Okamoto, T., Koga, K., and Makita, Z. (2002). Interferon-gamma-induced apoptosis and activation of THP-1 macrophages. *Life Sci* **71**(21), 2499-508.
- Isaacs, A., and Lindenmann, J. (1957). Virus interference. I. The interferon. *Proc R Soc Lond B Biol Sci* **147**(927), 258-67.
- Isaacs, A., Lindenmann, J., and Valentine, R. C. (1957). Virus interference. II. Some properties of interferon. *Proc R Soc Lond B Biol Sci* **147**(927), 268-73.
- Itsui, Y., Sakamoto, N., Kakinuma, S., Nakagawa, M., Sekine-Osajima, Y., Tasaka-Fujita, M., Nishimura-Sakurai, Y., Suda, G., Karakama, Y., Mishima, K., Yamamoto, M., Watanabe, T., Ueyama, M., Funaoka, Y., Azuma, S., and

- Watanabe, M. (2009). Antiviral effects of the interferon-induced protein guanylate binding protein 1 and its interaction with the hepatitis C virus NS5B protein. *Hepatology* **50**(6), 1727-37.
- Iwasaki, A., and Medzhitov, R. (2004). Toll-like receptor control of the adaptive immune responses. *Nat Immunol* **5**(10), 987-95.
- Iyer, S. S., Pulskens, W. P., Sadler, J. J., Butter, L. M., Teske, G. J., Ulland, T. K., Eisenbarth, S. C., Florquin, S., Flavell, R. A., Leemans, J. C., and Sutterwala, F. S. (2009). Necrotic cells trigger a sterile inflammatory response through the Nlrp3 inflammasome. *Proc Natl Acad Sci U S A* **106**(48), 20388-93.
- Janeway, C. A., Murphy, K. M., Travers, P., and M., W. (2008). "Janeway's Immunobiology." 7th ed. Garland Science.
- Johnson, L. L., and Sayles, P. C. (1997). Interleukin-12, dendritic cells, and the initiation of host-protective mechanisms against *Toxoplasma gondii*. *J Exp Med* **186**(11), 1799-802.
- Joiner, K. A., and Dubremetz, J. F. (1993). *Toxoplasma gondii*: a protozoan for the nineties. *Infect Immun* **61**(4), 1169-72.
- Joiner, K. A., Fuhrman, S. A., Miettinen, H. M., Kasper, L. H., and Mellman, I. (1990). *Toxoplasma gondii*: fusion competence of parasitophorous vacuoles in Fc receptor-transfected fibroblasts. *Science* **249**(4969), 641-6.
- Kafsack, B. F., Beckers, C., and Carruthers, V. B. (2004). Synchronous invasion of host cells by *Toxoplasma gondii*. *Mol Biochem Parasitol* **136**(2), 309-11.
- Kafsack, B. F., Carruthers, V. B., and Pineda, F. J. (2007). Kinetic modeling of *Toxoplasma gondii* invasion. *J Theor Biol* **249**(4), 817-25.
- Kaiser, F., Kaufmann, S. H., and Zerrahn, J. (2004). IIGP, a member of the IFN inducible and microbial defense mediating 47 kDa GTPase family, interacts with the microtubule binding protein hook3. *J Cell Sci* **117**(Pt 9), 1747-56.
- Kaufmann, S. H., Desnoyers, S., Ottaviano, Y., Davidson, N. E., and Poirier, G. G. (1993). Specific proteolytic cleavage of poly(ADP-ribose) polymerase: an early marker of chemotherapy-induced apoptosis. *Cancer Res* **53**(17), 3976-85.
- Kaushik, S., Massey, A. C., Mizushima, N., and Cuervo, A. M. (2008). Constitutive activation of chaperone-mediated autophagy in cells with impaired macroautophagy. *Mol Biol Cell* **19**(5), 2179-92.

- Keller, P., Schaumburg, F., Fischer, S. F., Hacker, G., Gross, U., and Luder, C. G. (2006). Direct inhibition of cytochrome c-induced caspase activation in vitro by *Toxoplasma gondii* reveals novel mechanisms of interference with host cell apoptosis. *FEMS Microbiol Lett* **258**(2), 312-9.
- Khaminets, A., Hunn, J. P., Konen-Waisman, S., Zhao, Y. O., Preukschat, D., Coers, J., Boyle, J. P., Ong, Y. C., Boothroyd, J. C., Reichmann, G., and Howard, J. C. (2010). Coordinated Loading of IRG Resistance GTPases on to the *Toxoplasma gondii* Parasitophorous Vacuole. *Cell Microbiol* **Accepted article**.
- Khan, A., Fux, B., Su, C., Dubey, J. P., Darde, M. L., Ajioka, J. W., Rosenthal, B. M., and Sibley, L. D. (2007). Recent transcontinental sweep of *Toxoplasma gondii* driven by a single monomorphic chromosome. *Proc Natl Acad Sci U S A* **104**(37), 14872-7.
- Khan, A., Taylor, S., Ajioka, J. W., Rosenthal, B. M., and Sibley, L. D. (2009). Selection at a single locus leads to widespread expansion of *Toxoplasma gondii* lineages that are virulent in mice. *PLoS Genet* **5**(3), e1000404.
- Khan, I. A., Schwartzman, J. D., Matsuura, T., and Kasper, L. H. (1997). A dichotomous role for nitric oxide during acute *Toxoplasma gondii* infection in mice. *Proc Natl Acad Sci U S A* **94**(25), 13955-60.
- Kim, L., and Denkers, E. Y. (2006). *Toxoplasma gondii* triggers Gi-dependent PI 3-kinase signaling required for inhibition of host cell apoptosis. *J Cell Sci* **119**(Pt 10), 2119-26.
- Klamp, T., Boehm, U., Schenk, D., Pfeffer, K., and Howard, J. C. (2003). A giant GTPase, VLIg-1, is inducible by interferons. *J. Immunol.* **171**, 1255-65.
- Kochs, G., Haener, M., Aebi, U., and Haller, O. (2002). Self-assembly of human MxA GTPase into highly ordered dynamin-like oligomers. *J Biol Chem* **277**(16), 14172-6.
- Kochs, G., and Haller, O. (1999a). GTP-bound human MxA Protein interacts with the nucleocapsids of Thogoto virus (Orthomyxoviridae). *J. Biol. Chem.* **274**, 4370-4376.
- Kochs, G., and Haller, O. (1999b). Interferon-induced human MxA GTPase blocks nuclear import of thogoto virus nucleocapsids. *Cell Biology* **96**, 2082-2086.
- Kochs, G., Trost, M., Janzen, C., and Haller, O. (1998). MxA GTPase:

- oligomerization and GTP-dependent interaction with viral RNP target structures. *Methods* **15**(3), 255-63.
- Koga, R., Hamano, S., Kuwata, H., Atarashi, K., Ogawa, M., Hisaeda, H., Yamamoto, M., Akira, S., Himeno, K., Matsumoto, M., and Takeda, K. (2006). TLR-dependent induction of IFN-beta mediates host defense against *Trypanosoma cruzi*. *J Immunol* **177**(10), 7059-66.
- Könen-Waisman, S., and Howard, J. C. (2007). Cell-autonomous immunity to *Toxoplasma gondii* in mouse and man. *Microbes Infect* **9**(14-15), 1652-61.
- Kotenko, S. V., Gallagher, G., Baurin, V. V., Lewis-Antes, A., Shen, M., Shah, N. K., Langer, J. A., Sheikh, F., Dickensheets, H., and Donnelly, R. P. (2003). IFN-lambdas mediate antiviral protection through a distinct class II cytokine receptor complex. *Nat. Immunol.* **4**, 69-77.
- Kroemer, G., and Levine, B. (2008). Autophagic cell death: the story of a misnomer. *Nat Rev Mol Cell Biol* **9**(12), 1004-10.
- Kuma, A., Hatano, M., Matsui, M., Yamamoto, A., Nakaya, H., Yoshimori, T., Ohsumi, Y., Tokuhiya, T., and Mizushima, N. (2004). The role of autophagy during the early neonatal starvation period. *Nature* **432**(7020), 1032-6.
- Labbe, K., and Saleh, M. (2008). Cell death in the host response to infection. *Cell Death Differ* **15**(9), 1339-49.
- Lafuse, W. P., Brown, D., Castle, L., and Zwillig, B. S. (1995). Cloning and characterization of a novel cDNA that is IFN-gamma-induced in mouse peritoneal macrophages and encodes a putative GTP-binding protein. *J Leukoc Biol* **57**(3), 477-83.
- Lang, C., Algnier, M., Beinert, N., Gross, U., and Luder, C. G. (2006). Diverse mechanisms employed by *Toxoplasma gondii* to inhibit IFN-gamma-induced major histocompatibility complex class II gene expression. *Microbes Infect* **8**(8), 1994-2005.
- Langermans, J. A., Nibbering, P. H., Van Vuren-Van Der Hulst, M. E., and Van Furth, R. (2001). Transforming growth factor-beta suppresses interferon-gamma-induced toxoplasma activity in murine macrophages by inhibition of tumour necrosis factor-alpha production. *Parasite Immunol* **23**(4), 169-75.
- Lapaque, N., Takeuchi, O., Corrales, F., Akira, S., Moriyon, I., Howard, J. C., and

- Gorvel, J. P. (2006). Differential inductions of TNF-alpha and IIGP, IIGP by structurally diverse classic and non-classic lipopolysaccharides. *Cell Microbiol* **8**(3), 401-13.
- Lapaquette, P., Glasser, A. L., Huett, A., Xavier, R. J., and Darfeuille-Michaud, A. (2010) Crohn's disease-associated adherent-invasive E. coli are selectively favoured by impaired autophagy to replicate intracellularly. *Cell Microbiol* **12**(1), 99-113.
- Lecomte, V., Chumpitazi, B. F., Pasquier, B., Ambroise-Thomas, P., and Santoro, F. (1992). Brain-tissue cysts in rats infected with the RH strain of *Toxoplasma gondii*. *Parasitol Res* **78**(3), 267-9.
- Lee, E. J., Heo, Y. M., Choi, J. H., Song, H. O., Ryu, J. S., and Ahn, M. H. (2008). Suppressed production of pro-inflammatory cytokines by LPS-activated macrophages after treatment with *Toxoplasma gondii* lysate. *Korean J Parasitol* **46**(3), 145-51.
- Lee, M. S., and Kim, Y. J. (2007). Pattern-recognition receptor signaling initiated from extracellular, membrane, and cytoplasmic space. *Mol Cells* **23**(1), 1-10.
- Lefevre, F., Guillomot, M., D'Andrea, S., Battegay, S., and La Bonnardiere, C. (1998). Interferon-delta: the first member of a novel type I interferon family. *Biochimie* **80**(8-9), 779-88.
- Lehmann, T., Marcet, P. L., Graham, D. H., Dahl, E. R., and Dubey, J. P. (2006). Globalization and the population structure of *Toxoplasma gondii*. *Proc Natl Acad Sci U S A* **103**(30), 11423-8.
- Leipe, D. D., Wolf, Y. I., Koonin, E. V., and Aravind, L. (2002). Classification and evolution of P-loop GTPases and related ATPases. *J Mol Biol* **317**(1), 41-72.
- Levine, B. (2005). Eating oneself and uninvited guests; autophagy-related pathways in cellular defense. *Cell* **120**(2), 159-62.
- Li, G., Zhang, J., Sun, Y., Wang, H., and Wang, Y. (2009). The evolutionarily dynamic IFN-inducible GTPase proteins play conserved immune functions in vertebrates and cephalochordates. *Mol Biol Evol* **26**(7), 1619-30.
- Lindenmann, J., Deuel, E., Fanconi, S., and Haller, O. (1978). Inborn resistance of mice to myxoviruses: macrophages express phenotype in vitro. *J Exp Med* **147**(2), 531-40.
- Lindenmann, J., Lane, C. A., and Hobson, D. (1963). The Resistance of A2g Mice to

- Myxoviruses. *J Immunol* **90**, 942-51.
- Ling, Y. M., Shaw, M. H., Ayala, C., Coppens, I., Taylor, G. A., Ferguson, D. J., and Yap, G. S. (2006). Vacuolar and plasma membrane stripping and autophagic elimination of *Toxoplasma gondii* in primed effector macrophages. *J Exp Med* **203**(9), 2063-71.
- Luder, C. G., Algnier, M., Lang, C., Bleicher, N., and Gross, U. (2003). Reduced expression of the inducible nitric oxide synthase after infection with *Toxoplasma gondii* facilitates parasite replication in activated murine macrophages. *Int J Parasitol* **33**(8), 833-44.
- Luder, C. G., Lang, T., Beuerle, B., and Gross, U. (1998). Down-regulation of MHC class II molecules and inability to up-regulate class I molecules in murine macrophages after infection with *Toxoplasma gondii*. *Clin Exp Immunol* **112**(2), 308-16.
- Luder, C. G., Walter, W., Beuerle, B., Maeurer, M. J., and Gross, U. (2001). *Toxoplasma gondii* down-regulates MHC class II gene expression and antigen presentation by murine macrophages via interference with nuclear translocation of STAT1alpha. *Eur J Immunol* **31**(5), 1475-84.
- Luft, B. J., and Remington, J. S. (1988). AIDS commentary. Toxoplasmic encephalitis. *J Infect Dis* **157**(1), 1-6.
- MacKenzie, C. R., Langen, R., Takikawa, O., and Daubener, W. (1999). Inhibition of indoleamine 2,3-dioxygenase in human macrophages inhibits interferon-gamma-induced bacteriostasis but does not abrogate toxoplasmatosis. *Eur J Immunol* **29**(10), 3254-61.
- MacMicking, J., Taylor, G. A., and McKinney, J. (2003). Immune control of tuberculosis by IFN-gamma-inducible LRG-47. *Science* **302**, 654-659.
- MacMicking, J. D. (2005). Immune control of phagosomal bacteria by p47 GTPases. *Curr Opin Microbiol* **8**(1), 74-82.
- Mariathasan, S., Weiss, D. S., Newton, K., McBride, J., O'Rourke, K., Roose-Girma, M., Lee, W. P., Weinrauch, Y., Monack, D. M., and Dixit, V. M. (2006). Cryopyrin activates the inflammasome in response to toxins and ATP. *Nature* **440**(7081), 228-32.
- Martens, S., and Howard, J. (2006). The Interferon-Inducible GTPases. *Annu Rev Cell Dev Biol* **22**, 559-589.

- Martens, S., Parvanova, I., Zerrahn, J., Griffiths, G., Schell, G., Reichmann, G., and Howard, J. C. (2005). Disruption of *Toxoplasma gondii* parasitophorous vacuoles by the mouse p47-resistance GTPases. *PLoS Pathog* **1**(3), e24.
- Martens, S., Sabel, K., Lange, R., Uthaiiah, R., Wolf, E., and Howard, J. C. (2004). Mechanisms regulating the positioning of mouse p47 resistance GTPases LRG-47 and IIGP1 on cellular membranes: retargeting to plasma membrane induced by phagocytosis. *J. Immunol.* **173**, 2594-606.
- Matzinger, P. (1994). Tolerance, danger, and the extended family. *Annu Rev Immunol* **12**, 991-1045.
- McClarty, G., Caldwell, H. D., and Nelson, D. E. (2007). Chlamydial interferon gamma immune evasion influences infection tropism. *Curr Opin Microbiol* **10**(1), 47-51.
- McKee, A. S., Dzierszynski, F., Boes, M., Roos, D. S., and Pearce, E. J. (2004). Functional inactivation of immature dendritic cells by the intracellular parasite *Toxoplasma gondii*. *J Immunol* **173**(4), 2632-40.
- Medzhitov, R. (2001). Toll-like receptors and innate immunity. *Nature Rev Immunol* **1**(2), 135-45.
- Medzhitov, R., and Janeway, C. A., Jr. (1997). Innate immunity: impact on the adaptive immune response. *Curr Opin Immunol* **9**(1), 4-9.
- Melzer, T., Duffy, A., Weiss, L. M., and Halonen, S. K. (2008). The gamma interferon (IFN-gamma)-inducible GTP-binding protein IGTP is necessary for toxoplasma vacuolar disruption and induces parasite egression in IFN-gamma-stimulated astrocytes. *Infect Immun* **76**(11), 4883-94.
- Miyairi, I., Tatireddigari, V. R., Mahdi, O. S., Rose, L. A., Belland, R. J., Lu, L., Williams, R. W., and Byrne, G. I. (2007). The p47 GTPases Iigp2 and Irgb10 regulate innate immunity and inflammation to murine *Chlamydia psittaci* infection. *J Immunol* **179**(3), 1814-24.
- Mizushima, N. (2002). Molecular mechanism of autophagy: the role of the Apg12 conjugation system. *Seikagaku* **74**(7), 523-37.
- Mizushima, N., Levine, B., Cuervo, A. M., and Klionsky, D. J. (2008). Autophagy fights disease through cellular self-digestion. *Nature* **451**(7182), 1069-75.
- Mogensen, K. E., Lewerenz, M., Reboul, J., Lutfalla, G., and Uze, G. (1999). The type I interferon receptor: structure, function, and evolution of a family

- business. *J Interferon Cytokine Res* **19**(10), 1069-98.
- Molestina, R. E., and Sinai, A. P. (2005a). Detection of a novel parasite kinase activity at the *Toxoplasma gondii* parasitophorous vacuole membrane capable of phosphorylating host IkappaBalpha. *Cell Microbiol* **7**(3), 351-62.
- Molestina, R. E., and Sinai, A. P. (2005b). Host and parasite-derived IKK activities direct distinct temporal phases of NF-kappaB activation and target gene expression following *Toxoplasma gondii* infection. *J Cell Sci* **118**(Pt 24), 5785-96.
- Moosmann, B., and Behl, C. (2000). Cytoprotective antioxidant function of tyrosine and tryptophan residues in transmembrane proteins. *Eur J Biochem* **267**(18), 5687-92.
- Mordue, D. G., Hakansson, S., Niesman, I., and Sibley, L. D. (1999). *Toxoplasma gondii* resides in a vacuole that avoids fusion with host cell endocytic and exocytic vesicular trafficking pathways. *Exp Parasitol* **92**(2), 87-99.
- Mordue, D. G., Monroy, F., La Regina, M., Dinarello, C. A., and Sibley, L. D. (2001). Acute toxoplasmosis leads to lethal overproduction of Th1 cytokines. *J Immunol* **167**(8), 4574-84.
- Moulder, J. W. (1985). Comparative biology of intracellular parasitism. *Microbiol Rev* **49**(3), 298-337.
- Müllenbeck, M. (2007). Bachelor thesis. University of Cologne, Cologne.
- Munn, D. H., Shafizadeh, E., Attwood, J. T., Bondarev, I., Pashine, A., and Mellor, A. L. (1999). Inhibition of T cell proliferation by macrophage tryptophan catabolism. *J Exp Med* **189**(9), 1363-72.
- Murray, H. W., and Cohn, Z. A. (1979). Macrophage oxygen-dependent antimicrobial activity. I. Susceptibility of *Toxoplasma gondii* to oxygen intermediates. *J Exp Med* **150**(4), 938-49.
- Nantais, D. E., Schwemmler, M., Stickney, J. T., Vestal, D. J., and Buss, J. E. (1996). Prenylation of an interferon-gamma-induced GTP-binding protein: the human guanylate binding protein, huGBP1. *J Leukoc Biol* **60**(3), 423-31.
- Nelson, D. E., Virok, D. P., Wood, H., Roshick, C., Johnson, R. M., Whitmire, W. M., Crane, D. D., Steele-Mortimer, O., Kari, L., McClarty, G., and Caldwell, H. D. (2005). Chlamydial IFN- γ immune evasion is linked to host infection tropism. *Proc Natl Acad Sci U S A* **102**(30), 10658-63.

- Nishida, Y., Arakawa, S., Fujitani, K., Yamaguchi, H., Mizuta, T., Kanaseki, T., Komatsu, M., Otsu, K., Tsujimoto, Y., and Shimizu, S. (2009). Discovery of Atg5/Atg7-independent alternative macroautophagy. *Nature* **461**(7264), 654-8.
- Obojes, K., Andres, O., Kim, K. S., Daubener, W., and Schneider-Schaulies, J. (2005). Indoleamine 2,3-dioxygenase mediates cell type-specific anti-measles virus activity of gamma interferon. *J Virol* **79**(12), 7768-76.
- Ogura, Y., Sutterwala, F. S., and Flavell, R. A. (2006). The inflammasome: first line of the immune response to cell stress. *Cell* **126**(4), 659-62.
- Olszewski, M. A., Gray, J., and Vestal, D. J. (2006). In silico genomic analysis of the human and murine guanylate-binding protein (GBP) gene clusters. *J Interferon Cytokine Res* **26**(5), 328-52.
- Papic, N. (2007). Ph. D. thesis. University of Cologne, Cologne.
- Papic, N., Hunn, J. P., Pawlowski, N., Zerrahn, J., and Howard, J. C. (2008). Inactive and active states of the interferon-inducible resistance GTPase, Irga6, in vivo. *J Biol Chem* **283**(46), 32143-51.
- Parkes, M., Barrett, J. C., Prescott, N. J., Tremelling, M., Anderson, C. A., Fisher, S. A., Roberts, R. G., Nimmo, E. R., Cummings, F. R., Soars, D., Drummond, H., Lees, C. W., Khawaja, S. A., Bagnall, R., Burke, D. A., Todhunter, C. E., Ahmad, T., Onnie, C. M., McArdle, W., Strachan, D., Bethel, G., Bryan, C., Lewis, C. M., Deloukas, P., Forbes, A., Sanderson, J., Jewell, D. P., Satsangi, J., Mansfield, J. C., Cardon, L., and Mathew, C. G. (2007). Sequence variants in the autophagy gene IRGM and multiple other replicating loci contribute to Crohn's disease susceptibility. *Nat Genet* **39**(7), 830-2.
- Pawlowski, N. (2009). Ph. D. thesis. University of Cologne, Cologne.
- Pawlowski, N., Khaminets, A., Hunn, J. P., Papic, N., Schmidt, A., Uthaiyah, R. C., Lange, R., Vopper, G., Martens, S., Wolf, E., and Howard, J. C. (in preparation). Activation of GTP Hydrolysis In Trans by the Immunity-Related GTPase Irga6 Mirrors the Catalytic Mechanism of the Signal Recognition Particle (SRP/SR α).
- Pestka, S., Krause, C. D., and Walter, M. R. (2004). Interferons, interferon-like cytokines, and their receptors. *Immunol Rev* **202**, 8-32.
- Petrilli, V., Dostert, C., Muruve, D. A., and Tschopp, J. (2007a). The inflammasome:

- a danger sensing complex triggering innate immunity. *Curr Opin Immunol* **19**(6), 615-22.
- Petrilli, V., Papin, S., Dostert, C., Mayor, A., Martinon, F., and Tschopp, J. (2007b). Activation of the NALP3 inflammasome is triggered by low intracellular potassium concentration. *Cell Death Differ* **14**(9), 1583-9.
- Pfefferkorn, E. R. (1990). *Cell Biology of Toxoplasma gondii*. W. H. Freeman and Company.
- Pfefferkorn, E. R. (1984). Interferon gamma blocks the growth of *Toxoplasma gondii* in human fibroblasts by inducing the host cells to degrade tryptophan. *Proc Natl Acad Sci U S A* **81**(3), 908-12.
- Pfefferkorn, E. R., and Guyre, P. M. (1984). Inhibition of growth of *Toxoplasma gondii* in cultured fibroblasts by human recombinant gamma interferon. *Infect Immun* **44**(2), 211-6.
- Plattner, F., and Soldati-Favre, D. (2008). Hijacking of host cellular functions by the Apicomplexa. *Annu Rev Microbiol* **62**, 471-87.
- Praefcke, G. J. K., and McMahon, H. T. (2004). The dynamin superfamily: universal membrane tubulation and fission molecules? *Nature Reviews Molecular Cell Biology* **5**, 133-147.
- Pua, H. H., Dzhagalov, I., Chuck, M., Mizushima, N., and He, Y. W. (2007). A critical role for the autophagy gene Atg5 in T cell survival and proliferation. *J Exp Med* **204**(1), 25-31.
- Pyo, J. O., Jang, M. H., Kwon, Y. K., Lee, H. J., Jun, J. I., Woo, H. N., Cho, D. H., Choi, B., Lee, H., Kim, J. H., Mizushima, N., Oshumi, Y., and Jung, Y. K. (2005). Essential roles of Atg5 and FADD in autophagic cell death: dissection of autophagic cell death into vacuole formation and cell death. *J Biol Chem* **280**(21), 20722-9.
- Read, T. D., Brunham, R. C., Shen, C., Gill, S. R., Heidelberg, J. F., White, O., Hickey, E. K., Peterson, J., Utterback, T., Berry, K., Bass, S., Linher, K., Weidman, J., Khouri, H., Craven, B., Bowman, C., Dodson, R., Gwinn, M., Nelson, W., DeBoy, R., Kolonay, J., McClarty, G., Salzberg, S. L., Eisen, J., and Fraser, C. M. (2000). Genome sequences of *Chlamydia trachomatis* MoPn and *Chlamydia pneumoniae* AR39. *Nucleic Acids Res* **28**(6), 1397-406.
- Remington, J. S., and Merigan, T. C. (1968). Interferon: protection of cells infected

- with an intracellular protozoan (*Toxoplasma gondii*). *Science* **161**(843), 804-6.
- Richter, M. F., Schwemmle, M., Herrmann, C., Wittinghofer, A., and Staeheli, P. (1995). Interferon-induced MxA protein. GTP binding and GTP hydrolysis properties. *J Biol Chem* **270**(22), 13512-7.
- Robertsen, B., Zou, J., Secombes, C., and Leong, J. A. (2006). Molecular and expression analysis of an interferon-gamma-inducible guanylate-binding protein from rainbow trout (*Oncorhynchus mykiss*). *Dev Comp Immunol* **30**(11), 1023-33.
- Rohde, A. (2007). Ph. D. thesis. University of Cologne, Cologne.
- Roshick, C., Wood, H., Caldwell, H. D., and McClarty, G. (2006). Comparison of gamma interferon-mediated antichlamydial defense mechanisms in human and mouse cells. *Infect Immun* **74**(1), 225-38.
- Roy, C. R., and Mocarski, E. S. (2007). Pathogen subversion of cell-intrinsic innate immunity. *Nat Immunol* **8**(11), 1179-87.
- Saeij, J. P., Arrizabalaga, G., and Boothroyd, J. C. (2008). A cluster of four surface antigen genes specifically expressed in bradyzoites, SAG2CDXY, plays an important role in *Toxoplasma gondii* persistence. *Infect Immun* **76**(6), 2402-10.
- Saeij, J. P., Boyle, J. P., and Boothroyd, J. C. (2005). Differences among the three major strains of *Toxoplasma gondii* and their specific interactions with the infected host. *Trends Parasitol* **21**(10), 476-81.
- Saeij, J. P., Boyle, J. P., Coller, S., Taylor, S., Sibley, L. D., Brooke-Powell, E. T., Ajioka, J. W., and Boothroyd, J. C. (2006). Polymorphic secreted kinases are key virulence factors in toxoplasmosis. *Science* **314**(5806), 1780-3.
- Saeij, J. P., Coller, S., Boyle, J. P., Jerome, M. E., White, M. W., and Boothroyd, J. C. (2007). *Toxoplasma* co-opts host gene expression by injection of a polymorphic kinase homologue. *Nature* **445**(7125), 324-7.
- Santiago, H. C., Feng, C. G., Bafica, A., Roffe, E., Arantes, R. M., Cheever, A., Taylor, G., Vieira, L. Q., Aliberti, J., Gazzinelli, R. T., and Sher, A. (2005). Mice deficient in LRG-47 display enhanced susceptibility to *Trypanosoma cruzi* infection associated with defective hemopoiesis and intracellular control of parasite growth. *J Immunol* **175**(12), 8165-72.
- Scaffidi, P., Misteli, T., and Bianchi, M. E. (2002). Release of chromatin protein

- HMGB1 by necrotic cells triggers inflammation. *Nature* **418**(6894), 191-5.
- Scanga, C. A., Aliberti, J., Jankovic, D., Tilloy, F., Bennouna, S., Denkers, E. Y., Medzhitov, R., and Sher, A. (2002). Cutting edge: MyD88 is required for resistance to *Toxoplasma gondii* infection and regulates parasite-induced IL-12 production by dendritic cells. *J Immunol* **168**(12), 5997-6001.
- Scharton-Kersten, T. M., Wynn, T. A., Denkers, E. Y., Bala, S., Grunvald, E., Hieny, S., Gazzinelli, R. T., and Sher, A. (1996). In the absence of endogenous IFN-gamma, mice develop unimpaired IL-12 responses to *Toxoplasma gondii* while failing to control acute infection. *J Immunol* **157**(9), 4045-54.
- Schmidt, S. K., Muller, A., Heseler, K., Woite, C., Spekker, K., MacKenzie, C. R., and Daubener, W. (2009). Antimicrobial and immunoregulatory properties of human tryptophan 2,3-dioxygenase. *Eur J Immunol* **39**(10), 2755-64.
- Schnaith, A., Kashkar, H., Leggio, S. A., Addicks, K., Kronke, M., and Krut, O. (2007). *Staphylococcus aureus* subvert autophagy for induction of caspase-independent host cell death. *J Biol Chem* **282**(4), 2695-706.
- Schroder, K., Hertzog, P. J., Ravasi, T., and Hume, D. A. (2004). Interferon-gamma: an overview of signals, mechanisms and functions. *J Leukoc Biol* **75**(2), 163-89.
- Schwab, J. C., Beckers, C. J., and Joiner, K. A. (1994). The parasitophorous vacuole membrane surrounding intracellular *Toxoplasma gondii* functions as a molecular sieve. *Proc Natl Acad Sci U S A* **91**(2), 509-13.
- Shapira, S., Harb, O. S., Margarit, J., Matrajt, M., Han, J., Hoffmann, A., Freedman, B., May, M. J., Roos, D. S., and Hunter, C. A. (2005). Initiation and termination of NF-kappaB signaling by the intracellular protozoan parasite *Toxoplasma gondii*. *J Cell Sci* **118**(Pt 15), 3501-8.
- Shenoy, A. R., Kim, B. H., Choi, H. P., Matsuzawa, T., Tiwari, S., and MacMicking, J. D. (2007). Emerging themes in IFN-gamma-induced macrophage immunity by the p47 and p65 GTPase families. *Immunobiology* **212**(9-10), 771-84.
- Sher, A., Collazzo, C., Scanga, C., Jankovic, D., Yap, G., and Aliberti, J. (2003). Induction and regulation of IL-12-dependent host resistance to *Toxoplasma gondii*. *Immunol Res* **27**(2-3), 521-8.
- Shi, Y., and Rock, K. L. (2002). Cell death releases endogenous adjuvants that selectively enhance immune surveillance of particulate antigens. *Eur J*

- Immunol* **32**(1), 155-62.
- Sibley, L. D., and Ajioka, J. W. (2008). Population structure of *Toxoplasma gondii*: clonal expansion driven by infrequent recombination and selective sweeps. *Annu Rev Microbiol* **62**, 329-51.
- Sibley, L. D., and Boothroyd, J. C. (1992). Virulent strains of *Toxoplasma gondii* comprise a single clonal lineage. *Nature* **359**(6390), 82-5.
- Sibley, L. D., Weidner, E., and Krahenbuhl, J. L. (1985). Phagosome acidification blocked by intracellular *Toxoplasma gondii*. *Nature* **315**(6018), 416-9.
- Sinai, A. P., Webster, P., and Joiner, K. A. (1997). Association of host cell endoplasmic reticulum and mitochondria with the *Toxoplasma gondii* parasitophorous vacuole membrane: a high affinity interaction. *J Cell Sci* **110** (Pt 17), 2117-28.
- Singh, S. B., Davis, A. S., Taylor, G. A., and Deretic, V. (2006). Human IRGM Induces Autophagy to Eliminate Intracellular Mycobacteria. *Science* **313**(5792), 1438-41.
- Song, B. D., and Schmid, S. L. (2003). A molecular motor or a regulator? Dynamin's in a class of its own. *Biochemistry*. **42**, 1369-76.
- Spekker, K., Czesla, M., Ince, V., Heseler, K., Schmidt, S. K., Schares, G., and Daubener, W. (2009). Indoleamine 2,3-dioxygenase is involved in defense against *Neospora caninum* in human and bovine cells. *Infect Immun* **77**(10), 4496-501.
- Steinfeldt, T., Könen-Waisman, S., Tong, L., Pawlowski, N., Lamkemeyer, T., Sibley, D. L., Hunn, J. P., and Howard, J. C. (submitted). Phosphorylation of IRG resistance proteins is an evasion strategy for virulent *T. gondii* strains.
- Su, C., Evans, D., Cole, R. H., Kissinger, J. C., Ajioka, J. W., and Sibley, L. D. (2003). Recent expansion of *Toxoplasma* through enhanced oral transmission. *Science* **299**(5605), 414-6.
- Subauste, C. S., and Wessendarp, M. (2006). CD40 restrains in vivo growth of *Toxoplasma gondii* independently of gamma interferon. *Infect Immun* **74**(3), 1573-9.
- Sunden-Cullberg, J., Norrby-Teglund, A., Rouhiainen, A., Rauvala, H., Herman, G., Tracey, K. J., Lee, M. L., Andersson, J., Tokics, L., and Treutiger, C. J. (2005). Persistent elevation of high mobility group box-1 protein (HMGB1) in

- patients with severe sepsis and septic shock. *Crit Care Med* **33**(3), 564-73.
- Suss-Toby, E., Zimmerberg, J., and Ward, G. E. (1996). Toxoplasma invasion: the parasitophorous vacuole is formed from host cell plasma membrane and pinches off via a fission pore. *Proc Natl Acad Sci U S A* **93**(16), 8413-8.
- Suzuki, Y., Orellana, M. A., Schreiber, R. D., and Remington, J. S. (1988). Interferon-gamma: the major mediator of resistance against *Toxoplasma gondii*. *Science* **240**(4851), 516-8.
- Taylor, G. A. (2004). p47 GTPases: regulators of immunity to intracellular pathogens. *Nature Reviews Immunology* **4**, 100-109.
- Taylor, G. A. (2007). IRG proteins: key mediators of interferon-regulated host resistance to intracellular pathogens. *Cell Microbiol* **9**(5), 1099-107.
- Taylor, G. A., Collazo, C. M., Yap, G. S., Nguyen, K., Gregorio, T. A., Taylor, L. S., Eagleson, B., Secret, L., Southon, E. A., Reid, S. W., Tessarollo, L., Bray, M., McVicar, D. W., Komschlies, K. L., Young, H. A., Biron, C. A., Sher, A., and Vande Woude, G. F. (2000). Pathogen-specific loss of host resistance in mice lacking the IFN-gamma-inducible gene IGTP. *Proc Natl Acad Sci U S A* **97**(2), 751-5.
- Taylor, G. A., Jeffers, M., Largaespada, D. A., Jenkins, N. A., Copeland, N. G., and Vande Woude, G. F. (1996). Identification of a novel GTPase, the inducible expressed GTPase, that accumulates in responses to interferon γ . *J. Biol. Chem.* **271**, 20399-20405.
- Taylor, G. A., Stauber, R., Rulong, S., Hudson, E., Pei, V., Pavlakis, G. N., Resau, J. H., and Vande Woude, G. F. (1997). The inducibly expressed GTPase localizes to the endoplasmic reticulum, independently of GTP binding. *J. Biol. Chem.* **272**, 10639-10645.
- Taylor, S., Barragan, A., Su, C., Fux, B., Fentress, S. J., Tang, K., Beatty, W. L., Hajj, H. E., Jerome, M., Behnke, M. S., White, M., Wootton, J. C., and Sibley, L. D. (2006). A secreted serine-threonine kinase determines virulence in the eukaryotic pathogen *Toxoplasma gondii*. *Science* **314**(5806), 1776-80.
- Thomas, S. M., Garrity, L. F., Brandt, C. R., Schobert, C. S., Feng, G. S., Taylor, M. W., Carlin, J. M., and Byrne, G. I. (1993). IFN-gamma-mediated antimicrobial response. Indoleamine 2,3-dioxygenase-deficient mutant host cells no longer inhibit intracellular *Chlamydia* spp. or *Toxoplasma* growth. *J Immunol*

- 150**(12), 5529-34.
- Tietzel, I., El-Haibi, C., and Carabeo, R. A. (2009). Human guanylate binding proteins potentiate the anti-chlamydia effects of interferon-gamma. *PLoS ONE* **4**(8), e6499.
- Tiwari, S., Choi, H. P., Matsuzawa, T., Pypaert, M., and MacMicking, J. D. (2009). Targeting of the GTPase Irgm1 to the phagosomal membrane via PtdIns(3,4)P(2) and PtdIns(3,4,5)P(3) promotes immunity to mycobacteria. *Nat Immunol* **10**(8), 907-17.
- Uthaiyah, R. C., Praefcke, G. J., Howard, J. C., and Herrmann, C. (2003). IIGP1, an interferon-gamma-inducible 47-kDa GTPase of the mouse, showing cooperative enzymatic activity and GTP-dependent multimerization. *J Biol Chem* **278**(31), 29336-43.
- van Pesch, V., Lanaya, H., Renauld, J. C., and Michiels, T. (2004). Characterization of the murine alpha interferon gene family. *J Virol* **78**(15), 8219-28.
- Vetter, I. R., and Wittinghofer, A. (2001). The guanine nucleotide-binding switch in three dimensions. *Science* **294**(5545), 1299-304.
- Willingham, S. B., Bergstralh, D. T., O'Connor, W., Morrison, A. C., Taxman, D. J., Duncan, J. A., Barnoy, S., Venkatesan, M. M., Flavell, R. A., Deshmukh, M., Hoffman, H. M., and Ting, J. P. (2007). Microbial pathogen-induced necrotic cell death mediated by the inflammasome components CIAS1/cryopyrin/NLRP3 and ASC. *Cell Host Microbe* **2**(3), 147-59.
- Wilson, C. B., and Remington, J. S. (1979). Activity of human blood leukocytes against *Toxoplasma gondii*. *J Infect Dis* **140**(6), 890-5.
- Wilson, C. B., Remington, J. S., Stagno, S., and Reynolds, D. W. (1980). Development of adverse sequelae in children born with subclinical congenital *Toxoplasma* infection. *Pediatrics* **66**(5), 767-74.
- Winsser, J., Verlinde, J. D., and et al. (1948). Isolation of toxoplasma from cerebrospinal fluid of a living infant in Holland. *Proc Soc Exp Biol Med* **67**(3), 292-4.
- Woodman, J. P., Dimier, I. H., and Bout, D. T. (1991). Human endothelial cells are activated by IFN-gamma to inhibit *Toxoplasma gondii* replication. Inhibition is due to a different mechanism from that existing in mouse macrophages and human fibroblasts. *J Immunol* **147**(6), 2019-23.

- Xie, Z., and Klionsky, D. J. (2007). Autophagosome formation: core machinery and adaptations. *Nat Cell Biol* **9**(10), 1102-9.
- Yamamoto, M., Standley, D. M., Takashima, S., Saiga, H., Okuyama, M., Kayama, H., Kubo, E., Ito, H., Takaura, M., Matsuda, T., Soldati-Favre, D., and Takeda, K. (2009). A single polymorphic amino acid on *Toxoplasma gondii* kinase ROP16 determines the direct and strain-specific activation of Stat3. *J Exp Med* **206**(12), 2747-60.
- Yarovinsky, F., and Sher, A. (2006). Toll-like receptor recognition of *Toxoplasma gondii*. *Int J Parasitol* **36**(3), 255-9.
- Yeretssian, G., Labbe, K., and Saleh, M. (2008). Molecular regulation of inflammation and cell death. *Cytokine* **43**(3), 380-90.
- Yousefi, S., Perozzo, R., Schmid, I., Ziemiecki, A., Schaffner, T., Scapozza, L., Brunner, T., and Simon, H. U. (2006). Calpain-mediated cleavage of Atg5 switches autophagy to apoptosis. *Nat Cell Biol* **8**(10), 1124-32.
- Zeng, J., Parvanova, I. A., and Howard, J. C. (2009). A dedicated promoter drives constitutive expression of the cell-autonomous immune resistance GTPase, Irga6 (IIGP1) in mouse liver. *PLoS ONE* **4**(8), e6787.
- Zerrahn, J., Schaible, U. E., Brinkmann, V., Guhlich, U., and Kaufmann, S. H. (2002). The IFN-inducible Golgi- and endoplasmic reticulum- associated 47-kDa GTPase IIGP is transiently expressed during listeriosis. *J Immunol* **168**(7), 3428-36.
- Zhang, H. M., Yuan, J., Cheung, P., Luo, H., Yanagawa, B., Chau, D., Stephan-Tozy, N., Wong, B. W., Zhang, J., Wilson, J. E., McManus, B. M., and Yang, D. (2003). Overexpression of interferon-gamma-inducible GTPase inhibits coxsackievirus B3-induced apoptosis through the activation of the phosphatidylinositol 3-kinase/Akt pathway and inhibition of viral replication. *J Biol Chem* **278**(35), 33011-9.
- Zhao, Y. (2008). Ph. D. thesis. University of Cologne, Cologne.
- Zhao, Y., Ferguson, D. J., Wilson, D. C., Howard, J. C., Sibley, L. D., and Yap, G. S. (2009a). Virulent *Toxoplasma gondii* evade immunity-related GTPase-mediated parasite vacuole disruption within primed macrophages. *J Immunol* **182**(6), 3775-81.
- Zhao, Y., Wilson, D., Matthews, S., and Yap, G. S. (2007). Rapid elimination of

- Toxoplasma gondii by gamma interferon-primed mouse macrophages is independent of CD40 signaling. *Infect Immun* **75**(10), 4799-803.
- Zhao, Y. O., Khaminets, A., Hunn, J. P., and Howard, J. C. (2009b). Disruption of the Toxoplasma gondii parasitophorous vacuole by IFN γ -inducible immunity-related GTPases (IRG proteins) triggers necrotic cell death. *PLoS Pathog* **5**(2), e1000288.
- Zhao, Y. O., Konen-Waisman, S., Taylor, G. A., Martens, S., and Howard, J. C. (2010). Localisation and mislocalisation of the interferon-inducible immunity-related GTPase, Irgm1 (LRG-47) in mouse cells. *PLoS ONE* **5**(1), e8648.
- Zhao, Y. O., Rohde, C., Lilue, J. T., Könen-Waisman, S., Khaminets, A., Hunn, J. P., and Howard, J. C. (2009c). Toxoplasma gondii and the Immunity-Related GTPase (IRG) resistance system in mice: a review. *Mem Inst Oswaldo Cruz* **104**(2), 234-40.
- Zhao, Z., Fux, B., Goodwin, M., Dunay, I. R., Strong, D., Miller, B. C., Cadwell, K., Delgado, M. A., Ponpuak, M., Green, K. G., Schmidt, R. E., Mizushima, N., Deretic, V., Sibley, L. D., and Virgin, H. W. (2008). Autophagosome-independent essential function for the autophagy protein Atg5 in cellular immunity to intracellular pathogens. *Cell Host Microbe* **4**(5), 458-69.

8 Summary

Toxoplasma gondii is a widespread protozoan parasite infecting all warm-blooded animals and causing disease in immunocompromised individuals and *in utero*. The pathogen depends on the intracellular life style residing in a specialized organelle, termed parasitophorous vacuole (PV), in order to survive and replicate. Cell-autonomous immunity, regulated by IFN γ , is essential to restrict growth of the parasite in mouse and man. In mouse cells, resistance to *T. gondii* is mediated by the family of IFN-inducible IRG proteins (p47 GTPases). Upon infection several IRG proteins associate with the PV and participate in vesiculation of the PV membrane leading to demise of the parasite and necrotic death of the cell. Until now, despite intrinsic interest, the phenomenon of IRG protein loading onto PV has not been well studied. In human cells, depletion of cellular tryptophan by IDO has been reported as the major mechanism of restriction of *T. gondii* proliferation exerted by IFN γ . IDO-independent restriction of *T. gondii* growth has been reported but not followed up.

The process of IRG protein association with *T. gondii* vacuoles emerged as a rapid, organized and diffusion-driven event where multiple resistance proteins sequentially bind to the vacuolar membrane forming homomeric and heteromeric complexes. The efficient loading process requires the autophagy factor Atg5 regulating correct localisation of IRG proteins prior to infection. Virulent strains of *T. gondii* inhibit IRG protein association with PVs independently of individual virulence determinants ROP5, ROP16 and ROP18. Impaired loading of IRG proteins onto *T. gondii* vacuoles leads to reduced elimination of the parasite in IFN γ -stimulated cells, underlining the importance of the phenomenon in cell-autonomous immunity to *T. gondii*.

This study shows that density of cultured cells is the key factor in determining the mode of *T. gondii* control in primary human cells. IFN γ -induced, proliferating cells control parasite replication independently of IDO. Consistent with absence of the IRG system in humans, the vacuolar membrane and enclosed parasite remain intact in IFN γ -induced human cells. However, similar to mouse cells, human cells die by necrosis, when infected with *T. gondii* and stimulated with IFN γ . This may not only suppress parasite growth but also amplify an antimicrobial response due to release of the proinflammatory “danger” signal HMGB1. Programmed necrosis could be efficiently suppressed at high densities of primary cells and in HeLa cell line, and tryptophan depletion becomes the main source of *T. gondii* control.

9 Zusammenfassung

Toxoplasma gondii ist ein weit verbreiteter parasitischer Protozoe, der potentiell alle warmblütigen Tiere infizieren kann und in Individuen mit geschwächtem Immunsystem und *in utero* schwere Krankheiten verursacht. Der Pathogen ist auf einen intrazellulären Lebensstil innerhalb eines speziellen Organells, der parasitophoren Vakuole (PV) angewiesen, welche für sein Überleben und seine Vermehrung notwendig ist. Das Wachstum des Parasiten in Mensch und Maus wird durch die $\text{IFN}\gamma$ regulierte, zell-autonome Immunität eingeschränkt. In Mauszellen wird die Resistenz gegen *T. gondii* durch die Familie der IFN-induzierbaren IRG Proteine (p47 GTPasen) vermittelt. Bei erfolgter Infektion assoziieren mehrere IRG Proteine mit der PV und tragen dazu bei, dass die PV-Membran vesikuliert, was schließlich zum Tod des Parasiten und nekrotischem Tod der Wirtszelle führt. Bis heute sind trotz immanentem Interesse die Vorgänge der IRG Proteinakkumulation auf der PV unzureichend untersucht. In menschlichen Zellen wurde der durch Stimulation mit $\text{IFN}\gamma$ bewirkt Abbau zellulären Tryptophans durch Indolamin-2,3-Dioxygenase (IDO) als wesentlicher Abwehrmechanismus identifiziert. IDO-unabhängige Mechanismen zur Einschränkung des Wachstums von *T. gondii* wurden zwar berichtet, jedoch nicht weiter verfolgt.

Das sich entwickelte Verständnis der IRG Proteinassoziation mit der Vakuole von *T. gondii* ist das eines schnellen, organisierten und diffusionsgetriebenen Vorganges, bei welchem mehrere der Proteine der Reihe nach an die Vakuolenmembran binden und dabei homo- und heteromere Komplexe bilden. Für die effiziente Akkumulation ist der Autophagy Regulator Atg5 notwendig, welcher schon vor erfolgter Zellinvasion des Parasiten für eine korrekte Lokalisation der IRG Proteine notwendig ist. Virulente *T. gondii*-Stämme sind in der Lage, unabhängig von den Virulenzdeterminanten ROP5, ROP16 und ROP18 die IRG Proteinassoziation mit der PV zu hemmen. In $\text{IFN}\gamma$ -stimulierten Zellen führt die beeinträchtigte Beladung von *T. gondii* Vakuolen mit IRG Proteinen zu einer verminderten Elimination des Parasiten, welches die Bedeutung dieses Vorganges im Rahmen der zell-autonomen Immunität gegen *T. gondii* weiter unterstreicht.

Die vorliegende Arbeit zeigt, dass für die Kontrolle von *T.gondii* in menschlichen Zellen die Dichte der kultivierten Zellen entscheidend ist. $\text{IFN}\gamma$ -stimulierte, proliferierende Zellen kontrollieren die Replikation des Parasiten IDO-unabhängig.

In Übereinstimmung mit dem Fehlen des IRG Systems in Menschen bleibt die Vakuolenmembran sowie der darin enthaltene Parasit in menschlichen, IFN γ -stimulierte Zellen intakt. In Analogie zu Mauszellen, sterben humane IFN γ -induzierte Wirtszellen jedoch durch nekrotischen Zelltod. Dies unterdrückt nicht nur die Ausbreitung des Parasiten, sondern verstärkt durch die Freisetzung des proinflammatorischen „Warnsignals“ HMGB1 auch die antimikrobielle Antwort. Der nekrotische Zelltod konnte durch eine hohe Dichte einiger primärer menschlicher Zellenlinien und HeLa zellen zum Zeitpunkt der Infektion effizient unterdrückt werden, so dass der Abbau von Tryptophan hier hauptverantwortlich für die Kontrolle von *T. gondii* war.

10 Acknowledgements

I am grateful to Jonathan Howard for giving me the opportunity to work in his group, for his support and advices. Thomas Langer for reviewing my work and being in my examination. Siegfried Roth for chairing my examination board. Matthias Cramer, Bettina Montazem and Karoline Bendig for the help in tackling various bureaucratic issues. Maria Leptin, Gerrit Praefcke, Hamid Kashkar and Mats Paulsson for stimulating discussions.

I am indebted to Stephanie Könen-Waisman for counting vacuoles, Rita Lange for cloning lessons, Gaby Vopper for the “nice pullover”, Christoph Rohde for the discussions about rock music, Tobias Steinfeldt for the big leaky gels and for reading my thesis, Claudia Poschner for being a great companion in cell culture, Nikolaus Pawlowski and Yang Zhao for fruitful discussions resulted in great scientific contributions, Julia Hunn for the constructive critique, Cemalettin Bekpen and Robert Finking for the moral help at the start, Nataša Papić for being kind, for supervising me during my lab rotation period and for taking a look at my thesis, Jia Zeng for teaching how work with *Toxoplasma*, Urs Benedikt Müller for the food for my soul, Maria Kampes for being there for me. Stephan Schüll, Marialice Heider, Martin Fleckenstein, Jingtao Li and all other members of the Howard lab, present and past, for helpful discussions and friendly atmosphere.

I thank the members of Thomas Langer, Gerrit Praefcke, Martin Krönke, Jürgen Dohmen, Manolis Pasparakis, Günter Schwarz, Dagmar Knebel-Mörsdorf, Dominique Soldati-Favre, Jens Brüning, John Boothroyd and Jon Boyle groups for various help. My thanks to the International Graduate School in Genetics and Functional Genomics and the Graduate School for Biological Sciences for funding and especially program coordinators Brigitte Wilcken-Bergmann and Isabell Witt for their professional help.

11 Erklärung

Ich versichere, dass ich die von mir vorgelegte Dissertation selbständig angefertigt, die benutzten Quellen und Hilfsmittel vollständig angegeben und die Stellen der Arbeit – einschließlich Tabellen, Karten und Abbildungen –, die anderen Werken im Wortlaut oder dem Sinn nach entnommen sind, in jedem Einzelfall als Entlehnung kenntlich gemacht habe; dass diese Dissertation noch keiner anderen Fakultät oder Universität zur Prüfung vorgelegen hat; dass sie – abgesehen von unten angegebenen Teilpublikationen – noch nicht veröffentlicht worden ist sowie, dass ich eine solche Veröffentlichung vor Abschluss des Promotionsverfahrens nicht vornehmen werde. Die Bestimmungen der Promotionsordnung sind mir bekannt. Die von mir vorgelegte Dissertation ist von Prof. Dr. Jonathan C. Howard betreut worden.

Köln, Mai 2010

12 Teilpublikationen

Zhao, Y. O., **Khaminets, A.**, Hunn, J. P., and Howard, J. C. (2009). Disruption of the *Toxoplasma gondii* parasitophorous vacuole by IFN γ -inducible immunity-related GTPases (IRG proteins) triggers necrotic cell death. *PLoS Pathog* **5**(2), e1000288.

Zhao, Y. O., Rohde, C., Lilue, J. T., Könen-Waisman, S., **Khaminets, A.**, Hunn, J. P., and Howard, J. C. (2009). *Toxoplasma gondii* and the Immunity-Related GTPase (IRG) resistance system in mice: a review. *Mem Inst Oswaldo Cruz* **104**(2), 234-40.

Khaminets, A., Hunn, J. P., Könen-Waisman, S., Zhao, Y. O., Preukschat, D., Coers, J., Boyle, J. P., Ong, Y. C., Boothroyd, J. C., Reichmann, G., and Howard, J. C. (2010). Coordinated Loading of IRG Resistance GTPases on to the *Toxoplasma gondii* Parasitophorous Vacuole. *Cell Microbiol* **Accepted article**.

Pawlowski, N., **Khaminets, A.**, Hunn, J. P., Papic, N., Schmidt, A., Uthaiyah, R. C., Lange, R., Vopper, G., Martens, S., Wolf, E., and Howard, J. C. (in preparation). Activation of GTP Hydrolysis In Trans by the Immunity-Related GTPase Irga6 Mirrors the Catalytic Mechanism of the Signal Recognition Particle (SRP/SR α).

13 Lebenslauf

Name: Aliaksandr Khaminets
Geburtsdatum: 24.07.1983
Geburtsort: Slonim, Weißrussland
Staatsangehörigkeit: Weißrussisch
Familienstand: Ledig
Email: akhaminets@googlemail.com
Adresse: Gleueler Str. 229, 50935 Köln, Deutschland

Ausbildung:

1988-1991 Schule, Oshmyani, Weißrussland
1991-2000 Schule, Slonim, Weißrussland
2000 Immatrikulation an der Biologischen Fakultät der
Weißrussische Staatliche Universität, Minsk, Weißrussland
2004-2005 Diplomarbeit in Fachrichtung Microbiologie am
Weißrussische Staatliche Universität, Minsk, Weißrussland
Nov. 2005 – März 2006 Rotationsperioden in den Laboren von Prof. Dr. Jonathan
Howard, Prof. Dr. Karin Schnetz und Prof. Dr. Thomas
Langer als Mitglied der „International Graduate School of
Genetics and Functional Genomics“ der Universität zu
Köln, Köln, Deutschland
April 2006 Promotionsstudiengang Biologie in Fachrichtung Genetik
am Abteilung von Prof. Dr. Jonathan C. Howard, Institut
für Genetik, Universität zu Köln, Köln, Deutschland